Copper Homeostasis and Neurodegenerative Disorders (Alzheimer's, Prion, and Parkinson's Diseases and Amyotrophic Lateral Sclerosis)

Elena Gaggelli,[†] Henryk Kozlowski,[‡] Daniela Valensin,[†] and Gianni Valensin*[,†]

Department of Chemistry, University of Siena, Via Aldo Moro 2, Siena 53100, Italy, and Faculty of Chemistry, University of Wroclaw, F. Joliot-Curie 14, 50-383 Wroclaw, Poland

Received May 13, 2005

Contents

* Corresponding author: telephone, ++39-0577-234231; fax, ++39-0577-234254; e-mail address, valensin@unisi.it.
[†] University of Siena.
[‡] University of Wroclaw.

1. Introduction and Comments

1.1. Neurodegeneration and Protein Aggregation

Neurological disorders of cognitive abnormalities, collectively denoted with the term "neurodegenerative diseases", imply the presence of excess misfolded proteins causing neuronal damage.[1] These aberrant proteins have a typical tendency to aggregate and form solid deposits as diverse as the plaques of Alzheimer's (AD) and prion (PrPD) diseases, the Lewy bodies of Parkinson's disease (PD), the nuclear and cytoplasmic inclusions of Huntington disease (HD), the Bunina bodies of familial amyotrophic lateral sclerosis (ALS), and many others[1−4] (Figure 1). In all of these disorders, proteins that are normally soluble convert into insoluble aggregates that can form intractable and frequently toxic deposits not only in the brain but also in skeletal and muscular tissue and in the heart and the liver.

Proteins, the major molecular components of cells, are involved in virtually every biological process taking place in living systems. Most proteins need to fold into unique, compact 3D structures to acquire their functionality, although intermediate states on the way to the final folded structure play significant roles in events such as translocation across membranes and trafficking to specific cellular locations.[5] A series of strategies has been developed to ensure that proteins fold, and remain properly folded, where and when they are required. These strategies include the folding catalysts and molecular chaperones, and the development of control mechanisms.[6−8]

Despite all control mechanisms, the failure of proteins to achieve their functional states may result in the onset of pathological and often fatal disorders. Newly translated misfolded proteins can still be managed by degradation pathways, mainly via the ubiquitin−proteasome system.[9] In some cases, however, proteins with a high propensity to misfold escape all protective mechanisms and assemble into large aggregates that can be highly organized and extremely stable. Amyloidoses, in which proteins assemble into amyloid fibrils, belong to such a family of disorders associated with polypeptide aggregation. The list of diseases associated with amyloid deposition keeps growing. More than 20 different human amyloid disorders are known so far, and they also include type II diabetes.[10] Aging cells and several age-related pathologies are also characterized by accumulation of oxidatively damaged proteins.[11−13]

The increasing importance of amyloid diseases to human health has prompted major research efforts to identify the molecular mechanisms that give rise to pathological symptoms. The essence of the mechanism of protein aggregation

10.1021/cr040410w CCC: $59.00
Published on Web 06/01/2006

Gianni Valensin (born 1946) received his degree in Chemistry from the University of Florence, Italy, in 1970. He was appointed Full Professor of Physical Chemistry in 1986 at the University of Basilicata, Italy, and, later, Full Professor of Inorganic Chemistry in 1990 at the University of Siena, Italy. He is currently the President of the NMR Centre of the University of Siena.

Elena Gaggelli (born 1947) received her degree in Pharmaceutical Chemistry from the University of Siena, Italy, in 1970. She was appointed Full Professor of Inorganic Chemistry in 2002 at the University of Siena, Italy. She was a Research Associate at the State University of New York with Prof. Paul C. Lauterbur in 1983.

Gianni Valensin and Elena Gaggelli share common research interests that include molecular mechanisms of neurodegeneration, structural and dynamic features of Cu(II) complexes with peptides, proteins, and aminoglycosidic ligands, effects of calcium on conformational selection processes, small-molecule/macromolecule interactions, and NMR metabonomics of human biofluids.

Henryk Kozlowski is Full Professor at the University of Wroclaw, where he obtained his Ph.D. (1973) and habilitation (1977). He was a pioneer of bioinorganic chemistry in Poland. He is coauthor of 410 research publications in coordination and bioinorganic chemistry. His main research interests include molecular mechanisms of neurodegenerative diseases; structure and thermodynamics of bioinorganic systems; metal interactions with natural peptides and their derivatives, pesticides, nucleotides, and nucleic acids; molecular mechanisms of metal-related toxicity and carcinogenesis; chelating agents for toxic metals; and effects of toxic metals on biomolecules.

is that monomeric species initially form small oligomers that then nucleate the growth of rudimentary fibrillar structures. These species can reorganize and assemble further to produce characteristic long and often twisted threadlike fibrils.[6,14] Thus, there are distinct steps in the aggregation process where intervention might be able to prevent or reverse the formation of protein aggregates, as recently pointed out by Dobson.[15]

Until very recently, it has generally been agreed that only a small number of polypeptide chains are prone to form the amyloid fibrils associated with clinical disorders. A number of recent studies by Dobson et al. have, however, shown that suitable conditions can be found where proteins unrelated to diseases form aggregates in vitro and that such aggregates have structural and cytotoxic properties closely resembling those of amyloid fibrils formed in diseased tissues.[16] Independent of variations in primary and secondary structures, when proteins form amyloid fibrils, they all adopt the cross-β-sheet arrangement that is the hallmark of these structures.[17] It is therefore evident that major conformational rearrangements are usually required for the formation of amyloid structures (Figure 2).[18] According to this picture, the conversion process can be schematically divided into two steps.[18]

Daniela Valensin (born 1973) received an M.Sc. degree in Chemistry in 1998 and a Ph.D. degree in Inorganic Chemistry in 2002 at the Chemistry Department of the University of Siena, where she is now a postdoctoral student. Her main scientific interests involve many aspects of nuclear magnetic resonance applied to bioinorganic systems.

(i) A conformational change leads to the formation of an ensemble of species competent for self-association, often referred to as "amyloidogenic intermediate(s)". In such species, the involved peptide chain exposes at least part of its hydrophobic residues to the solvent under conditions in which intermolecular interactions can occur. In the case of globular proteins, the formation of amyloidogenic intermediates involves the disruption of the native structure to a greater or lesser extent;[2] in natively unfolded proteins or unstructured peptides, this step may involve the formation of partially folded species with a high propensity to aggregate.[19]

(ii) Self-association of the amyloidogenic intermediates occurs and eventually leads to the formation of amyloid fibrils. The aggregation process is complex, generally following a nucleation/polymerization mechanism and involving a variety of conformational rearrangements and multiple steps of assembly.[20]

Atomic models of amyloid fibrils have not been available because of difficulties in creating sufficiently large amyloid crystals. Very recently, a seven-residue peptide fragment of the translation termination factor Sup35 was shown to form amyloid fibrils and closely related microcrystals that allowed the atomic structure to be determined.[21] The fragment could bind other copies of itself with the formation of two "tightly interdigitating β-sheets", yielding exclusion of water and a dry, stable interface.

The progressive identification of genes implicated in the various neurodegenerative disorders and the simultaneous development of cellular and animal models have resulted in the generally accepted belief that mutations in the genes yield

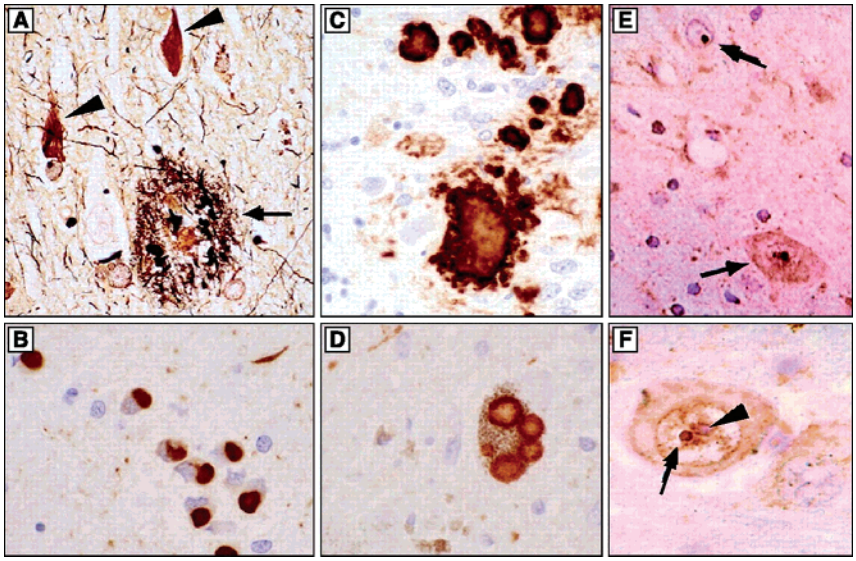

Figure 1. Aggregation of misfolded proteins in visible inclusions in neurodegenerative diseases. (A) Alzheimer's disease: arrowhead, intracellular neurofibrillary tangles; arrow, extracellular amyloid plaque. (B) Fibrillar tau inclusions in Pick's disease. (C) PrP^{Sc} amyloid deposition in prion disease. (D) Multiple Lewy bodies in a nigral neuron in Parkinson's disease. (E) Neuronal intranuclear inclusions of mutant ataxin-3 in Machado−Joseph's disease. (F) Higher power micrograph of nuclear inclusion of mutant ataxin-3. Reprinted from *Science*. Taylor et al., *Science* 296:1991 (2002).

abnormal processing of the toxic protein with consequent accumulation and deposition of the misfolded protein. However, gene mutations account for a few percent of the widely occurring neurodegenerative disorders that are mainly determined by impaired homeostatic control of free radicals and metal ions.

1.2. Oxidative Stress in Cells and Tissues

The human brain is estimated to produce more than 10^{11} free radicals per day,[22] and imbalance in pro-oxidant vs antioxidant homeostasis results in "oxidative stress" with the generation of several potentially toxic reactive oxygen species (ROS), including both the radical and nonradical species that participate in the initiation and/or propagation of radical chain reactions. When molecular oxygen is reduced to water in the electron transport chain, there is a stepwise addition of four electrons, resulting in the formation of several hydrogen-containing ROS, such as hydroperoxyl radical, superoxide radical, hydrogen peroxide, and the hydroxyl radical. Other ROS are generated by the Haber−Weiss or Fenton reactions:

$$O_2^- + H_2O_2 \rightarrow OH^- + OH^\bullet + O_2 \text{ (Haber−Weiss reaction)}$$

$$M^{n+} + H_2O_2 \rightarrow OH^- + OH^\bullet + M^{(n+1)+} \text{ (Fenton reaction)}$$

The superoxide ion is mainly produced by the electron-transport chains in the mitochondria and microsomes through electron leakage. This phenomenon increases with increase in oxygen utilization, and it is therefore especially important in the brain, which uses elevated quantities of oxygen for its metabolism.[23] Superoxide radicals are also formed by metal ion-dependent oxidative reactions and by the action of several enzymes.

The superoxide anion does not cross cell membranes and, by itself, is not very reactive toward cell constituents. Dismutation of superoxide yields hydrogen peroxide, which is also produced by some oxidases. Hydrogen peroxide is also a comparatively inactive molecule, but unlike superoxide, it can easily cross cell membranes. Hydrogen peroxide and superoxide may undergo further transformations and give rise to the highly reactive hydroxyl radicals through the Haber−Weiss reaction or (in the presence of transition metal ions, especially iron and copper in their low oxidation states)[24] through Fenton reactions. This property, combined with the membrane permeability of hydrogen peroxide, gives superoxide and hydrogen peroxide the ability to affect the integrity of distant molecules within the cell.

ROS are implied in normal cellular life as modulators of internal biological processes, including signal transduction, transcription, or apoptosis. However, due to the high chemical reactivity, levels of ROS exceeding the normal needs of the cell are potentially very dangerous for the structural and functional integrity of the cell itself. In fact, ROS can either directly modify cellular DNA, proteins, and lipids or initiate chain reactions, yielding extensive oxidative damage to these critical molecules. Although cells possess a variety of defense mechanisms and repair systems against ROS, these can sometimes be inadequate, leading to oxidative stress in which the production of ROS overwhelms the antioxidant defenses of the organism. Oxidative stress can be regarded as an imbalance between pro-oxidant/free radical production and opposing antioxidant defenses. Acute oxidative stress and chronic oxidative stress have been implicated in a large number of human degenerative diseases, affecting a wide variety of physiological functions, such as atherosclerosis, diabetes, ischemia/reperfusion injury, inflammatory diseases, cancer, neurological diseases, hypertension, ocular diseases, pulmonary diseases, and hematological diseases. Even aging and age-related loss of physiological fitness have been attributed to the chronic effects of ROS on various biological macromolecules.

The brain is particularly vulnerable to oxidative stress,[25] since it consumes approximately one fifth of the total oxygen inspired and carries out the turnover of large quantities of ATP at a high rate. Since approximately 5% of the oxygen consumed by cells is estimated to be reduced to ROS,

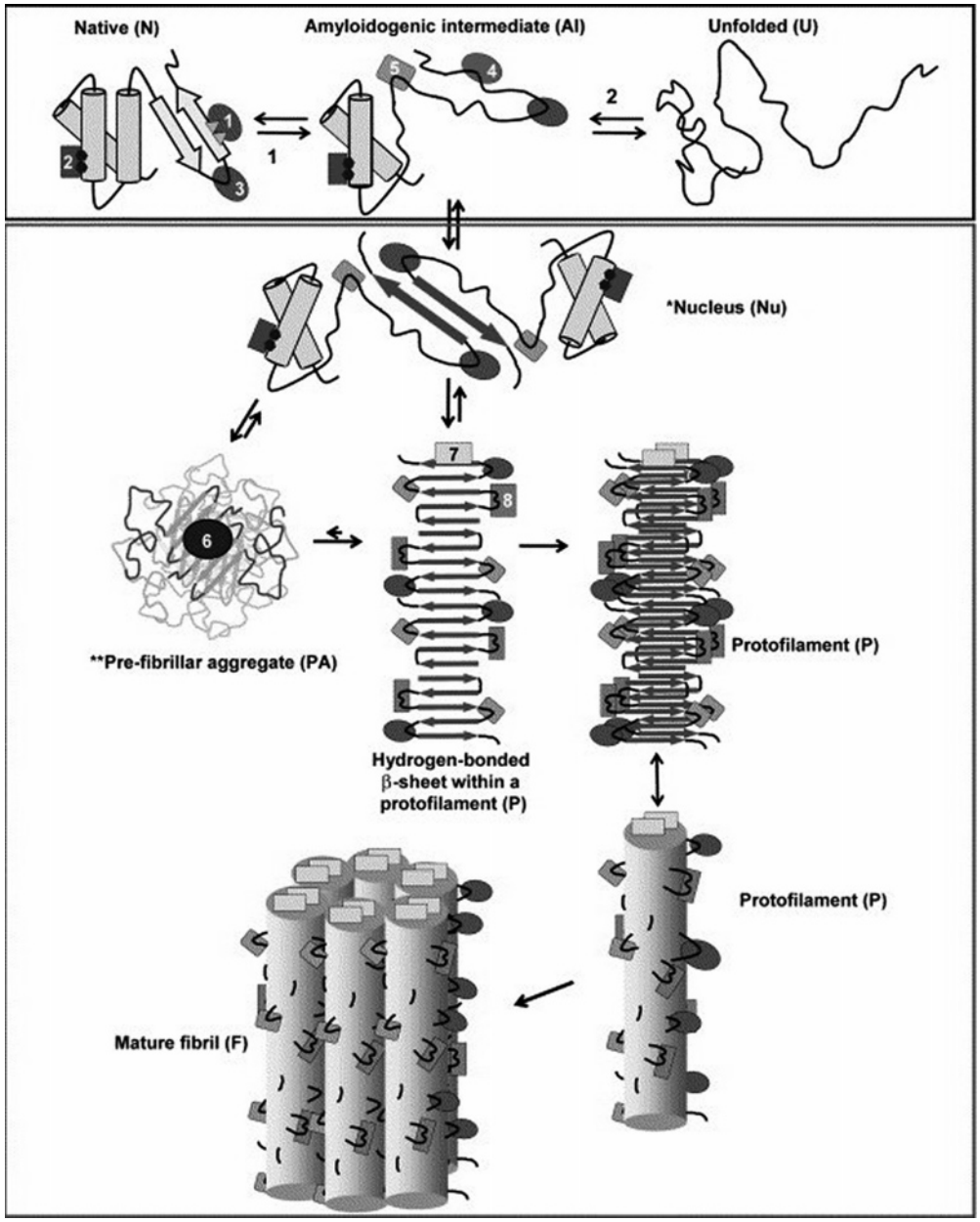

Figure 2. Mechanism of formation of amyloid fibrils that can be produced. The first step (upper box) is the formation of an amyloidogenic intermediate via the partial unfolding of the native state (1) or via partial folding of otherwise naturally unfolded species (2). The second step is the self-association of the amyloidogenic intermediates, which eventually leads to the formation of amyloid fibrils (lower box). The amyloidogenic intermediates have a high tendency to aggregate and become stabilized by the formation of intermolecular β-sheets. Small oligomers are formed initially that act as nuclei to direct the further growth of aggregates (Here the nucleus is for simplicity shown as a dimer). This growth leads to the formation of higher order oligomers referred to as prefibrillar aggregates (PA). These aggregates convert into protofilaments (P) directly or indirectly, and finally into mature fibrils (F). Such fibrils usually consist of two to six protofilaments that are often twisted around each other to form a ropelike structure. Adapted with permission from ref 18. Copyright 2004 Elsevier.

relatively higher amounts of ROS may be generated in the brain as compared to other tissues that use less oxygen. Moreover, the brain is rich in poly-unsaturated fatty acids, which are particularly susceptible to ROS damage.

Oxidative stress has been implicated not only in normal brain aging but also in many neurodegenerative disorders.[22,26] As a matter of fact, AD, PD, and ALS are all characterized by extensive oxidative damage to cell membranes, proteins, and DNA.

1.3. Neurobiology of Metal Ions

The discovery that many proteins and enzymes rely on metal ions for their structure and function raised a new research territory at the interface of chemistry and biology, and led to merging of fundamental concepts of biochemistry and inorganic chemistry into the foundation of the discipline of "Bioinorganic Chemistry".[27]

The interest of the bioinorganic chemist in the study of neurochemistry and neurophysiology has long been minimal and largely limited to the role and function played by calcium, magnesium, potassium, and sodium. This outlook has dramatically changed, and the progress made in the study of the central nervous system can now open great opportunities for the comprehensive understanding of the roles of transition metal ions in synaptic transmission, in memory formation, and in neurological diseases, i.e., for "Metallo-

neuro-chemistry".[18,28] In fact, growing evidence is being collected of relationships between the biochemistry of Fe, Cu, Mn, and Zn and the generation of (or defense against) oxygen and protein radicals that mediate the major neurological diseases. In particular, the view has emerged that the brain is a specialized organ able to concentrate metal ions. For the purposes of the present review, the attention will be confined to copper ions, with a few references only to the relevance of other ions.

It has long been believed that the concentration of free metal ions in the brain is too low to be physiologically significant and that, as a consequence, involvement of metal ions in neurological disorders may only arise from toxicological exposure to Cu, Fe, Zn, or Mn. The diseased state has then long been ascribed to ingestion of or exposure to the metals, causing an abnormal protein interaction.

It is slowly emerging that, in terms of total concentrations, the brain has more than enough of the mentioned metal ions in its tissue to damage or dysregulate numerous proteins and metabolic systems.[29−31] It follows that the brain, like all other organs and tissues, must have efficient homeostatic mechanisms and buffers in place to prevent the abnormal discompartmentalization of metal ions. Also, the blood−brain barrier (BBB) is relatively impermeable to fluctuating levels of plasma metal ions. It is known that several of the metal regulatory transport systems are energy dependent (e.g. the Wilson's disease Cu-ATPase). Therefore, damage to the BBB and alterations in the ATP production/consumption in the brain are two characteristics of several neurodegenerative disorders that could perturb metal levels and lead to deranged protein behavior. Hence, there is no need to hypothesize toxic exposure to explain abnormal metal−protein interactions in vivo. In other words, it does not matter how low the absolute concentration of a given metal ion normally found in the brain is, but rather, it is relevant to evaluate the routes of its homeostatic control, that, once impaired, may allow degeneration into the pathological state.

There are two generic reactions of relevance to neurodegenerative disease: (i) a metal−protein association leading to protein aggregation (Zn(II), Cu(II), Fe(III)) or (ii) a metal-catalyzed protein oxidation leading to protein damage and denaturation (Cu(II), Fe(III), Mn(II)).

The aim of the present review is to provide a comprehensive overview of literature dealing with the relationship between oxidative stress, impaired copper homeostasis, and neurological disorders. The effects of the other relevant metal ions will be only partially addressed, with special emphasis on their agonist or antagonist effects. A brief survey of structural features of complexes formed by Cu(II) and model peptides will be provided since it has given relevant clues to the understanding of electronic, spectroscopic, and geometric features in copper−protein complexes. The metabolic pathways of copper ingestion, transport, and delivery will be considered in order to lay down the basic principles of copper homeostatic control. Finally, the involvement of copper in Alzheimer's disease, amyotrophic lateral sclerosis, Parkinson's disease, and prion diseases will be given prominence, because the mechanisms underlying the onset of these pathologies are better understood than those of all other amyloidoses.

2. Copper Binding Motifs in Peptides and Proteins

Peptides are very effective and often specific ligands for a variety of metal ions. They contain a range of potential donor atoms, and the complexes formed exist in a variety of conformations. Coordination of Cu(II) to peptides with noncoordinating side chains starts at the N-terminal amino nitrogen, which acts as an anchoring binding site, preventing metal ion hydrolysis. The adjacent carbonyl oxygen is the second donor, completing the chelate ring.[32] As the pH is raised, the metal ion succeeds in deprotonating successive peptide nitrogens, forming $Cu-N^-$ bonds, until eventually a $[CuH_{-3}L]^{2-}$ species (4N complex) is formed around pH 9−10, with the −3 indicating the number of ligand atoms undergoing metal-induced deprotonation.

The formation of stable five-membered chelate rings by consecutive nitrogens is the driving force of the coordination process, lowering the p*K* value of the first amide nitrogen by as much as 10 log units. The deprotonations of particular amide nitrogens are usually well separated from each other, indicating the lack of cooperativity in the binding process.

Consideration of the Asn-Ser-Phe-Arg-Tyr-NH_2 (NSFRY-NH_2) pentapeptide reveals that the coordination modes to Cu(II) are analogous, but the formation of a 4N complex is observed at a much lower pH, indicating an extreme stability enhancement of almost 5 orders of magnitude.[33] This exceptionally high complex stability has been ascribed to metal-ion-promoted conformational organization. The other feature found for this system is the cooperative transition from the 2N to the 4N complex. Aromatic rings of Phe, Tyr, or Trp were shown to generally enhance complex stability through direct electronic interactions with the metal ion, the stacking between two rings, or general hydrophobic effects,[34] but mainly in short di- or tripeptides.

The occurrence of proline as the N-terminal residue provides an effective anchoring site for metal ions, whereas its introduction into the peptide chain in position two, three, or further results in a peptide bond that does not have an amide proton that may be displaced by metal ions. As a consequence, the simple stepwise coordination of consecutive amide nitrogens, discussed above, is no longer possible. For these reasons, this phenomenon was named the "breakpoint"[35] and was extensively investigated. On the other hand, the presence of a Pro residue in the peptide sequence increases the propensity of a peptide chain to bend.

The most interesting feature of these systems is the favored formation of large macrochelate loops, with Cu(II) bound to the N-terminal amino group and a distant donor. The latter might be either a main chain amide or a donor group of a normally noncoordinating side chain, like the Tyr phenolate, the ϵ-NH_2 of Lys, or the lateral carboxylate of Glu.

2.1. Histidine and Histidine-Containing Peptides

The histidine residue possesses a very efficient nitrogen donor in its side chain imidazole ring. The cooperativity of all three donor groups of this amino acid in metal binding is made possible by the formation of two fused chelate rings: the five-membered $\{NH_2, COO^-\}$ (amino acid-like) one and the six-membered $\{NH_2, N_{im}\}$ (histamine-like) one.

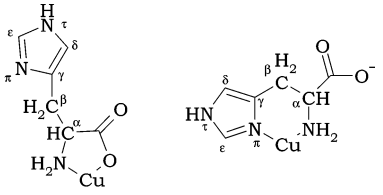

The high thermodynamic stability of five- and six-membered rings versus larger ones results in the selection of the N-π (or N-1) rather than the N-τ (or N-3) imidazole nitrogen. Such terdentate binding makes histidine a primary low molecular weight chelator in living systems. It is interesting to note that the administration of Cu-histidine, when initiated early in life, is the most effective treatment for Menkes disease, a genetic neurodegenerative disorder due to impaired copper metabolism.[36] The specificity of histidine in metal ion binding is preserved in His-containing peptides. The His residue provides two nitrogen donors and a six-membered chelate ring for coordination. However, the coordination properties of a His residue within a peptide sequence depend enormously on the position of this residue in a peptide chain.

(a) His-1 Peptides. These bind Cu(II) differently from ordinary peptides. The $\{NH_2, N_{im}\}$ chelate of the His-1 residue, analogous to histamine,[37] is so efficient that it hinders the deprotonation of amide groups by Cu(II). The pH of the first amide deprotonation is elevated from ~5 to well above 6.

(b) His-2 Peptides. The amine, the imidazole, and the amide nitrogen of the intervening His simultaneously participate in metal binding. The predominant complex is $CuH_{-1}L$, detected at a pH as low as 4 and remaining as the most important species through pH 10.[38] The high stability of this complex results from the formation of a pair of fused chelate rings.

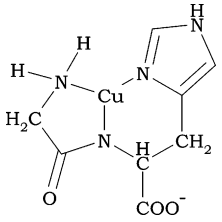

(c) His-3 Peptides. The presence of the His residue in position three of the peptide chain allows for the simultaneous formation of three fused chelate rings and, thus, the saturation of the coordination plane. The Cu(II) complexation reaction proceeds cooperatively, with both amide groups deprotonating and bonding to Cu(II) between pH 4 and 5.[39] The 4N complexes formed in this way are the most stable ones formed by peptides. For example, the tripeptide Gly-Gly-His is 10-fold more effective in binding Cu(II) than Gly-His, and ~200-fold more effective than NSFRY-NH_2, the strongest ligand among non-His peptides.

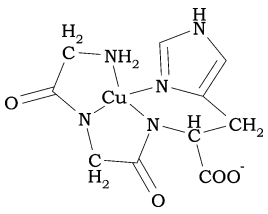

(d) His-4 Peptides and Beyond. When His occurs at the fourth position or is even further from the N-terminus, competition between the amino terminus and the imidazole nitrogen might occur at the first anchoring site. Many investigations have provided evidence that anchoring of Cu(II) at the His residue is preferred over the N-terminal binding.[40,41]

2.2. NMR Studies of Histidine-Containing Peptides Interacting with Cu(II)

The study of Cu(II) complexes with peptides and many other ligands may take advantage of numerous spectroscopic techniques, such as UV−vis, CD, EPR, and X-ray, as well as of mass spectrometry and potentiometric titrations. The possible approaches have been the object of many recent excellent reviews.[42−46] Although NMR finds a prominent role in delineating structures of diamagnetic and paramagnetic metal complexes in solution, it is evident that such a role has been largely limited in the investigation of Cu(II) interacting with histidine-containing peptides.

Addition of paramagnetic ions to solutions of any NMR detectable ligand is in fact expected to dramatically affect nuclear relaxation rates and chemical shifts in a way strictly related to metal location within the molecular frame. The desired structural information is then gained by applying developed theories of paramagnetic NMR.[47] However, if compared to such general trends, what is commonly observed with histidine-containing peptides that strongly bind Cu(II) is that NMR spectra are practically unaffected even at very high metal/ligand ratios;[40,41] only the imidazole protons of the considered peptides are somehow broadened, which ratifies the common view of histidine providing the first and most relevant anchoring point for Cu(II) at pH values consistent with imidazole first deprotonation.[40,41,48−52] This is why the use of NMR has generally been limited to qualitatively demonstrate the involvement of His (or other eventual residues) in metal binding without taking any advantage of the potential of the technique in obtaining structural details.

An example is reported in Figure 3, which shows the effects of adding Cu(II) on the NMR spectra of two synthetic His-containing peptides.[53] If it were not for some broadening experienced by the arrowed aromatic protons of histidine, one might conclude that copper(II) does not change the appearance of the spectra, as if it were not binding the peptides. In contrast with such an observation, all other experimental techniques support the strong interaction of copper. This apparent paradox can be explained by taking contributions of the exchange rate from the metal coordination sphere into account.[40,53]

In solutions of ligands containing paramagnetic ions as cosolute, both the longitudinal (R_{1obs}) and the transverse (R_{2obs}) nuclear relaxation rates are averaged over the values of the free ligand molecules in the bulk (R_{1f} or R_{2f}) and those of the ligand molecules residing in the metal coordination sphere and experiencing the effects of the electron spin magnetic moment (R_{1b} or R_{2b}):

$$R_{1obs} = \frac{1}{T_{1obs}} = \frac{p_f}{T_{1f} + k_{on}^{-1}} + \frac{p_b}{T_{1b} + k_{off}^{-1}}$$

$$R_{2obs} = \frac{1}{T_{2obs}} = \frac{p_f}{T_{2f} + k_{on}^{-1}} + \frac{p_b}{T_{2b} + k_{off}^{-1}}$$

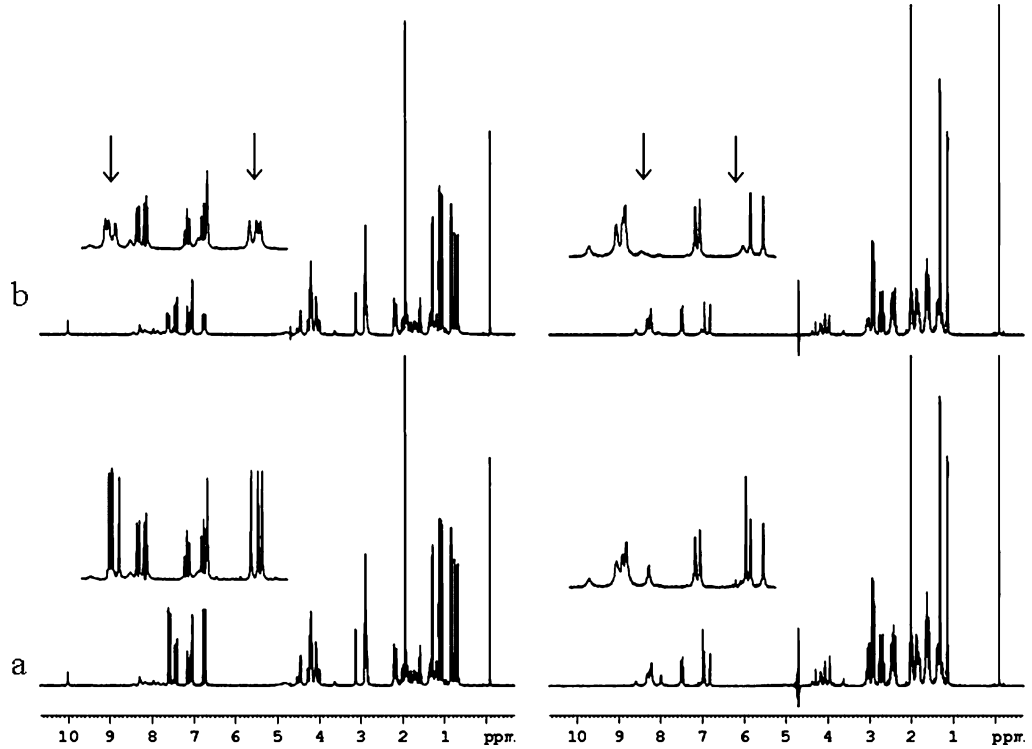

Figure 3. ^{1}H NMR spectra of (a) APP(145−155) 2 mM in H_2O/D_2O at pH 7.3; (b) APP(145−155) 2 mM in H_2O/D_2O at pH 7.3 after addition of 0.02 equiv of Cu(II); (c) PrP106−113 2.6 mM in H_2O/D_2O at pH 5.6; and (d) PrP106−113 2.6 mM in H_2O/D_2O at pH 5.6 after addition of 0.1 equiv of Cu(II). The arrows help locate the aromatic protons of histidine in the NMR spectra. Adapted with permission from ref 53. Copyright 2005 The Royal Society of Chemistry.

In these equations, p_f and p_b are the fractional populations of the ligand in each environment, and k_{on} and k_{off} are the kinetic rate constants for entrance into and exit from the metal coordination sphere. Since entrance into the metal coordination sphere is a high-rate diffusion-controlled process, $k_{on}^{-1} \ll T_{1f}$, T_{2f} usually holds, which yields the so-called paramagnetic contributions to nuclear relaxation rates:[47]

$$R_{1p} = R_{1obs} - p_f R_{1f} = \frac{p_b}{T_{1b} + k_{off}^{-1}}$$

$$R_{2p} = R_{2obs} - p_f R_{2f} = \frac{p_b}{T_{2b} + k_{off}^{-1}}$$

The paramagnetic contributions are easily measured, and $R_{1b} = 1/T_{1b}$ can be obtained, which is the structure-sensitive term, as accounted for by the Solomon equation, which, for systems with $S = {}^1/_2$, is given by[54]

$$R_{1b} = \frac{1}{10}\left(\frac{\mu_0}{4\pi}\right)^2 \frac{\hbar^2 \gamma_I^2 \gamma_S^2}{r^6}\left\{\frac{\tau_c}{1 + (\omega_I - \omega_S)^2 \tau_c^2} + \frac{3\tau_c}{1 + \omega_i^2 \tau_c^2} + \frac{6\tau_c}{1 + (\omega_I + \omega_S)^2 \tau_c^2}\right\}$$

where μ_0 is the permeability of a vacuum, γ_I and γ_S are the nuclear and electron magnetogyric ratios, respectively, ω_I and ω_S are the nuclear and electron Larmor frequencies, r is the metal−nucleus distance, and τ_c is the effective correlation time, generally determined, in the case of copper(II), by the reorientation correlation time of the metal complex and measured from the value of the cross-relaxation rate, σ, of the β-CH_2 protons[55] or from the ratio between the nonselective and selective relaxation rates of the backbone protons of the free peptides.[56]

It follows that the contribution of exchange, if not negligible, must be evaluated in independent ways and that the exchange rate may become a limiting factor and level off the paramagnetic contribution to nuclear relaxation rates and, hence, to NMR line widths. This may effectively be the case for copper(II) strongly associated to His-containing peptides, where the inverse of the off-rate kinetic constant (k_{off}^{-1}) may become so long that the dipolar contribution to nuclear relaxation rates is washed out. This being the case, the exclusive line broadening of the imidazole protons might arise from a faster exchange rate rather than from its unique involvement in binding.

The effects of exchange can be nicely verified by comparing the output of different NMR experiments performed on the same sample. Figure 4A reports the low-field (lower traces) and high-field (upper traces) regions of the ^{1}H NMR spectrum of the PrP106−126 peptide in the presence of Cu(II) at a 1:5 metal/ligand ratio.[53] It is evident that only the H_δ and H_β of His-111 are broadened (the H_ϵ signal is obscured by other signals), while all other resonances are poorly affected. However, Figure 4B shows the α-region of the ^{1}H−^{13}C HSQC spectra of the same peptide before and after the addition of 0.2 equiv of Cu(II) ions. The circled Lys-106, Thr-107, Lys-110, His-111, and Gly-126 H_α−C_α connectivities are somehow affected by the presence of paramagnetic ions. Such different broadening of H_α in the two spectra is accounted for by H_α and C_α experiencing different paramagnetic contributions (due to different distances from the metal and magnetogyric ratios) such that k_{off}^{-1} does not limit, in the case of C_α, the detection of the dipolar interaction.

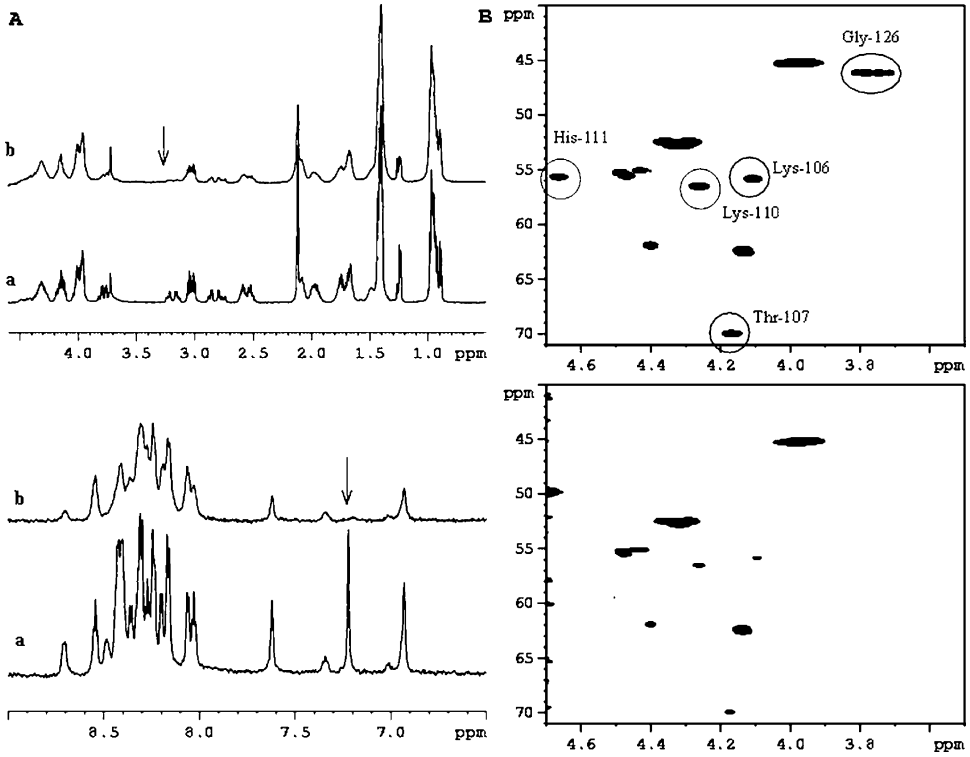

Figure 4. (A) Selected regions of ^{1}H NMR spectra of PrP106−126 1.8 mM in H_2O/D_2O at pH 5.7 before (a) and after the addition of 0.2 equiv of Cu(II) (b). The arrows indicate the most affected His protons. (B) ^{1}H−^{13}C HSQC spectra of PrP106−126 1.8 mM in H_2O/D_2O at pH 5.7 and $T = 298$ K before (upper) and after the addition of 0.2 equiv of Cu(II) (bottom). The most affected circled cross-peaks belong to Gly-126, His-111, Lys-106, Lys-110, and Thr-107. Reprinted with permission from ref 53. Copyright 2005 The Royal Society of Chemistry.

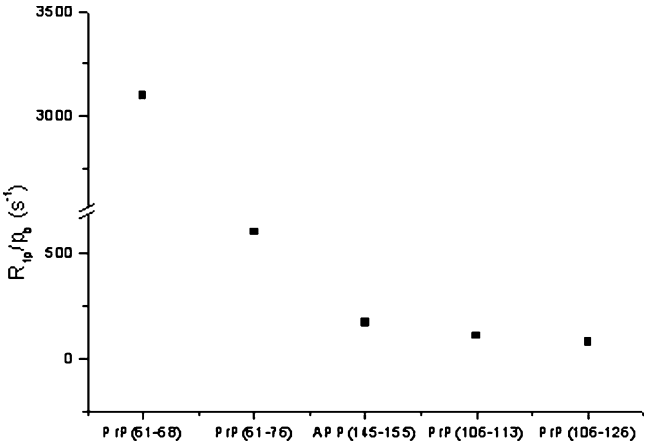

Figure 5. R_{1p}/p_b values of Hϵ His protons for Cu(II) complexes of peptide sequences derived from human prion protein (PrP) and human amyloid precursor protein (APP). Adapted with permission from ref 53. Copyright 2005 The Royal Society of Chemistry.

The interplay between exchange rate and paramagnetic effects can be further exemplified by considering the normalized values of paramagnetic contributions to His H_ϵ in diverse peptides (Figure 5).[53] Since the $Cu^{2+}-H_\epsilon$ distance is fixed at 0.31 nm in any case, the different values are exclusively determined by the exchange rate.

The conclusion is that, in most cases, the exchange rate must be independently calculated in order to evaluate the R_{1b} values from experimental observations. This allows the geometric and structural constraints to be obtained and, therefore, the opportunity to gain valuable information on the 3D structure of Cu(II) complexes, as will be extensively shown for peptides taken from proteins involved in neurodegenerative disorders.

2.3. Copper Metalloproteins

2.3.1. The ATCUN Motif

The amino terminal Cu(II) and Ni(II) (ATCUN ≡ H_2N-XX-His, with X any amino acid) motif has been extensively studied for ∼45 years.[57] The first concept of a small metal binding site on albumins[58] has progressively changed to a Cu(II) (and Ni(II)) binding motif that can be found in several naturally occurring proteins or designed for insertion into proteins to provide them with DNA cleavage capability. The ATCUN motif requires (i) a free amino terminus, (ii) an His residue in position 3, and (iii) two intervening peptide nitrogens, and it is formally equivalent to the binding site provided by tri- or oligopeptides having a His-3 residue. However, in the ATCUN motif of human serum albumin (H_2N-Asp-Ala-His-...), the Asp side chain carboxyl was shown to be involved in forming a pentacoordinated structure.[59] The ATCUN motif, encountered in human, bovine, and rat albumins, neuromedin C and K, protamine P2a, and histatins, binds Cu(II) specifically and reversibly, releasing Cu(II) with appropriate ligands and reflecting its role as a copper transport site in albumins. The properties of the ATCUN motif were extensively summarized by Harford and Sarkar.[60] More than 20 years ago, the Cu(II)-bound ATCUN motif was shown to possess antitumor activity,[61] which was ascribed to production of hydroxyl radical via Fenton chemistry.

2.3.2. Copper-Containing Metalloproteins

A huge number of copper-containing metalloproteins has been reported so far, with the number increasing almost every day. These proteins play important roles in electron transfer and dioxygen binding, activation, and reduction. According to the structure of the catalytic copper-containing site, these

proteins have been classified into type-1 or blue (plastocyanin, azurin, pseudoazurin, amicyanin, rusticyanin, stellacyanin, etc.), type-2 (amine oxidases, galactose oxidase, superoxide dismutase, etc.), and type-3 (hemocyanin, ceruloplasmin, laccase, nitrite reductase etc.). The function, the number, and the type of Cu ligands and the structure of these proteins have been summarized in excellent reviews and textbooks.[62−71] Relevant structural and functional properties of many copper-containing proteins are summarized in recently published Handbooks of Metalloproteins.[72,73]

3. Elements of Copper Homeostasis

3.1. Introduction

Copper is too redox active to exist in an unbound form in the cell without causing oxidative damage: an upper limit of 10^{-18} M for the free concentration of Cu(II) in unstressed cells has been evaluated,[74,75] and new metabolic systems handling copper have been recently discovered. Damage to the tight regulation of Cu(II) homeostasis is expected to contribute to several neurodegenerative conditions. In fact, although Cu(II) is essential for life and for the function of numerous enzymes of interest to neurobiology (tyrosinase, ceruloplasmin, cytochrome *c* oxidase, dopamine β-hydroxylase, etc.), free or incorrectly bound Cu(II) may act as a catalyst for the generation of the most damaging radicals, such as the hydroxyl radical. Inappropriate compartmentalization or elevation of Cu(II) in the cell and inappropriate binding of Cu(II) to cellular proteins are currently being explored as sources of pathological oxidative stress in several neurodegenerative disorders.

Maintenance of cellular copper homeostasis requires membrane copper transporters and a family of proteins, termed "copper chaperones", that deliver copper to specific targets in the cell. Copper transporters and chaperones identified in lower eukaryotes are also present in mammals, indicating remarkable evolutionary conservation of the systems involved in copper trafficking within cells.

The body of a healthy, 70-kg human adult contains <110 mg of Cu, much of it in the liver (10 mg), brain (8.8 mg), blood (6 mg), skeleton (including the bone marrow; 46 mg), and skeletal muscle (because of its size; 26 mg).[76] Most of this copper is probably functional, being involved in cuproenzymes. The Recommended Dietary Allowance for adult men and women is 0.9 mg of copper/day, and the Tolerable Upper Intake Level has been set at 10 mg/day.[77]

The identification of the genes affected in two human disorders of copper transport, Menkes (ATP7A, copper deficiency disorder) and Wilson (ATP7B, copper toxicity disorder) diseases, provided important new information about the molecules that regulate systemic and cellular copper concentrations. Both genes encode copper ATPases that are members of the P-type ATPases family of cation transporters (vide infra). These proteins are copper efflux pumps that regulate the amount of copper leaving the cell and that, in addition, supply copper to cuproenzymes in the trans-Golgi network.

ATP7A and ATP7B play an important role in the physiological regulation of copper. A model of systemic copper homeostasis indicating the points at which these two proteins are thought to act in regulating copper levels and distribution in the body is shown in Figure 6.[78] Copper is primarily absorbed in the small intestine; the liver is central to copper homeostasis, and most of the newly absorbed copper first enters this organ. In the liver, copper is supplied to endogenous enzymes, incorporated into ceruloplasmin, and secreted into the blood; if in excess, it is secreted in the bile.

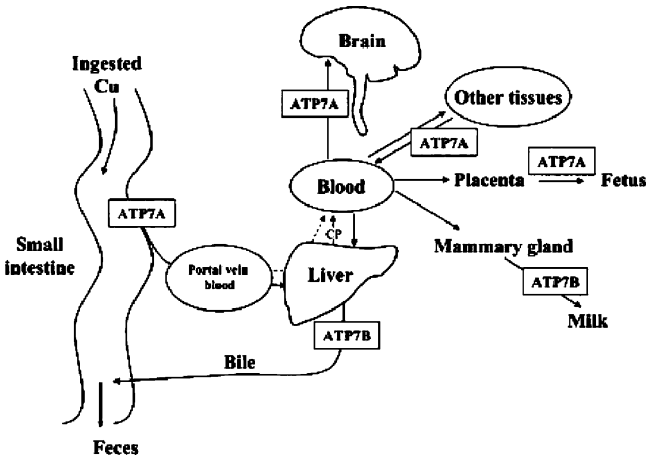

Figure 6. Model for the homeostatic regulation of copper in mammals. The flow of copper is shown by the arrows. The steps involving the Cu ATPases, ATP7A and ATP7B, are indicated. CP indicates the ceruloplasmin, the main copper protein in the blood. Reprinted with permission from ref 78. Copyright 2003 American Society for Nutrition.

The transport of copper to the brain requires a mechanism for transport across the blood−brain barrier. This step is blocked in Menkes disease, suggesting the Cu-ATPase ATP7A is the copper pump involved. Copper is transported into neurons and astrocytes by the protein Ctr1, originally discovered in yeast and later characterized in mammals (vide infra).[79,80] The delivery of copper to target enzymes depends on at least three metallochaperone systems: (a) the Cox17 system delivers copper to mitochondria for insertion in Cytochrome oxidase;[81] (b) the copper chaperone for superoxide dismutase (CCS) system delivers copper to superoxide dismutase (SOD) in the cytoplasm;[82] and (c) the Atox1 or

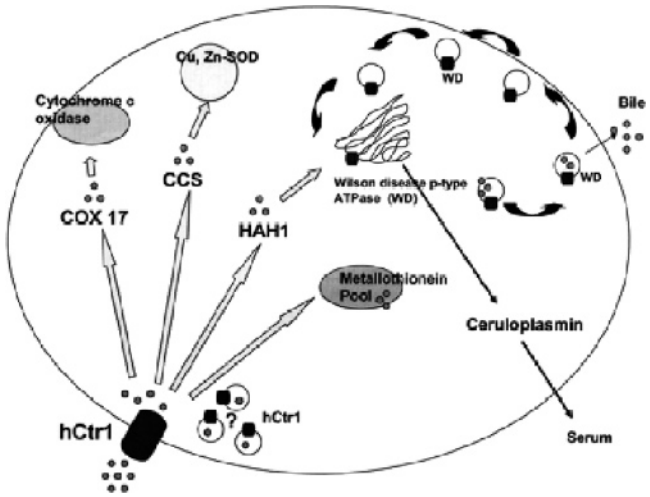

Figure 7. Model of copper trafficking in a hepatocyte. Copper enters the hepatocyte via the copper transport protein, hCtr1. Copper, once inside the hepatocyte, has one of four possible fates: (i) joining the copper/metallothionein pool, (ii) trafficking to the mitochondria for cytochrome *c* oxidase incorporation via the copper chaperone cox17, (iii) binding to CCS for delivery to Cu,Zn−SOD, or (iv) trafficking to the Wilson disease P-type ATPase, which resides in the trans-Golgi network, by HAH1 for subsequent copper incorporation into the cuproprotein ceruloplasmin. Reprinted with permission from ref 84. Copyright 2003 American Society for Nutrition.

HAH1 system delivers copper to ATP7A in the trans-Golgi network for successive incorporation in other Cu proteins such as Ceruloplasmin.[83]

Copper may also join the copper/metallothionein pool. This general view is schematized in Figure 7,[84] but it may be largely incomplete, since extensive research on neurodegenerative disorders is providing increasing evidence of the roles played by other neuronal membrane proteins, such as the prion and the amyloid precursor protein, in dealing with copper trafficking in the brain.

3.2. The Human Copper Transporter (HCTR1)

Human Ctr1 (190 amino acids), contains a methionine and histidine rich extra-cellular N-terminus. Ctr1 mRNA is ubiquitously expressed, with the highest levels found in the liver and lower levels detected in the brain and spleen. Ctr1 has three transmembrane domains, exists as a homotrimer, and has been shown to be extensively glycosylated (Figure 8).[85,86] Uptake of copper by Ctr1 (i) is energy independent, (ii) is stimulated by acidic extracellular pH and high K^+ concentrations, and (iii) is time dependent and saturable. The stimulation of copper uptake by K^+ and the observation in yeast that copper uptake is coupled with K^+ efflux may indicate that copper uptake by Ctr1 is mediated by a $Cu^+/2K^+$ antiport mechanism. Ctr1 occurs as a pool of intracellular molecules that can be quickly recruited to the plasma membrane in times of copper shortage and then endocytosed upon high copper concentration in the medium.[87]

The hCtr1, like the ATP7A/B copper exporters, is post-translationally regulated by copper availability. Elevated copper stimulates its rapid endocytosis and degradation.[88] This process may function to attenuate copper uptake and prevent overaccumulation of this potentially toxic metal. In examining the role of conserved extracellular motifs in regulating the copper-responsive endocytosis and degradation of hCtr1, it was shown that the Mets motif closest to the first transmembrane region was required to stimulate endocytosis in response to low micromolar copper levels but not elevated concentrations.[86] Moreover, mutation of either methionine of the ^{150}MXXXM^{154} motif completely abolished copper-responsive endocytosis and degradation of hCtr1 even under high copper concentrations.[86]

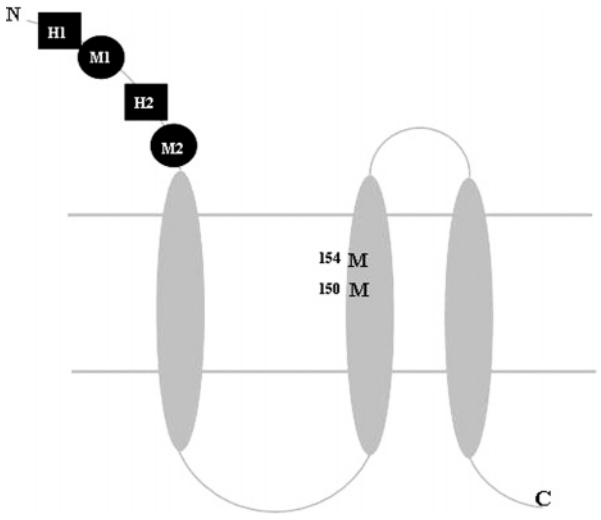

Figure 8. Schematic diagram of the hCtr1 protein showing the methionine rich motifs, M1 and M2 (black circles), the histidine rich sequences, H1 and H2 (black squares), and the Met-150 and Met-154 residues of the conserved MXXXM motif.

Recently, it has been shown that hCtr1 mediates saturable Cu uptake and that the rapid Cu-dependent internalization of hCtr1 is not a required step in transmembrane copper transport.[89] It has been, therefore, suggested that hCtr1 acts as a conventional transporter, providing a permeation pathway for Cu through the membrane.

3.3. Menkes and Wilson P-Type ATPases

Wilson (WND) and Menkes (MNK) diseases represent the most well recognized and understood disorders of copper homeostasis, with marked neurological manifestations. These diseases are associated with mutations in the P-type ATPase ATP7A (MNKP, Menkes protein) and ATP7B (WNDP, Wilson protein). MNKP and WNDP are functionally homologous, share 67% protein identity, are located in the trans-Golgi network membranes, and differ in tissue and developmental expression only.

The functional relationship between these two proteins in the central nervous system is poorly understood. Due to its localization in the choroid plexus, MNKP is thought to control the overall supply of copper to the brain, but the physiological functions that these two ATPases have in different regions of either the adult or the developing brain are largely unknown. Very recently, high-resolution imaging and functional assays have been used to demonstrate that MNKP and WNDP show cell-specific distribution in the adult cerebellum, have distinct enzymatic characteristics, and are regulated differently during development:[90] WNDP is continuously expressed in Purkinje neurons, where it delivers copper to ceruloplasmin, while MNKP is a faster copper transporter.

MNKP and WNDP have eight transmembrane domains and contain six Met-X-Cys-X-X-Cys copper binding motifs at the N-terminus. Like all other P-type ATPases, they use energy from ATP hydrolysis to translocate metal cations across lipid bilayers. Under normal copper conditions, both are predominately localized to the trans-Golgi network, where they function in the copper secretory pathway, delivering copper for incorporation into nascent cuproproteins. When the cell is exposed to high levels of copper, MNKP redistributes from the TGN to the cell surface, where it is thought to rid the cell of excess copper in response to copper overload. The structure of the second domain of the human Menkes protein (MNK2), formed by 72 residues, has been determined by NMR in both the apo and copper-loaded forms.[91] The loop involved in copper binding is part of a hydrophobic patch, which is maintained in both forms. Conformational mobility is observed in the apo form in the same loop. The solution structure of the expressed first N-terminal Cu binding motif MNK1(2−79) has been very recently reported together with that of the Cu(I) complex.[92] The effects of the pathogenic mutation A629P occurring within the sixth Cu binding soluble domain have been addressed in terms of a structural comparison which shows an increased solvent accessibility of the protein β-sheet.[93]

3.4. Metallothionein

Metallothioneins (MTs) have been found throughout all the kingdoms and constitute a superfamily of Cys rich polypeptides with a low molecular mass (4−8 kDa).[94,95] MTs are able to chelate metal ions such as Cd(II), Zn(II), and Cu(I).[96] A number of animal MT structures with Zn(II) and/or Cd(II) ions are available and reveal that MTs are

composed of two domains (α and β), each presenting a metal−thiolate cluster. In animals, MTs are known to be involved in metal homeostasis, and some can protect cells against Cd toxicity. Similarly, information obtained by gene expression analysis and functional expression in microorganisms suggests that plant MTs may be involved in metal homeostasis[97] and Cu tolerance.[98] However, in contrast to the case for animals, direct information about the role of MT proteins from plants is scarce because of difficulties in purifying them. Difficulties in identifying and purifying plant MTs may arise from the instability of these proteins in the presence of oxygen. There is, however, a critical need for more protein data.

Several biological roles have been proposed for MT: (a) detoxification of nonessential metals such as Cd and Hg; (b) detoxification/storage of excessive essential metals such as Cu and Zn; (c) sequestration of radicals/reactive oxygen species, alkylating agents, or peroxynitrite; and (d) transfer/transport of essential heavy metals.

All of these biological roles can be explained by the chemical reactions based on the chemical nature of the mercaptide bond (sulfur−metal bond). In the case of Cu, MT is known to detoxify excessive Cu; in fact, accumulation of Cu beyond the biosynthetic capacity of MT causes acute hepatitis owing to the production of reactive oxygen species.

The 3D structures of MTs from mammalian and crustacean species that have been determined so far show a monomeric protein composed of two globular domains, each encompassing a metal−thiolate cluster. The evolutionary-distant sea urchin metallothionein isoform A (MTA) is a 64-residue metalloprotein, which contains essentially the same number of metal-chelating Cys-Cys and Cys-Xxx-Cys motifs and metal ions as the mammalian MTs. There is, however, no obvious sequence homology relationship. To gain an insight into the metal organization in this protein, DNA for sea urchin MTA was cloned, the protein was expressed, and its structure was determined by NMR.[99] The 3D structure of Cd_7-MTA reveals two globular domains, each encompassing a metal−thiolate cluster (i.e. a Cd_4Cys_{11} cluster in the amino-terminal domain and a Cd_3Cys_9 cluster in the carboxy-terminal domain).[96]

Whereas a number of mammalian MT structures with Zn(II) and/or Cd(II) ions are available, such information has been lacking for Cu(I) MTs until recently. The only exception has been a structural model for Cu_7-MT from yeast, determined by NMR and containing a single $Cu_7(Cys)_8$ cluster, as obtained by using ^{107}Ag as a probe.[100] Because Ag(I) and Cu(I) have different coordination properties, however, the determined structural features of the Ag(I) cluster do not necessarily apply to the Cu(I) cluster.

This question has been addressed in the NMR reinvestigation of Cu_7-MT from yeast.[101] In this work, a highly refined structure of the polypeptide chain was determined and the seven Cu(I) ions were fitted into the protein cleft formed by a spatial arrangement of the CysS ligands. The calculations suggested a variety of possible Cu(I) cluster structures fully compatible with the determined geometrical constraints of the protein.

The crystal structure of yeast copper thionein (Cu-MT), determined at 1.44 Å resolution, has been recently reported.[102] The Cu-MT structure shows the largest known oligonuclear Cu(I) thiolate cluster in biology, consisting of six trigonally and two digonally coordinated Cu(I) ions. This is at variance with the results from previous spectroscopic determinations, which were performed on MT samples containing seven rather than eight metal ions. The protein backbone has a random coil structure with the loops enfolding the copper cluster, which is located in a cleft where it is bound to 10 cysteine residues. The protein structure is somewhat different from that of Ag_7-MT and similar, but not identical, to that of Cu_7-MT. Besides the different structure of the metal cluster, the main differences lie in the cysteine topology and in the conformation of some portions of the backbone. The present structure suggests that Cu-MT, in addition to its role as a safe depository for copper ions in the cell, may play an active role in the delivery of copper to metal-free chaperones.

3.5. Copper Chaperones

Copper chaperones were first isolated in the baker's yeast *Saccharomyces cerevisiae*,[103,104] and functional homologues have been noted in humans,[83] sheep,[105] mice,[106] *Arabidopsis thaliana*,[107] and *Caenorhabditis elegans*.[108] The prototypical copper chaperone conducts Cu(I) in the cytoplasm and transfers this "cargo" directly to a specific partner protein.[109]

3.5.1. Atox1

A small antioxidant protein, Atx1, subsequently shown to be a copper chaperone, was discovered in studying the suppression of oxygen toxicity in yeast mutants lacking SOD.[110] Shortly after that, a homologue in humans and other mammals, Atox1 (or HAH1), was discovered.[111] Human Atox1 contains 68 amino acids. Once Cu(I) enters a cell, it binds to the copper binding site of Atox1 and is transferred to its docking partners in the secretory pathway (Figure 7).

Atox1 is the prototypical copper chaperone protein acting as a soluble cytoplasmic copper(I) receptor that can adopt either a two- or three-coordinate metal center in the active site; the unusual structure and dynamics of this protein suggested a copper exchange function with related protein domains in MNKP and WNDP.[104]

The 1.02 Å resolution X-ray structure of the Hg(II) form of Atx1 (HgAtx1) revealed the overall secondary structure, the location of the metal binding site, the detailed coordination geometry for Hg(II), and specific amino acid residues that may be important in interactions with the target protein.[112] A mechanism was suggested in which facile metal ion transfer occurs between the metal binding sites of the diffusible copper donor and membrane-tethered copper-acceptor proteins. The Atx1 structural motif represents a prototypical metal ion trafficking unit that is likely to be employed in a variety of organisms for different metal ions.

Starting from the sequences of Atx1 and the first soluble domain of the copper-transporting ATPase *Ccc*2, both from yeast, a search on the available genomes was performed using a homology criterion and a metal binding motif x′-x″-C-x‴-x⁗-C.[113] It was found that metallochaperones and their physiological partner ATPases recognize one another, via an interplay of electrostatics, hydrogen bonding, and hydrophobic interactions, in a manner that precisely orients the metal binding side chains for rapid metal transfer between otherwise tight binding sites.

Shortly after the yeast work was published, a homologue in humans and other mammals, Atox1, was discovered. Atox1 interacts with MNKP in the hepatocyte and is thus required for proper biliary excretion of excess copper as well as delivery of copper for holoceruloplasmin synthesis. Molecular modeling predicted a structure of two α-helices

overlaying a four-stranded antiparallel β-sheet with a potential metal binding site involving two conserved cysteine residues,[114] identified as copper ligands by site-directed mutagenesis.

The crystal structure of HAH1 was determined in the presence of Cu(I), Hg(II), and Cd(II).[115] The 1.8 Å resolution structure of CuHAH1 revealed a copper ion coordinated by Cys residues from two adjacent HAH1 molecules. An extended hydrogen-bonding network, unique to the complex of two HAH1 molecules, stabilizes the metal binding sites and suggests specific roles for several conserved residues. The obtained structures provided models for intermediates in metal ion transfer and suggested a detailed molecular mechanism for protein recognition and metal ion exchange between MT/HCXXC-containing domains.

Using a solid-phase-based assay completed with Biacore studies, evidence was provided that HAH1 forms homodimers in the presence of copper with an apparent affinity constant of 6 μM.[116] The copper-loaded HAH1 was shown to independently interact with each of the six individual metal binding domains of the copper-translocating MNKP.

The C-terminus of human HAH1 was produced in *Escherichia coli* and characterized in solution by NMR spectroscopy, both with and without copper(I).[117] Only minor structural rearrangements were shown upon copper(I) binding. In particular, the variation of interatomic interactions around the metal binding region is limited to a movement of Lys60 toward the metal site. The protein structures are similar to those obtained by X-ray crystallography in a variety of derivatives, with backbone RMSD values below 1 Å. In the holoprotein, Cu(I) is confirmed to be two coordinate.

3.5.2. CCS (Copper Chaperone for SOD1)

A protein termed the copper chaperone for superoxide dismutase (CCS) was designated as the factor responsible for copper incorporation into SOD1.[82] Comparison of the amino acid sequences of SOD1 and CCS revealed a striking homology between the enzyme and its putative chaperone, including residues involved in SOD1 homodimerization such that a mechanism could be hypothesized by which copper may be delivered to SOD1 by CCS through direct protein−protein interaction.

A direct interaction between CCS and SOD1 in vitro and in vivo was soon reported and proved to be mediated via the homologous domains in each protein.[118] Importantly, CCS was shown to interact not only with wild-type SOD1 but also with SOD1 containing the common missense mutations resulting in familial amyotrophic lateral sclerosis (vide infra).

The 1.8 Å resolution structure of the yeast copper chaperone for superoxide dismutase (yCCS) revealed a protein composed of two domains: (i) the N-terminal domain very similar to the metallochaperone Atx1 and, hence, likely to play a role in copper delivery and/or uptake and (ii) a second domain resembling SOD1 in overall fold but lacking all of the structural elements involved in catalysis.[119] In the crystal, two SOD1-like domains were interacting to form a dimer with a subunit interface remarkably similar to that in SOD1, suggesting a structural basis for target recognition by this metallochaperone.

The three-dimensional structure of CCS was homology modeled using the periplasmic protein from the bacterial mercury-detoxification system and the structure of one subunit of the human SOD dimeric enzyme as templates.[120] On the basis of the three-dimensional model, a mechanism for the transfer of copper from CCS to SOD was proposed accounting for electrostatic acceptor recognition, copper storage, and copper-transfer properties.

The X-ray structure of the largest domain of human CCS (hCCS domain II), solved at 2.75 Å resolution, was again ratifying an overall structure closely related to that of SOD1, consisting of an eight-stranded β-barrel and a zinc binding site formed by two extended loops.[121] The first of these loops provided the ligands to a bound zinc ion, analogous to the zinc subloop in SOD1. The second structurally resembles the SOD1 electrostatic channel loop but lacks many of the residues important for catalysis. Like SOD1 and yCCS, hCCS forms a dimer using a highly conserved interface. In contrast to SOD1, however, the hCCS structure does not contain a copper ion bound in the catalytic site. Notably, the structure reveals a single loop proximal to the dimer interface which is unique to the CCS chaperones.

To clarify whether the oligomerization state during copper transfer was determined by either a heterodimer comprising one monomer of CCS and one monomer of SOD1 or a dimer of dimers involving interactions between the two homodimers, the protein−protein complex formation was investigated by gel filtration chromatography, dynamic light scattering, analytical ultracentrifugation, and chemical cross-linking experiments.[122] yCCS and a H48F mutant SOD1 formed a complex with the correct molecular mass for a heterodimer and no higher order oligomers were detected, thus suggesting that in vivo copper loading of yeast SOD1 occurs via a heterodimeric intermediate.

hCCS was shown to activate either human or yeast enzymes in vitro by direct protein to protein transfer of the copper cofactor.[123] A limiting stoichiometry of one copper and one zinc per hCCS monomer was determined, and the protein, unlike yCCS, was found to be a homodimer regardless of copper occupancy.

Disulfide formation in SOD1 by O_2 was shown to be greatly accelerated by the Cu-bound form of CCS in vivo and in vitro even in the presence of excess reductants during the stepwise conversion of the immature form of the enzyme to the active state.[124] The immature form of SOD1 was found to be most susceptible to oxidative insult and to aggregation reminiscent of that observed in amyotrophic lateral sclerosis. Thus, Cu−CCS mediation of correct disulfide formation in SOD1 was suggested to be important for regulation of enzyme activity and for prevention of misfolding or aggregation.

In the same way, activity assays with pure proteins and cell extracts revealed that O_2 (or superoxide) is required for activation of SOD1 by CCS.[125] Such CCS function provides oxidant-responsive post-translational regulation of SOD1 activity and may be relevant to a wide array of physiological stresses that involve a sudden elevation of oxygen availability.

3.5.3. Cox17

The third classical copper chaperone, Cox17, was also discovered first in yeast as a small 8 kDa protein required for cytochrome *c* oxidase (CCO) functioning.[126] Cox17 is found both in the cytoplasm and in the mitochondrial intermembrane space. It delivers copper to other CCO assembly proteins. In humans, two related proteins, Sco1 and Sco2, are necessary for the transfer of copper to CCO subunit II.[127]

The Cox17 protein binds Cu(I) through cysteine side chains but exhibits some important differences from other Cu-trafficking proteins. In some forms of the isolated protein, Cu was first suggested to be trigonally coordinated, either in a single hexanuclear cluster or in two trinuclear Cu(I) clusters, in a manner more similar to that of the metallothioneins and Cu(I) transcription factors than to those of the other Cu chaperones.[128] However, later determined 3D structures of yeast apo- and Cu-loaded Cox17[129] were revealing for a two-coordinated Cu(I) ion with ligation to conserved Cys23 and Cys26 residues, a site reminiscent of those observed for the Atx1 family chaperones. Evaluation of this coordination site and the specific role of the Cox17 protein is ongoing, but recent studies suggest that Cox17 is not necessarily involved in conducting Cu to the mitochondria. Rather, it plays a key role, along with other proteins such as Sco1, in the assembly of the active cytochrome *c* oxidase (CCO) in the intermembrane space of the mitochondria. Folding studies by NMR of oxidized apo-Cox17 demonstrated the possible formation of one conformer stabilized by two disulfide linkages that was binding a single Cu(I) ion in digonal coordination, as well as of one additional conformer capable of binding up to four Cu(I) ions in a polynuclear cluster.[130] Both conformers were suggested to possibly act as Cu(I) donors to Sco1 and Cox11.[130] The crystal structure of human apo-Sco1, determined at 2.8 Å resolution,[131] disclosed a strict similarity to other redox active proteins, such as thioredoxins. The obtained structure, together with the fact that one fatal missense mutation in SCO1 lies in a region away from the Cu binding site, led to the suggestion that SCO proteins act as redox signaling molecules rather than as copper chaperones. The coordination chemistry of yeast Cox11 involves a dinuclear cluster of two Cu(I) ions bound by three cysteines each that may be a cometallochaperone for the Cu_B site in CCO.[132,133] Cox17 was shown to be a specific copper donor to both Sco1 and Cox11, by using in vitro studies with purified proteins that revealed Cox17 to represent a novel copper chaperone that delivers copper to two proteins.[134]

4. Alzheimer's Disease (AD)

4.1. Introduction

Alzheimer's disease is the most common neurodegenerative disease, directly affecting ~10% of humans by age 65 and ~50% by age 85.[135] AD, first discovered in 1907,[136] is an irreversible and progressive disease that results in memory loss, unusual behavior, personality changes, and a decline in thinking ability. AD is accompanied by three main structural changes in the brain:[137,138] (i) diffuse loss of neurons; (ii) intracellular protein deposits (the neurofibrillary tangles, NFT) consisting of phosphorylated tau protein; and (iii) extracellular protein deposits (amyloid (Aβ) or senile plaques) surrounded by dystrophic neurites.

Based on these neuropathological markers, two major hypotheses were initially proposed.

(i) According to the *amyloid cascade hypothesis*, neurodegeneration in AD begins with the abnormal processing of the amyloid precursor protein (APP) and results in the production, aggregation, and deposition of the Aβ peptide.[139] Apparently, the amyloid cascade may facilitate NFT formation and cell death.

(ii) According to the *neuronal cytoskeletal degeneration hypothesis*, cytoskeletal changes are the main events that lead to neurodegeneration in AD, as the hyperphosphorylation and aggregation of tau are related to the activation of cell death processes.[140]

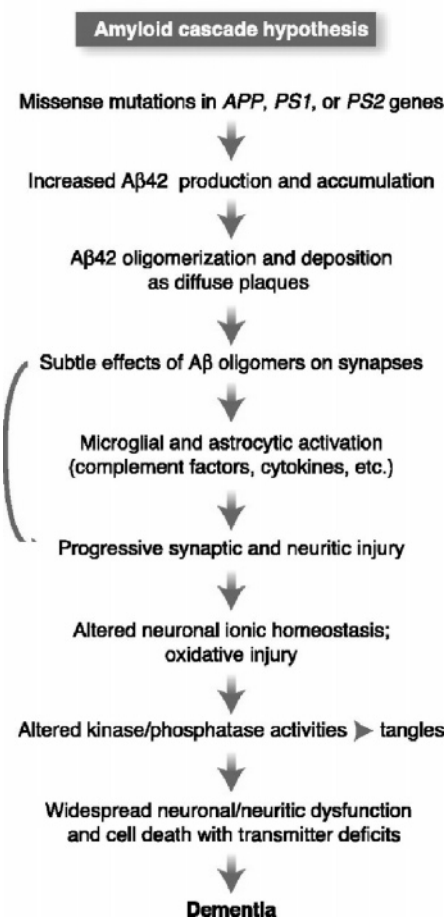

Figure 9. Sequence of pathogenic events leading to AD proposed by the amyloid cascade hypothesis. The curved arrow indicates that Aβ oligomers may directly injure the synapses and neurites of brain neurons, in addition to activating microglia and astrocytes. Reprinted with permission from *Science* (http://www.aaas.org), ref 139. Copyright 2002 AAAS.

The "amyloid cascade" hypothesis has received considerable support from genetic studies. In fact, AD, predominantly a disease of old age, may also be an inherited disorder of midlife (familial AD or FAD), with implication of the following genes: (a) the amyloid precursor protein (APP) gene,[141] which encodes the Aβ peptide, and (b) the presenilin protein genes (PS1 and PS2), which encode transmembrane proteins.[142,143]

The genetic framework for the amyloid cascade hypothesis is summarized in Figure 9.[139] While the study of FAD individuals has proved to be significant in the understanding of the onset of the disease in its familial form (~1% of AD cases), the onset as well as the reasons for the selective neuronal vulnerability of AD sporadic cases remains unclear. Synaptic abnormalities may represent the proximate cause of dementia in AD, and a novel hypothesis suggests that AD is a synaptic failure.[144,145] Synapse loss, in fact, provides a better correlate of the pattern and severity of cognitive impairment than amyloid plaques or neurofibrillary tangles.[146] Interestingly, this new hypothesis can be fixed in the amyloid cascade hypothesis, where Aβ deposition into early soluble oligomers can perform synaptotoxic effects in vitro and in vivo and hence major changes in intracellular signaling pathways that mediate Aβ-induced neurotoxicity.[147]

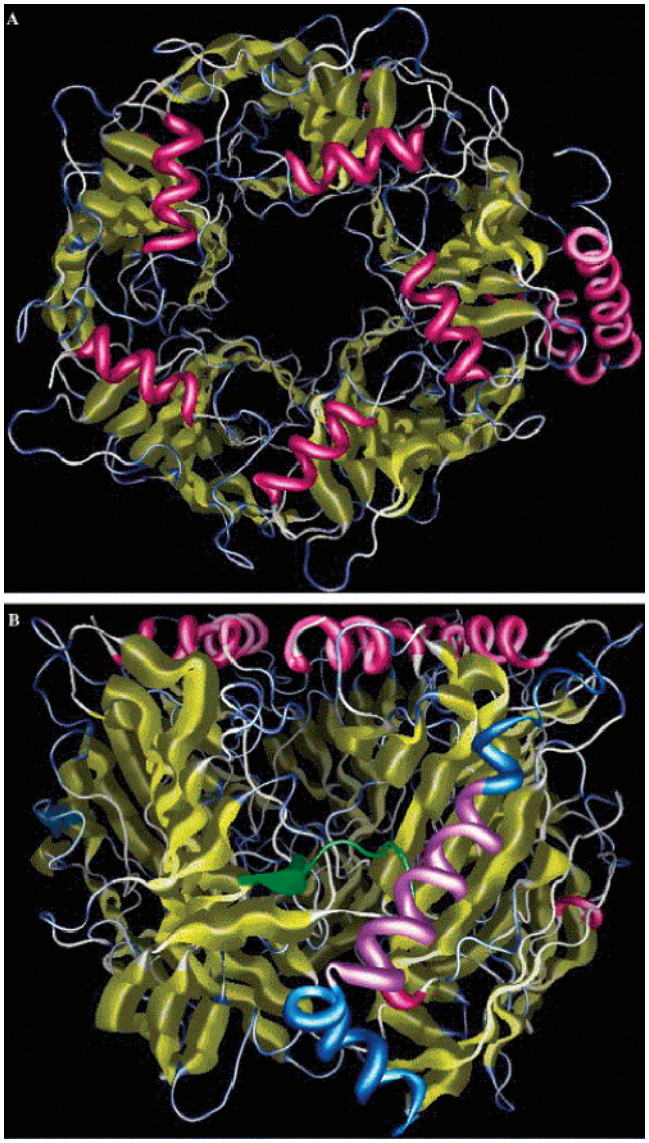

Figure 10. Base docking model of the α7nAChR−Aβ1−42 complex. In each subunit, α-helices are pink and β-sheets are yellow. (A) Top view of the complex, showing that the Aβ1−42 does bind parallel to the receptor. (B) Front view of the complex; here it is observed that the fragment V12−K28 (purple) interacts with loop C of the α7nAChR (green). The rest of the Aβ1−42 is blue. Reprinted with permission from ref 154. Copyright 2004 Elsevier.

It has long been known that acetylcholine metabolism is diminished during the AD pathology, which gave rise to the "cholinergic hypothesis" for AD etiology, stating that a dysfunction of acetylcholine-containing neurons in the brain contributes substantially to the cognitive decline observed in elderly people and AD patients.[148] One of the several proteins associated with amyloid plaque deposits is acetylcholinesterase (AChE), an enzyme that in AD brains is associated predominantly with the amyloid core of mature senile plaques. AChE is also incorporated into amyloid aggregates in vitro by forming macromolecular complexes with the growing Aβ fibrils.[149] AChE interacts with Aβ via a hydrophobic environment close to the peripheral anionic binding site of the enzyme and, thus, promotes amyloid fibril formation.[150,151]

Support for the cholinergic hypothesis has been provided by investigations of the interaction between Aβ and nicotinic acetylcholine receptors (nAChRs) that contain the α7 subunit (α7 nAChRs), since such complexes might be a key factor in the formation of AD plaques and degeneration of the cholinergic neurons.[152] Many studies have demonstrated that Aβ binds selectively and with high affinity to α7 nAChRs.[153] α7 nAChR is a pentameric channel which gates the selective flow of Ca^{2+} and Na^{+} ions and is highly expressed in basal forebrain cholinergic neurons that project to the hippocampus and cortex. Within these cholinergic neurons, α7 nAChR modulates calcium homeostasis and the release of acetylcholine from synaptic terminals.

A functional model of the α7 nAChR has been recently built, and subsequently the α7 nAChR−Aβ complex has been generated for the first time through an automated docking algorithm.[154] The final complex showed that the most important interactions occur between the residues Val12-Lys28 from the Aβ peptide and loop C of the receptor (Figure 10).

4.2. Amyloid Precursor Protein (APP)

APP is a family of glycosylated transmembrane proteins which are ubiquitously expressed, but most abundantly in the brain. The APP gene maps to chromosome 21 in humans[155,156] and constitutes a family of different isoforms, which are named according to their length in amino acids. The full-length APP is schematized in Figure 11,[157] which

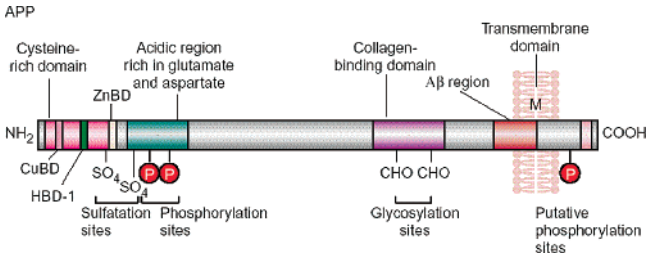

Figure 11. Schematic representation of APP. Reprinted with permission from ref 157. Copyright 2002 Elsevier.

highlights the toxic Aβ region (red box) and the copper (CuBD), zinc (ZnBD), heparin (HBD-1), and collagen binding domains.[158] APP695 is the most abundant APP transcript in the brain.[159] In addition to the APP isoforms derived from transcripts of chromosome 21, there are also two other variants that are C-terminally truncated and lack the β-amyloid fragment (amyloid precursor-like proteins, APLP1 and APLP2), which map to chromosome 19 in humans. APP can be localized to many membranous structures in the cell such as the endoplasmic reticulum and Golgi compartments, as well as to the cell membrane.

The cloning and characterization of APP revealed that it possessed many features reminiscent of a membrane-anchored receptor molecule. Among the many putative functions ascribed to APP,[160,161] a relevant role in modulating copper (and iron) homeostasis has been suggested on the basis that *App* knockout mice have elevated Cu levels in brain and liver.[162] Conversely, overexpression of the C-terminal fragment of APP, which contains Aβ, results in significantly reduced Cu and Fe levels in transgenic (C100) mouse brain;[163] APP, in the same way as the prion protein (vide infra), may be involved in the copper transport from the extracellular to the intracellular space,[164−166] similar to the copper incorporation system that operates in yeast.

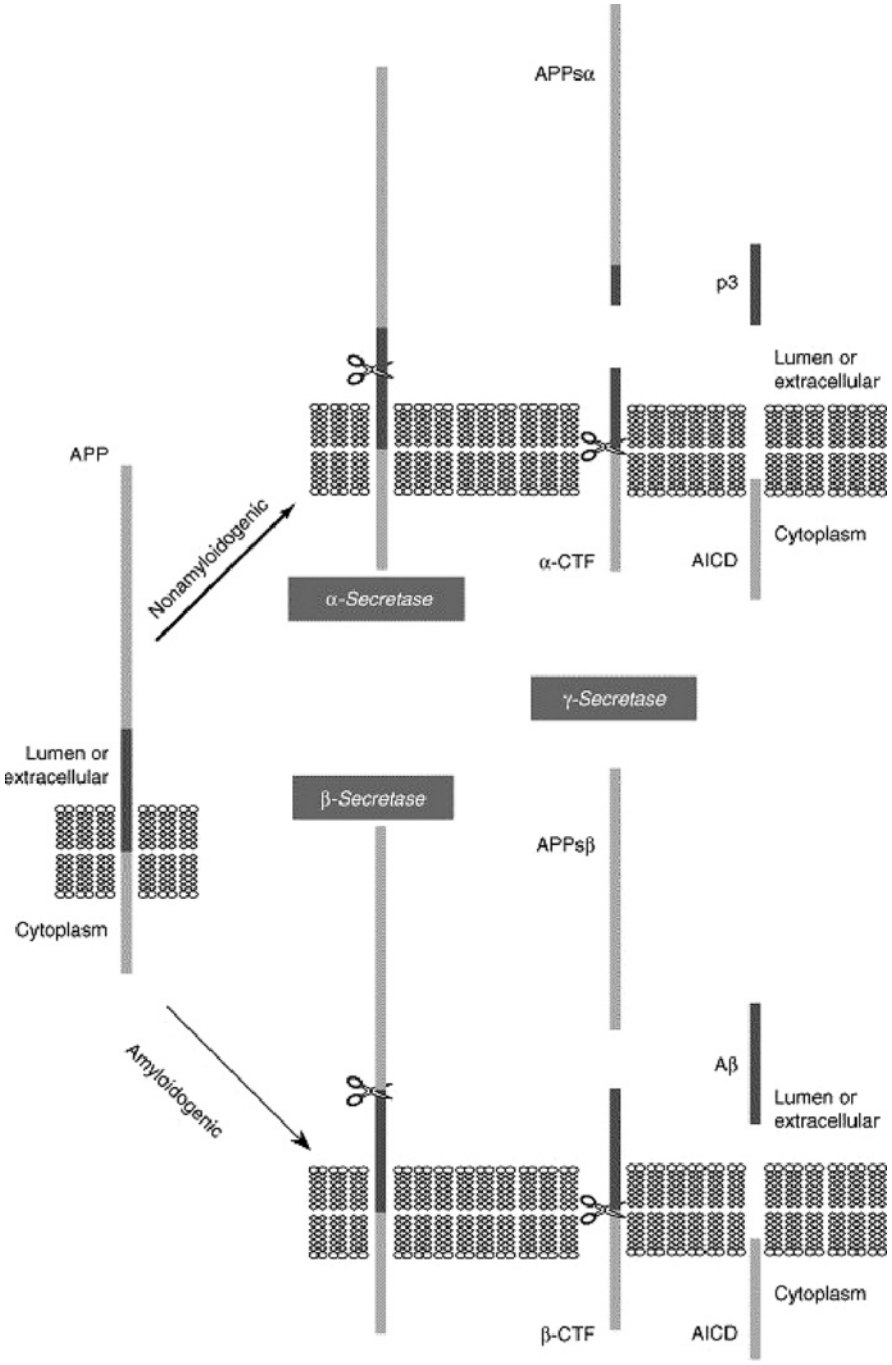

Figure 12. Proteolytic processing of amyloid precursor protein (APP) by the secretases. The majority of APP is processed in the nonamyloidogenic pathway (thick arrow); APP is first cleaved by α-secretase within the amyloid-β peptide (Aβ) domain (darker shaded region), leading to APPsα secretion and precluding Aβ generation. Membrane-anchored α-carboxy terminal fragment (CTF) is then cleaved by γ-secretase within the membrane, releasing the p3 peptide and APP intracellular domain (AICD). Alternatively, amyloidogenesis (thin arrow) takes place when APP is first cleaved by β-secretase, producing APPsβ. Aβ and AICD are generated upon cleavage by γ-secretase of the β-CTF fragment retained in the membrane. Scissors indicate the cleavage sites of α-, β-, and γ-secretase. Reprinted with permission from ref 169. Copyright 2004 Elsevier.

4.3. APP Processing: The Secretases

Aβ is generated intracellularly by the proteolytic processing of APP by two proteases known as β- and γ-secretase.[159] A third secretase, α-secretase, cleaves the Aβ sequence itself and is therefore usually considered as nonamyloidogenic (Figure 12). Another view of cleavage sites and membrane spanning of APP is given in Figure 13.[158]

α-Secretase (a member of the ADAM family of metalloproteases) and β-secretase (a membrane-bound aspartyl protease also called BACE) cleave the ectodomain of APP, resulting in the shedding of APPsα and APPsβ. γ-Secretase finally cleaves the transmembrane domain of the APP carboxy terminal fragments, releasing the p3 and the Aβ peptide, respectively, into the extracellular milieu and the APP intracellular domain into the cytoplasm. The strongest evidence that abnormal proteolytic processing and increased Aβ generation are central to the disease process comes from studies of very rare inherited forms of AD.[167] Missense mutations in APP and in the presenilins, the core proteins of the γ-secretase complex, all affect Aβ generation, ag-

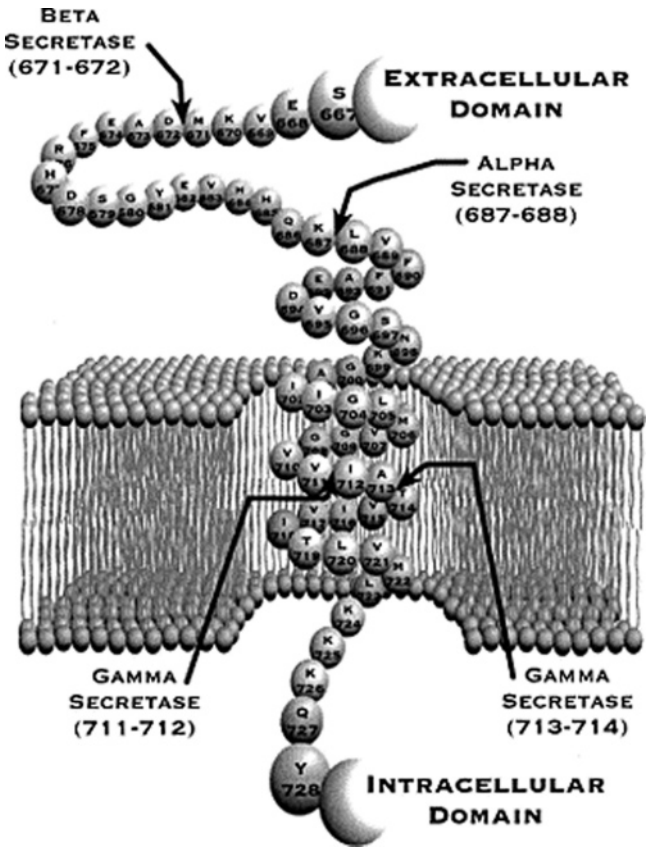

Figure 13. Schematic view of the membrane spanning and cleavage sites of APP_{770}. The $A\beta_{40}$ fragment, generated by β- and γ-cleavage, comprises residues 672−711 of APP_{770} while the $A\beta_{42}$ fragment spans residues 672−713. The p3 fragment, generated by α- and γ-cleavage, spans residues 688−711 and 713. The helical region of the transmembrane domain extends past the α-cleavage site and is important in secretase recognition. Reprinted with permission from ref 158. Copyright 2003 Elsevier.

gregation, or degradation.[168] Moreover, all mutations identified in APP are clustered around the three secretase cleavage sites (Figure 14).[169]

Gene mutations alter the normal processing of APP with production of more amyloidogenic species.[170] Currently, the nature of the neurotoxic Aβ species is very difficult to define, because monomers, soluble oligomers, insoluble oligomers, and insoluble amyloid fibrils are expected to accumulate and exist in dynamic equilibrium in the brain. The toxicity of Aβ and other amyloidogenic proteins has been recently related to soluble oligomeric intermediates rather than to insoluble fibrils.[139] These soluble oligomers (Aβ-derived diffusible ligands or ADDLs)[171] include spherical particles of 2.7 to 4.2 nm in diameter and curvilinear structures called "protofibrils",[172] and they represent protein micelles. Since Aβ is an amphipathic surface-active peptide, oligomer formation displays a critical concentration dependence and is correlated with the appearance of a hydrophobic environment.[173] By producing antibodies that specifically recognize micellar Aβ and not soluble, low-molecular-weight Aβ or Aβ fibrils, it was shown that all soluble oligomers display a common structure that is unique to soluble oligomers regardless of sequence.[174] Soluble oligomers were shown to have a unique distribution in human AD brain that is distinct from that of fibrillar amyloid.

4.4. Amyloid Peptides

The main alloforms of Aβ found in amyloid deposits are 40 and 42 amino acids long. The sequence of human Aβ42 is as follows:

```
          10        20        30        40
DAEFRHDSGYEVHHQKLVFFAEDVGSNKGAIIGLMVGGVVIA
```

Despite the small structural difference between Aβ40 and Aβ42, they display distinct clinical, biological, and biophysical behavior. The concentration of secreted Aβ42 is ~10% that of Aβ40, yet the longer form is the predominant component in parenchymal plaques.[175] An increase in the Aβ42/Aβ40 concentration ratio is associated with familial forms of early onset AD,[176] and treatments that reduce Aβ42 levels have been shown to correlate with decreased risk for progression of AD.[177] In addition, Aβ42 displays enhanced neurotoxicity relative to Aβ40.[178] Studies of the kinetics of Aβ fibril formation have shown that Aβ42 forms fibrils significantly faster than Aβ40,[179] leading to the statement "Aβ42 is more amyloidogenic than Aβ40". A combination of biochemical, spectroscopic, and morphologic methods was used to study the initial oligomerization and assembly of Aβ40 and Aβ42 (Figure 15);[180] monomers rapidly oligomerize into paranuclei, that can then oligomerize to form larger, beaded structures. Paranuclei are the initial, and minimal, structural units from which Aβ42 assemblies evolve. The equilibrium between monomer and paranucleus is rapid, while the conversion to protofibrils is slower but is also reversible. Protofibrils may form through a "linear" pathway involving (a) oligomerization of monomers into paranuclei, (b) paranucleus self-association to form larger oligomers, and then (c) maturation of these large oligomers into protofibrils. However, direct addition of monomers or paranuclei to protofibrils or fibrils may occur as well. The final step in the overall pathway is protofibril maturation into fibrils, a process that appears irreversible, at least kinetically. The data showed that Aβ40 and Aβ42 have distinct behaviors at the earliest stage of assembly, monomer oligomerization, which may explain the particularly strong association of Aβ42 with AD and suggest approaches for appropriate targeting of therapeutic agents for AD.

NMR structural studies showed that Aβ40 is mostly unstructured in aqueous solution[181,182] and that it adopts a helix−turn−helix structure upon addition of trifluoroethanol or sodium dodecyl sulfate (SDS).[183] Solid-state NMR structural data, obtained from Aβ40 in the fibrillized state, showed a loop similar to that observed in SDS solution-state structure.[184] In the solid-state structure, the only charged side chains in the core are those of Asp23 and Lys28, which form a salt bridge. The C-terminus of the peptide folds back onto the hydrophobic core, so that the hydrophobic core and the aliphatic side chains of the C-terminus come in close contact.

NMR and CD have recently been used to show that Aβ40 undergoes chemical exchange between a monomeric, soluble state and an oligomeric, aggregated state under physiological conditions.[185] The intermediate was assigned an α-helical structure by CD. The oligomer was assigned a MW > 100 kDa by solution-state DOSY-NMR. Saturation transfer difference NMR experiments demonstrated that the oligomer was related to monomeric Aβ and assisted the identification of the hydrophobic core (residues 15−24) as mainly involved in interactions between mono- and oligomeric Aβ molecules.

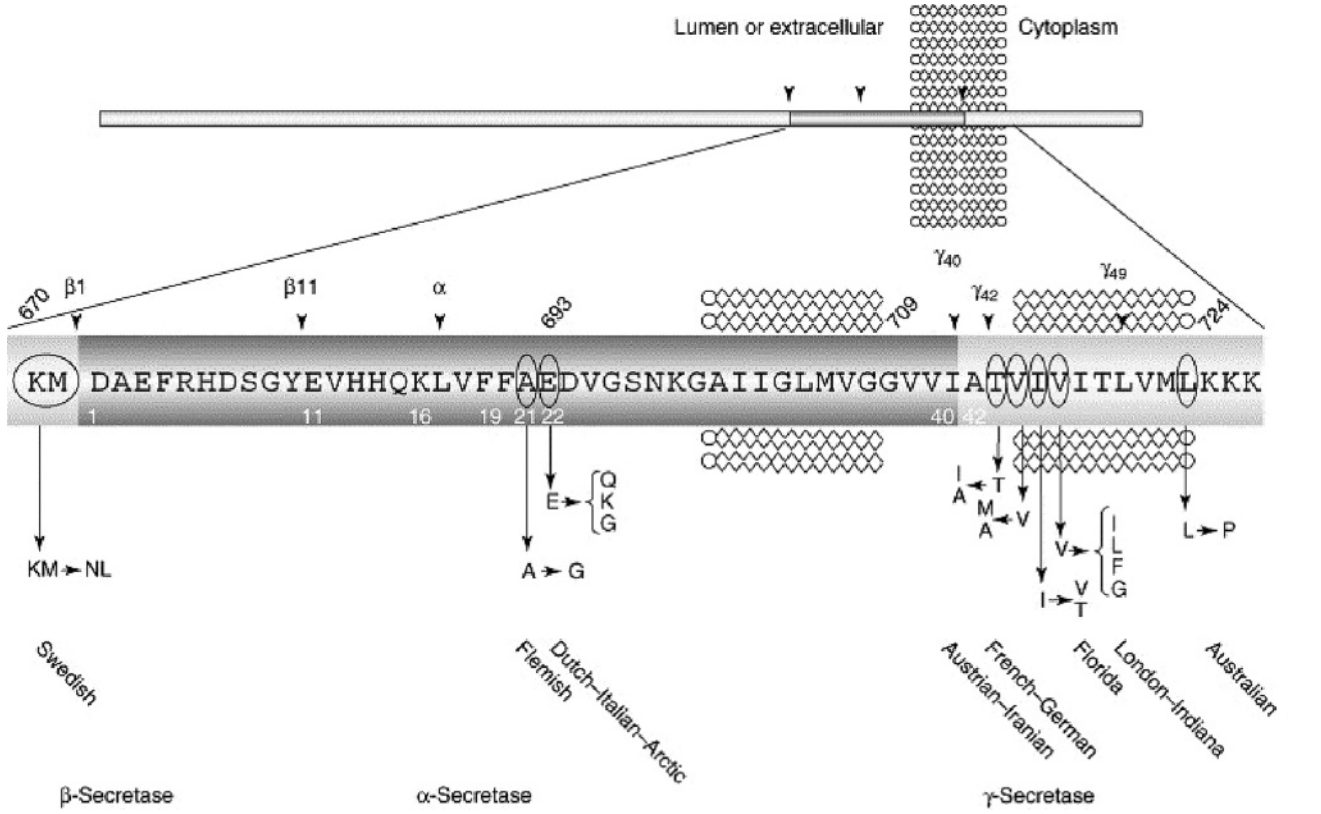

Figure 14. The mutations causing familial Alzheimer's disease (AD) in amyloid precursor protein (APP) surround the cleavage sites of the three secretases. The amino acid sequence of the region encompassing amyloid-β peptide (Aβ) is given; amino acids mutated in familial AD are circled, and the corresponding amino acid changes (KM → NL: KM mutated in NL) are indicated. The country from where the families originate is also mentioned in the schematic (this is sometimes used in the literature as an alternative name for the mutations). Amino acid numbering of APP is written in black, and that of Aβ in white. Arrowheads indicate the cleavage sites of α-, β-, and γ-secretase. Reprinted with permission from ref 169. Copyright 2004 Elsevier.

Variation of the anionic strength in the buffer was inducing a shift of equilibrium between mono- and oligomeric states, thus possibly allowing for the stabilization of intermediate structures.

H/D exchange monitored by NMR facilitates the identification of backbone amide protons involved in the protective secondary structure within globular proteins at single-residue resolution,[186] and it has been applied to amyloid fibrils synthesized from β-2 microglobulin, transthyretin, and fragments of the Aβ peptide (residues 25−35) and prion protein.[187−190] The same technique has recently been applied to the analysis of amyloid fibrils of full-length Aβ40 to reveal the residues involved in a highly protective hydrogen-bonded structure.[191] Kinetics exchange showed that about half the backbone amide protons exchange during the first 25 h, while the other half remain unexchanged because of solvent inaccessibility and/or hydrogen-bonded structure. Successive heteronuclear $^{1}H-^{15}N$ HSQC spectra, collected by fibrils of ^{15}N enriched Aβ, identified the backbone amides not exchanging in the fibril. The N and C-termini of the peptide were seen to be accessible to the solvent in the fibril state such that backbone amides of these residues were readily exchanging with bulk deuterium. In contrast, the residues in the middle of the peptide (residues 16−36) were mostly protected, suggesting that many of the residues in this segment of the peptide are involved in a β structure in the fibril. Two residues, Gly25 and Ser26, exhibit readily exchangeable backbone amide protons and therefore may be located on a turn or a flexible part of the peptide. The data substantially supported current models for how the Aβ peptide folds when it engages in the amyloid fibril structure.

Nanoelectrospray mass spectrometry and ion mobility spectrometry have recently been used to investigate conformational differences in monomers and small oligomers and the energetics and mechanisms of initial oligomerization reactions in Aβ42 and its [Pro19]Aβ42 alloform.[192] The Phe19 → Pro19 substitution was found to block fibril formation, and solution-like structures of Aβ monomers could be electrosprayed and characterized. Unfiltered solutions of Aβ42 produced only monomers and large oligomers, whereas [Pro19]Aβ42 solutions produced abundant monomers, dimers, trimers, and tetramers but no large oligomers. When passed through a 10 000 amu filter and immediately sampled, Aβ42 solutions produced monomers, dimers, tetramers, hexamers, and an aggregate of two hexamers that may be the first step in protofibril formation. The results were consistent with photochemical cross-linking data that supported an aggregation mechanism, where specific regions and residues control Aβ oligomerization and the controlling elements differ between Aβ40 and Aβ42.[193]

The initial step in the pathway of aggregation of the Aβ protein has been studied through the simulation of the structure and stability of the $A\beta_{10-35}$ dimer in aqueous solution.[194] A protocol based on shape complementarity was used to generate an assortment of possible dimer structures. The generated structures were evaluated using rapidly computed estimates of the desolvation and electrostatic interaction energies to identify a putative stable dimer structure. The potential of mean force associated with the dimerization of the peptides in aqueous solution was computed for both the hydrophobic and the electrostatic driving forces using umbrella sampling and classical mo-

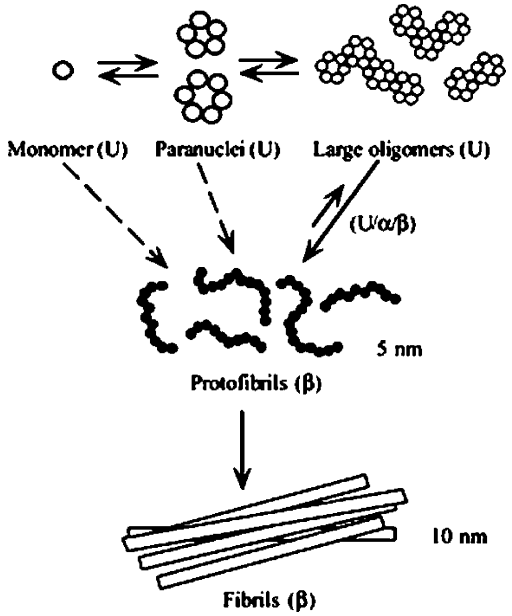

Figure 15. Simple model of Aβ42 assembly. Monomers, paranuclei, and large oligomers are predominately unstructured (U) but do contain β-sheet/β-turn (β) and helical (α) elements. Protofibril formation involves substantial conformational rearrangements, during which unstructured, α-helix, and β-strand elements (U/α/β) transform into predominately β-sheet/β-turn structures. Dotted arrows indicate the direct addition of monomers or paranuclei to protofibrils or fibrils. The diameters of the protofibrils and fibrils are indicated, but the structures in the scheme are not drawn to scale. Reprinted with permission from ref 180. Copyright 2003 National Academy of Sciences, U.S.A.

lecular dynamics simulation at constant temperature and pressure with explicit solvent and periodic boundary conditions. The comparison of the two free energy profiles suggested that the structure of the peptide dimer is determined by the favorable desolvation of the hydrophobic residues at the interface. Molecular dynamics trajectories originating from two putative dimer structures indicated that hydrophobic interactions were primarily stabilizing the peptide dimer and that the conformations of the peptide monomers were undergoing substantial structural reorganization in the dimerization process. The finding that the φ-dimer (Figure 16)[194] may constitute the ensemble of a stable Aβ_{10-35} dimer has important implications for fibril formation. In particular, the expulsion of water molecules at the interface might be a key event, just as in the oligomerization of Aβ_{16-22} fragments. It was conjectured that events prior to the nucleation process themselves might involve crossing free energy barriers which depend on the peptide−peptide and peptide−water interactions. Consistent with existing experimental studies, the peptides within the ensemble of aggregated states show no signs of the formation of a secondary structure.

4.5. Role of Oxidative Stress in AD

Various types of oxidative damage have been noted in AD, including glycation, protein oxidation, lipid peroxidation, and nucleic acid oxidation.[195]

Oxidative stress from excessive free radical generation may also be the main cause of the neuronal cell loss in AD.[30,196] The potential for oxidative damage from reactive oxygen intermediates in the aging brain is further enhanced by the high oxygen consumption and relatively low antioxidant

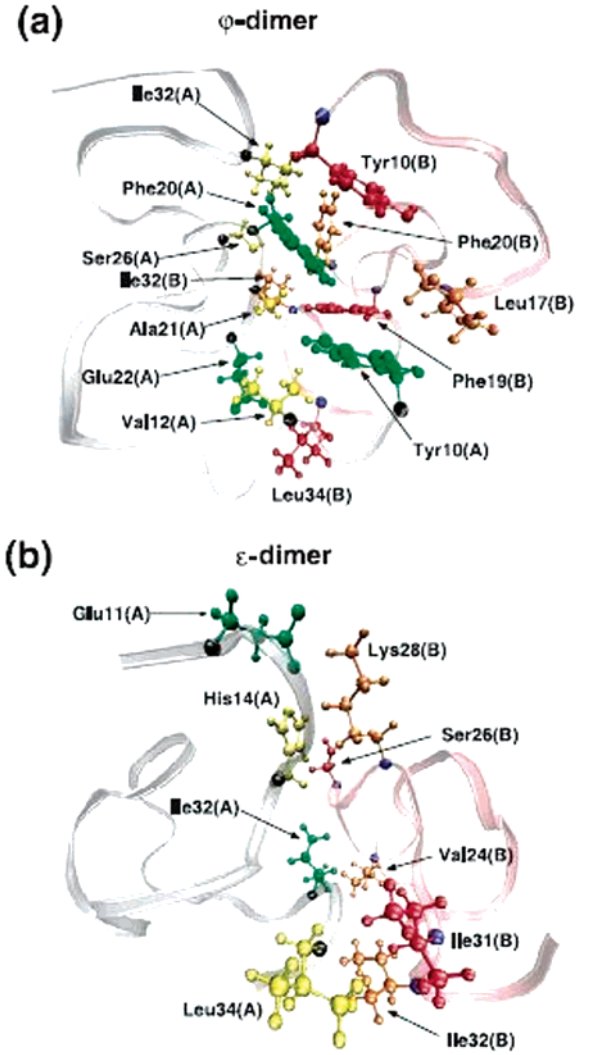

Figure 16. Putative dimer structures of Aβ_{10-35} derived by minimization of the desolvation energy function (a) and of the electrostatic interaction energy (b). The side chains at the dimer interface are depicted explicitly. Reprinted with permission from ref 194. Copyright 2005 Elsevier.

levels in brain tissue. Oxidative stress is a direct or mediated consequence of metal-catalyzed production of reactive oxygen species. The damage associated with redox-active heavy metal activity and potential disease mechanisms that might be targeted for therapy have been recently reviewed.[197]

An Aβ42-centered model for neurodegeneration in the AD brain based on the oxidative stress associated with Aβ42 has been developed,[198] suggesting that the amyloid peptide induces and antioxidants inhibit protein oxidation, lipid peroxidation, ROS production, and many other markers of oxidative stress. Consistent with this model, a proteomics approach has been applied to Alzheimer's disease. Differences in protein expression and post-translational modification (mostly oxidative modification) of proteins from AD brain and peripheral tissue, as well as in brain from rodent models of AD, have been observed.[199]

The increased oxidative modification of macromolecules likely results from increased intracellular production of membrane permeable H_2O_2 by abnormal mitochondria or increased extraneuronal production of H_2O_2 from activated microglia. Reaction of H_2O_2 with reduced metal ions via Fenton and Haber−Weiss chemistry leads to the generation of the hydroxyl radical ($^{\bullet}$OH) that induces many oxidative

modifications in macromolecules (e.g., 8-hydroxyguanosine, carbonyls). Since the •OH, reacting in the microsecond time span, cannot diffuse beyond nanometer distances, sites of nucleic acid and protein modification are indicative of the site of •OH generation and therefore the sites of Cu and Fe binding. The •OH-mediated oxidative modifications associated with AD neuronal cytoplasm and lesions are consistent with the chronic dysregulation of metal ion binding in the cytoplasm of pyramidal neurons and lesions of the AD brain. Dysregulation of transition metal metabolism and their extra- and intracellular accumulation in the AD brain have been repeatedly demonstrated and reviewed.[200]

Increases in metal ion accumulation and oxidative stress in the AD brain are associated with changes in the concentration of soluble and deposited Aβ. A number of stress conditions upregulate APP expression and Aβ generation. One common end point leading to this change in the expression and processing of APP and Aβ deposition is the shortage of energy supply, related oxidative stresses, and apoptosis. Not only does an energy shortage promote APP expression, but it also routes the metabolism of APP from the nonamyloidogenic to the amyloidogenic pathway. Inhibition of mitochondrial energy metabolism alters the processing of APP to generate amyloidogenic derivatives,[201] while oxidative stresses (H_2O_2 and UV) have been shown to increase the generation of Aβ peptides in neuroblastoma cells, as a consequence of increased generation of Aβ from APP.[202]

It is therefore evident that Aβ synthesis is modulated by stress conditions, perhaps as a result of altered metal ion metabolism. In support of this hypothesis, the amyloid plaque load in the cortex has been shown to be inversely correlated with oxidative stress.[203] That is, as amyloid load increases, cytoplasmic oxidative damage decreases. Thus, formation of diffuse amyloid plaques may be considered as a compensatory response that reduces oxidative stress.

An increase in Aβ generation under the oxidative experimental conditions described above may be aimed at chelating metal ions in order to prevent oxidation. It has been suggested that Aβ deposition possibly acts as a sink for trapping potentially harmful transition metal ions (particularly redox active metal ions) that can be released from metal binding proteins by oxidative and mildly acidic conditions and that would otherwise catalyze adverse oxidation of biomolecules.[204] The capture of metal ions in turn promotes the aggregation into Aβ deposits. It is not surprising that the brain, which concentrates transition metal ions,[200] has developed mechanisms to sequester metal ions to prevent their abnormal distribution under stress conditions.

4.6. Direct Involvement of Copper in AD

Besides all the evidence reported so far, several lines of evidence connect copper to both the cell biology of APP and the neurodegeneration of AD. For example, APP and Aβ are able to bind and reduce copper,[164,165,205−208] copper forms a high-affinity complex with the Aβ peptide[209] and promotes its aggregation,[204,210] and Aβ neurotoxicity depends on catalytically generated H_2O_2 by Aβ-copper complexes in vitro.[211] Moreover, copper (together with zinc and iron) is accumulated in the amyloid deposits of Alzheimer's brains,[29] which are partially disassembled by copper chelators.[212] Copper also mediates dityrosine-mediated oligomerization of Aβ in vitro and in vivo (vide infra).[213] Interestingly, both Aβ and copper are synaptically liberated in cholinergic pathways. Although Aβ-copper complexes might induce neuropathology by other mechanisms such as oxidative stress, current studies support the notion that copper-mediated aggregation of Aβ may play a role in AD.[214]

It has recently been shown that the addition of trace amounts of copper (0.12 ppm) to water given to cholesterol-fed rabbits can induce Aβ accumulation, including senile plaque-like structures in the hippocampus and temporal lobe, and can significantly retard learning ability.[215] Aβ metabolism appears, therefore, to be extraordinarily sensitive to small changes in copper concentrations that might be transduced across the blood brain barrier, as supported by the selective Cu(II) binding sites possessed by both Aβ and APP. A function for the Cu(II) binding site on Aβ is implied by the structural similarity of the coordinating residues with those of the femtomolar-affinity Cu(II) binding site on superoxide dismutase 1.[216,217] Aβ may therefore be part of a metal clearance system, which becomes corrupted in AD.[218] As a matter of fact, APP(135−156) has been shown to protect against Cu(II)-induced neurotoxic effects.[219] APP(135−156) lacking two histidine residues showed protection against Cu(II), whereas APP(135−156) mutated in cysteine 144, a key residue in the reduction of Cu(II) to Cu(I), did not protect against Cu(II) neurotoxicity.

4.6.1. APP and Copper

The APP copper binding domain (CuBD) is located in the N-terminal cysteine rich region next to the growth-factor-like domain (Figure 17).[220,221] The CuBD sequence is similar among the different APP family paralogues and orthologues, suggesting an overall conservation in its function or activity. In vivo studies show that APP expression is a key modulator of neuronal copper homeostasis since APP knockout mice have increased copper levels in the brain.[160] The APP CuBD can also modulate Cu(I)-mediated neurotoxicity[222] and, depending on the orthologue, can either promote or inhibit copper neurotoxicity.[223] The interaction between the APP−Cu(I) species and hydrogen peroxide can result in Cu(I) oxidation to Cu(II) and APP fragmentation.[224] Of importance to Alzheimer disease pathology is the finding that increasing the copper concentration modulates APP processing, resulting in greatly reduced Aβ production and increased levels of the cell-bound and secreted forms of APP.[225]

To understand the interaction of copper with the APP CuBD at the molecular level, the 3D structure of the CuBD (APP residues 124−189) was determined by NMR spectroscopy.[221] The copper binding and redox activity of the

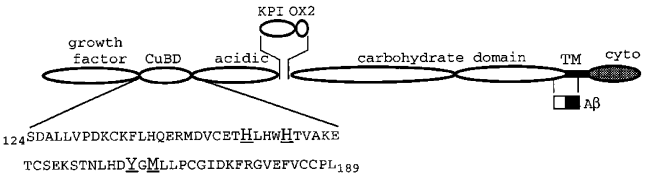

Figure 17. Schematic representation of APP showing important regions of the molecule. The N-terminal growth factor domain is followed by CuBD (together these constitute the cysteine rich region of the molecule), an acidic region, Kunitz-type protease inhibitor (KPI), OX2 domains that occur in some APP isoforms, a series of domains attached to carbohydrate, a transmembrane (TM) region, and a cytoplasmic (cyto) tail. The location of the Aβ region, a major component of Alzheimer's disease plaques, is shown. The sequence of CuBD is shown with the copper binding ligands in underlined type. Reprinted with permission from ref 221. Copyright 2003 The American Society for Biochemistry & Molecular Biology.

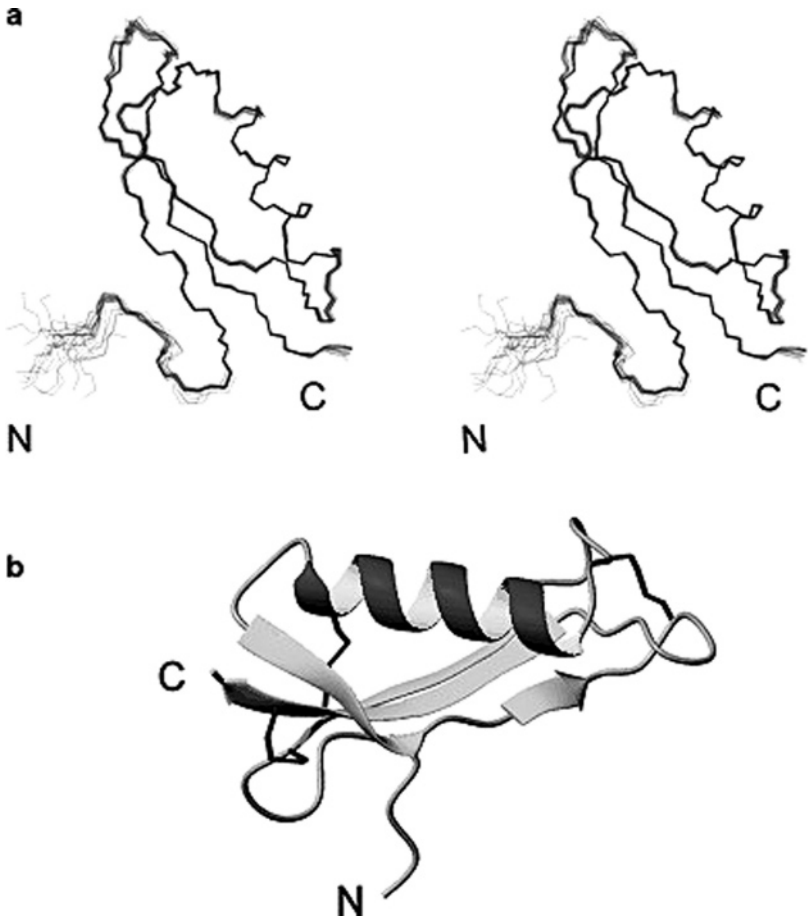

Figure 18. APP CuBD structure. (a) Stereoview of the backbone traces of the structure of CuBD as determined by NMR spectroscopy showing the 21 lowest energy structures. The structures are well ordered with only the three N-terminal residues unstructured, and they have good stereochemical properties with more than 98% of the backbone angles falling in the allowed regions of the Ramachandran plot. (b) Ribbon diagram of the structure closest to the mean. Reprinted with permission from ref 221. Copyright 2003 The American Society for Biochemistry & Molecular Biology.

recombinant CuBD were found to be very similar to those of the intact protein,[223] and the structure obtained in the absence of copper (Figure 18) was well defined and consisted of an α-helix packed against a triple-stranded β-sheet. The Cys133-Cys187 disulfide bond linked strands β1 and β3, and the other Cys158−Cys186 bond linked the α-helix to strand β3. The Cys144−Cys174 bond connected two loops at the other end of the molecule. Very few buried hydrophobic residues were found in the vicinity of this last disulfide bond, suggesting a role in stabilizing the structure in a region that does not have any secondary structure. The structure was found to be further stabilized by a small hydrophobic core (Leu-136, Trp-150, Val-153, Ala-154, Leu-165, Met-170, Val-182, and Val-185), and rigidity along the entire backbone was indicated by $\{^1H\}-^{15}N$ NOE data. The surface of CuBD was shown to be highly charged with several areas of negative (Glu-156, Glu-160, Glu-183, Asp-167, and Asp-131) and positive (Lys-132, Lys-134, Lys-161, His-147, His-151, and Lys-155) potential.

The analysis of peak broadening in the $^1H-^{15}N$ HSQC spectrum by Cu(II) suggested the presence of two binding sites, one tetrahedral one centered on His-147, His-151, Tyr-168, and Met-170 (Figure 19) and another physiologically irrelevant site involving the N-terminus.[221]

The orientation of the metal binding site indicated that subtle side-chain movements could yield a tetrahedral site suitable for coordinating Cu(I) (Figure 19) by two histidines, a methionine, and a cysteine residue in a tetrahedral arrangement.[226] The binding site in CuBD appeared novel and a search of the Protein Data Bank failed to identify a copper site with the same ligands. Only peptidylglycine monoxygenase containing a redox active Cu(II) binding site consisting of a tetrahedral arrangement of two His, one Met, and one water molecule was found,[227] but beyond this, no sequence or structural similarities could be revealed.

Inferences on the redox chemistry associated with the Cu−APP interactions were made based on the tetrahedral arrangement of Cu(II) ligands. It is in fact known that (i) four coordinate Cu(II) ions favor a square-planar coordination sphere, (ii) Cu(I) prefers a tetrahedral arrangement, (iii) histidine residues are common ligands for Cu sites, (iv) thioether ligands stabilize Cu(I) in model compounds, and (v) oxygen ligands are more common in Cu(II) complexes (e.g. an oxygen ligand in stellacyanin may be responsible for the very low reduction potential).[228] Hence, the tyrosine ligand in APP may facilitate binding of Cu(II), while the relatively rigid tetrahedral site would facilitate the reduction of Cu(II), which, in the absence of other reductants, results in Met-170 oxidation.

The fact that the CuBD domain of APP is exposed to solvent is in contrast with the cases of other Cu(I) sites that are normally sequestered inside proteins in order to avoid generation of ROS via Fenton chemistry. Occurrence of such reactions was indeed observed upon the binding of copper to the APP CuBD.[225] On the other hand, surface exposure of the CuBD is reminiscent of the case for Cu(I) sites of

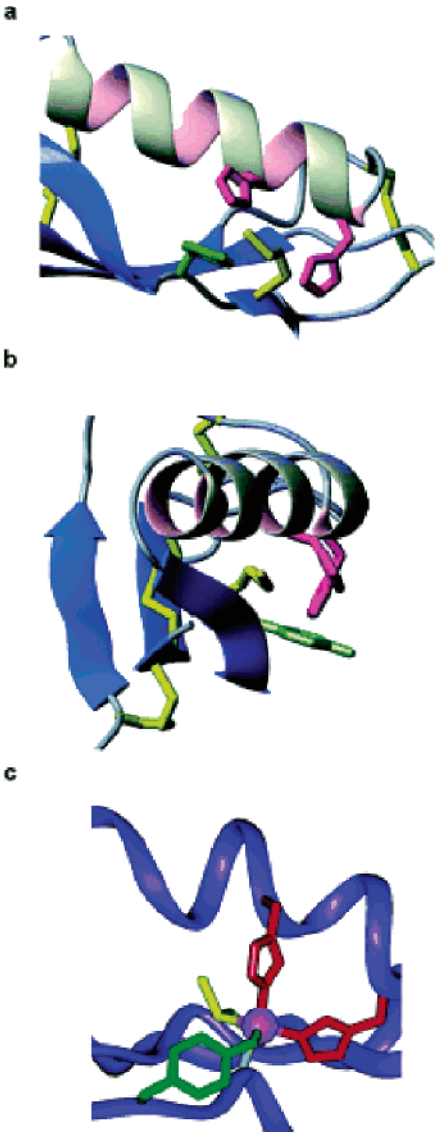

Figure 19. Metal binding site. (a and b) Orthogonal views of the putative metal binding site consisting of residues His-147, His-151, Tyr-168, and Met-170. (c) Model of Cu(I) coordinated in a tetrahedral configuration to His-147, His-151, Tyr-168, and Met-170. Reprinted with permission from ref 221. Copyright 2003 The American Society for Biochemistry & Molecular Biology.

copper chaperone proteins.[229] These considerations led to the general mechanism depicted in Figure 20.

(1) Membrane-bound APP acts as a "copper sensor/scavenger" and binds copper in response to copper levels in the extracellular *milieu* and/or inside the cell.[162,163] Cu(II) binding favors Cu(II) reduction, since the site is optimized for Cu(I) and APP dimerization.

(2) Binding of Cu(I) constitutes the signal for APP processing via the nonamyloidogenic route.[224,225] Conformational changes or oligomerization induced by reduction may trigger the signal transduction pathway, as supported by experimental evidence.[205] In fact, (i) metal binding was observed to be generally accompanied by protein aggregation, and (ii) APP processing is generally accompanied by APP oligomerization.[230]

(3) The release of the APP "chaperone" ectodomain from the membrane would allow the transportation of the metal to a nearby copper "transporter/receptor". Such a hypothesis agrees with the surface location of the Cu(I) site and may explain the role of APP in copper homeostasis[162,163] and copper modulation of APP processing.[225]

Interestingly, in a search of proteins having folds similar to that shown in Figure 18, three were found to be involved in copper chaperone activity, including the Menkes copper-transporting ATPase fragment, the metallochaperone Atx1, and the SOD1 copper chaperone.

The NMR approach described in section 2.2 was used to investigate the copper(II) binding features of two N- and C-terminal-protected APP fragments, APP(145−155) and APP(145−157), containing the critical residues of the CuBD.[52] NMR findings were supported by UV−vis, CD, and EPR spectra. It was shown that (i) the imidazole rings of all three His residues (His-147, His-149, and His-151) are involved in metal coordination; (ii) metal binding induces deprotonation of Leu-148 and His-149 amide nitrogens that complete the donor set to copper(II) in the species dominant at neutral pH; and (iii) the unusual coordination scheme of the His-Xxx-His-Xxx-His consensus sequence justifies the high specificity for Cu(II) when compared to SOD-like or albumin-like peptides or even to amyloid Aβ fragments. It was underlined that the delineated structural features (Figure 21)[52] may represent the key for interpreting the required conservation of His-147 and His-151 residues for the neurotoxic redox cycling between Cu(II) and Cu(I) by soluble APP.[231]

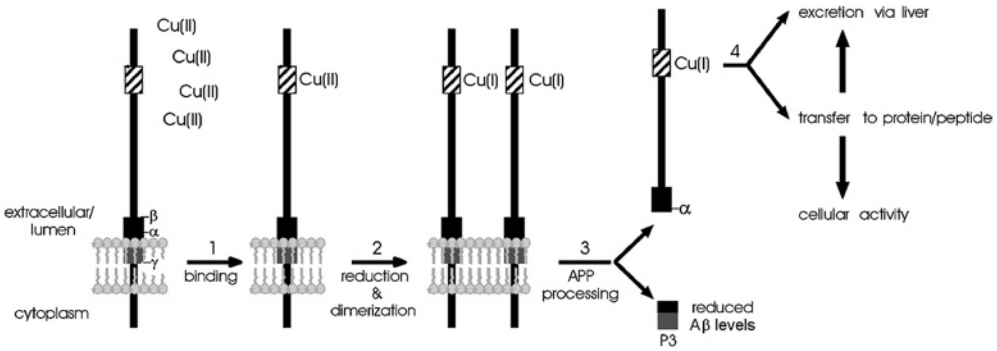

Figure 20. Model outlining the mechanism and biological consequences of the CuBD−copper interaction. (1) Binding of copper to the APP CuBD (hatched box). (2) The CuBD favors the reduction of Cu(II) to Cu(I) and subsequent APP dimerization. (3) The APP·Cu(I) complex promotes the processing of APP via the nonamyloidogenic pathway, resulting in the secretion of α-secretase-cleaved APP·Cu(I) and the P3 peptide. This results in a decrease in Aβ levels and an increase in α-secretase-cleaved APP. The secreted APP·Cu(I) can then act as a copper transporter to transport the Cu(I) away from the tissue for excretion via the liver. Alternatively, the APP could act as a copper chaperone and transfer the copper to an as yet unidentified cuproprotein. Reprinted with permission from ref 221. Copyright 2003 The American Society for Biochemistry & Molecular Biology.

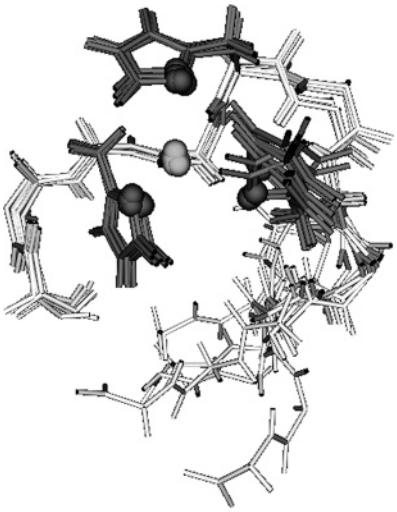

Figure 21. The first eight best structures of the Cu(II)−APP(145−155) complex. Structure calculation was based on obtained metal proton distances and was performed by restrained molecular dynamics with simulated annealing in the torsional angle space. The figure was created with MOLMOL 2K.1.0. Adapted with permission from ref 52. Copyright 2004 The Royal Society of Chemistry.

4.6.2. Aβ and Copper

Early electron microscopic studies indicated that fibrils of senile plaques (SP) from AD brains are apparently composed of two 2−4 nm filaments (4−8 nm in diameter).[232] X-ray diffraction patterns from unfixed human brain fractions and from purified amyloid cores isolated from SP suggested a β-pleated sheet structure with repeat distances in the fibers at 0.48 and 1.06 nm.[233] Together with many other data, an ordered protein structure in the SP was claimed.[234]

The structure and detailed composition of isolated amyloid plaque cores has been investigated with Raman microscopy.[235] Spectra obtained for SP cores isolated from the AD brain were essentially identical both within and among the brains. The Raman data ratified that the SP cores are composed largely of Aβ and that the structure is β-sheet with the possibility of a parallel β-helix, one of several all parallel β-domain folds, first discovered in the structure of Pectate Lyase C.[236] Raman bands characteristic of methionine sulfoxide showed that extensive methionine oxidation had occurred in the intact plaques. The Raman spectra also demonstrated that Zn(II) and Cu(II) are coordinated to histidine residues in the SP cores. Treatment of the senile plaques with EDTA reversed Cu binding to SP histidines and led to a broadening of amide features, indicating a "loosening" of the β-structure. These results indicate that Aβ in vivo is a metalloprotein, and the loosening of the structure following chelation treatment suggested a possible means for the solubilization of amyloid deposits. The amount of copper in extracts of plaque cores was measured at ~0.8 mg/L.[237] The involvement of copper in AD pathogenesis is further supported by the fact that this metal (together with other metals) binds Aβ in vitro. The main results obtained so far are summarized in Table 1. Different and sometimes conflicting results have been obtained, as will be discussed later, but it is without doubt that Aβ is a strong chelator for Cu(II) and this association has been claimed to be operative either in modifying the morphology of fibrils, as already observed for Zn^{2+},[238] or in mediating redox production of H_2O_2 from O_2,[239] or in modifying the aggregation rate,[204] as well as the type of aggregate formed.[240]

As for the Cu(II) binding site of Aβ (Table 1), speciation curves have demonstrated a marked pH dependence of metal binding affinities and metal binding sites. Moreover, rat and mouse Aβ peptides, with the G5R, Y10F, and H13R mutations, have been observed to yield speciation curves substantially diverse from those of human Aβ. Involvement of the imidazole rings of His6 and His14 has been apparently verified by all reported investigations, whereas the implication of the imidazole ring of His 13 or the amino terminal group as the third N donor has long been debated, as has been the nature of the oxygen donor that completes the Cu(II) coordination sphere. The latest results are quite convincing in rejecting the proposal of the involvement of Tyr phenolate oxygen as a Cu(II) binder and in supporting the role of the amino terminal group as the third nitrogen donor.

The stoichiometry, stability constants, and solution structure of the complexes formed in the reaction of Cu(II) with hAβ6, hAβ10, mAβ6, and mAβ10 were determined by potentiometric and UV−vis, CD, and EPR spectroscopic methods.[241] All fragments formed complexes with the same coordination modes. The coordination of the metal ion starts from the N-terminal Asp residue, which stabilizes significantly the 1N complex as a result of chelation through the N-terminal amino group and the β-carboxylate group. In the wide pH range 4−10, the imidazole nitrogen of His-6 is coordinated to form a macrochelate. Results show that, in the pH range 5−9, the human fragments form the complex with a different coordination mode compared to that of the mouse fragments. The low pK_1(amide) values (~5) obtained for the mouse fragments may suggest the coordination of the amide nitrogen of His-6, while in the case of the human fragments the coordination of the amide nitrogen of Ala-2 is suggested.

Potentiometric and spectroscopic (UV−vis, CD, NMR, and EPR) studies were also performed on copper(II) binding to a short N-terminal (11−16) fragment of human (Glu-Val-His-His-Gln-Lys) and mouse (Glu-Val-Arg-His-Gln-Lys) Aβ.[242] It was found that the human fragment was forming complexes with coordination through the imidazole nitrogens of both histidine residues and that amide nitrogens start to be involved in binding at higher pH values. The imidazole nitrogen of the histidine residue of the mouse Aβ was acting as the anchoring binding site, and at higher pH the 3N and 4N complexes are formed with the amide nitrogens coordinated. In a wide pH range including physiological pH, the human fragment was found to be much more effective in copper(II) binding than the mouse fragment.

Cu(II) bound to soluble and fibrillar Aβ has been characterized by EPR.[243] Addition of stoichiometric amounts of Cu(II) to soluble Aβ produced an EPR signal at 10 K with observable Cu(II) hyperfine lines. A nearly identical spectrum was observed for Aβ fibrils assembled in the presence of Cu(II). The EPR parameters were consistent with a type 2 Cu(II) center with three nitrogen donor atoms and one oxygen donor atom in the coordination sphere of Cu(II). The temperature dependences of the EPR signals were following a normal Curie behavior, indicating a mononuclear Cu(II) site. Fibrils assembled in the presence of Cu(II) contained one Cu(II) ion per peptide. The ligand donor atom set to Cu(II) was not changing during organization of Aβ monomers into fibrils, and neither soluble nor fibrillar forms of Aβ40 with Cu(II) contained antiferromagnetically exchange-coupled binuclear Cu(II) sites in which two Cu^{2+} ions are bridged by an intervening ligand.

Table 1.

peptide	solvent	method	observations	K_d (μM)	binding site	ref
hAβ6	H_2O	potentiometric curves, EPR, UV−vis, CD	$CuH_{-2}L$ dominant at neutral pH	log β provided	3N His, 2 amide NH	241
hAβ9	H_2O	potentiometric curves, EPR, UV−vis, CD	$CuH_{-1}L$ dominant at neutral pH	log β provided	3N His, 1 amide NH, NH_2	241
mAβ9	H_2O	potentiometric curves, EPR, UV−vis, CD	$CuH_{-1}L$ dominant at neutral pH	log β provided	3N His, 1 amide NH, NH_2	241
hAβ16	H_2O	Raman spectroscopy aggregation assays	induction of aggregates at pH < 6.6		His-Cu-His bridges (insoluble) His, 3 amide NH (soluble)	245
	H_2O	potentiometric curves, EPR, UV−vis, CD	CuH_2L dominant at neutral pH	log β provided	3N His, His, His	433
	H_2O	fluorescence		47		434
mAβ16	H_2O	potentiometric curves, EPR, UV−vis, CD	$CuH_{-1}L$ and CuHL dominant at neutral pH	log β provided	2N (CuHL) His, His 3N ($CuH_{-1}L$) His, 2 amide NH	433
hAβ28	H_2O/D_2O	NMR, EPR, CD	formation of precipitate no reduction to Cu(I)		3N1O His,His,His,Tyr	216
	H_2O	potentiometric curves, EPR, UV−vis, CD	CuHL dominant at neutral pH	log β provided	3N His, His, NH_2	433
	H_2O	EPR (20 K), CD, NMR, fluorescence	EPR spectra are pH dependent	0.1−0.01	3N1O (pH 5) 4N (pH 10) His, His, His, NH_2	244
	H_2O	EPR (20 K)				434
	H_2O	EPR (110 K)	pH dependence and Cu(II) conc dependence	28	type 2 square-planar Cu(II) change of coordination at pH 5.5−6 and 7−7.5	217
mAβ28	H_2O	potentiometric curves, EPR, UV−vis, CD	CuHL dominant at neutral pH	log β provided	3N His, amide NH, NH_2	433
rAβ28	H_2O/D_2O	NMR, EPR, CD	formation of precipitate no reduction to Cu(I)		2N2O	216
hAβ40	H_2O	competitive metal capture analysis		5.0×10^{-5} (pH 7.4) 2.5×10^{-4} (pH 6.6)		209
	SDS/D_2O	NMR, EPR	no reduction to Cu(I)		3N1O His,His,His,Tyr	216
	H_2O	Raman spectroscopy aggregation assays	induction of aggregates at pH < 6.6		His-Cu-His bridges (insoluble) His + 3 amide NH (soluble)	245
	H_2O	fluorescence		1.6 (pH 7.4)		435
	H_2O	EPR, cyclic voltammetry	76% reduction to Cu(I)		3N1O	206
	H_2O + glycerol 50%	EPR (10 K)	protofilaments 6 nm wide 1:1 ratio in fibrils		3N1O in both soluble complex and fibrils	243
	H_2O + glycerol 50%	EPR (20 K), fluorescence	filaments 5.5 nm wide 1:1 ratio in fibrils	11	3N1O in both soluble complex and fibrils His, His, NH_2, O donor not Tyr	434
hAβ42	H_2O	competitive metal capture analysis		6.3×10^{-12} (pH 7.4) 5.0×10^{-11} (pH 6.6)		209
	H_2O	fluorescence		2.0 (pH 7.4)		435
	H_2O	EPR (77 K)	role of Tyr-10 in reduction to Cu(I)		3N1O	281
	H_2O	Raman spectroscopy	senile plaque cores were also investigated extensive Met oxidation observed		His residues	235

A range of complementary spectroscopies has recently been used to characterize the binding of Cu(II) to Aβ and the structural changes induced in Aβ upon copper coordination.[244] The fragment Aβ(1−28) was used, since residues 29−42 are highly hydrophobic and are not believed to be associated with direct coordination of the metal ion.[216,245] EPR showed that Aβ(1−28) binds two Cu(II) ions sequentially and that both coppers have axial, type 2 coordination geometry, square-planar or square-pyramidal, with nitrogen and oxygen ligands. The occurrence of a dinuclear Cu site bridged by imidazole was excluded. CD indicated a structural transition of Aβ caused by copper. Competition studies indicated an affinity of $K_a \sim 10^7$ M^{-1} at pH 7.4. ^1H NMR gave evidence of histidine residues and not tyrosine involved in Cu(II) coordination. Using analogues of Aβ(1−28) in which each of the histidine residues had been replaced by alanine or in which the N-terminus had been acetylated suggested that the N-terminus and His-13 are crucial for Cu(II) binding and that His-6 and His-14 are also implicated (Figure 22) at pH > 7.5, where substitution of the O donor occurs.

Binding of Cu(II) by synthetic human Aβ induces its aggregation[204,209,210,246] and formation of fibrils,[243,247] although some authors failed to observe this last phenomenon, most probably because of experimental conditions.[240] Early studies indicated that histidine residues were important for Aβ aggregation since the loss of histidine residues, such as in rat Aβ, or histidine modification, results in greatly diminished aggregation of Aβ by Cu(II), Zn(II), or Fe(III).[204,248] These results indicate that histidine residues are essential for metal-

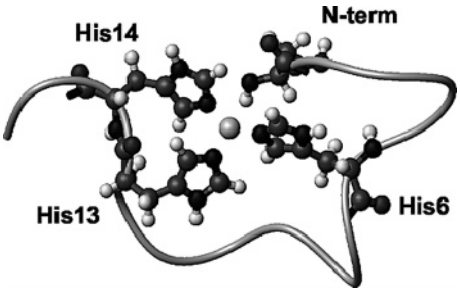

Figure 22. Model of Aβ coordinating Cu^{2+}. Coordinating ligands include the N-terminal amino group and the imidazole rings of His-6, His-13, and His-14 in a square-planar geometry. The model illustrates the dominant coordination geometry of the first mole equivalent of copper at physiological pH. Coordination at higher pH (pH 8.5 and above) probably involves main-chain amide coordination. A MolMol representation was obtained using distance geometry (DYANA), in which the metal−ligand bond lengths (1.9 Å) and angles (square-planar geometry) were constrained. Reprinted with permission from ref 244. Copyright 2004 The American Society for Biochemistry & Molecular Biology.

mediated assembly of Aβ and may explain why cerebral Aβ deposition is not a feature of aged rats even though soluble Aβ40 is produced by rat neuronal tissue.

The high concentrations of redox active Cu and Fe, and redox inactive Zn present in the cortex and hippocampus and the release of Cu and Zn from the synapse during transmission coupled with the lowered pH of the inflammatory AD brain provide an ideal environment in which Aβ could aggregate. Interestingly, Aβ simultaneously binds equal amounts of Cu(II) and Zn(II) in phosphate-buffered saline at pH 7.4 (~1.7 atoms each) when equimolar concentrations of both metal ions are present.[209] However, when the pH is lowered to pH 6.6, Cu(II) ions effectively remove almost all Zn(II) ions from Aβ. This may be a trigger for the initiation of the redox properties described below.

The importance of copper to Alzheimer's disease is emphasized by the neurotoxic interaction between the Aβ peptide and copper. The Aβ peptide binds copper with a high affinity and reduces Cu(II) to Cu(I) through recruitment of biological reductants such as cholesterol, ascorbic acid, L-DOPA, or dopamine.[211] The result is the catalytic generation of hydrogen peroxide (H_2O_2) and Aβ aggregation. Aβ and copper can interact to form an oligomeric complex that binds copper at a copper/zinc superoxide dismutase-like binding site. It is plausible that copper binding to CuBD and Aβ are linked phenomena. The modulation of copper levels by the APP CuBD would influence Aβ-Cu interactions, resulting in increased H_2O_2 production from Aβ-Cu or an overall increase in neuronal reactive oxygen intermediate production. Changes in copper levels will also affect APP processing into Aβ, thus controlling the production of neurotoxic Aβ.

Biochemical studies strongly imply a crucial role for Cu(II) and Fe(III) interactions with Aβ species in AD. The affinity of variant Aβ40 and Aβ42 species for Zn(II) is equal, but the affinity for Cu(II) and Fe(III) differentiates them in a way that echoes their participation in AD pathology [hAβ42 > hAβ40 > mAβ 42 > mAβ40].

Cu(II) and Fe(III) interactions with Aβ mediate the toxicity of the peptide in cell culture. Aβ catalyses H_2O_2 generation through the reduction of Cu^{2+} (and Fe^{3+}), using O_2 and biological reducing agents (e.g. cholesterol, vitamin C, catecholamines) as substrates.[211] Consistent with these biochemical properties being responsible for disease, it has been found that the neurotoxicity of Aβ in culture is mediated by AβCu^{2+} (or AβFe^{3+}) forming H_2O_2 and, again, differs thus: hAβ42 > hAβ40 ≫ mAβ40.[249] Conversely, Aβ is not toxic in the absence of Cu^{2+}· H_2O_2 is freely permeable across all tissue boundaries. Unless scavenged by defenses such as catalase and glutathione peroxidase, it will react with reduced metal ions (Fe^{2+}, Cu^{+}) to generate the hydroxyl radical (Fenton reaction), which in turn generates the lipid peroxidation adducts, protein carbonyl modifications, and nucleic acid adducts (such as 8-OH guanosine) in various cellular compartments. Such oxidative damage typifies, as already stated, AD neuropathology and precedes Aβ deposition in AD.[250]

The simultaneous generation by Aβ of Cu(I) (or Fe(II)) with H_2O_2 makes the peptide vulnerable to attack by ROS. Aβ is markedly vulnerable to cross-linking and oxidation induced by Cu(II) ions, which lead to side-chain damage (especially of histidine), and sodium dodecyl sulfate (SDS)-resistant oligomerization.[222] SDS-resistant oligomerization of Aβ enhances its neurotoxicity (vide supra), and it will be important to determine whether the mechanism of this modification in AD is Cu-mediated. Oxidative oligomers are resistant to proteolysis; therefore, oxidized Aβ oligomers are likely to become subunits for Zn^{2+}-induced assembly into the amyloid mass, as schematized in Figure 23.[218] As a first step, increased Fe and Cu levels may cause overproduction of APP and Aβ, and "hypermetalation" of Aβ follows from medium acidosis. Catalytic production of H_2O_2 from O_2 and biological reducing agents may then occur. Successive reaction of AβCu with H_2O_2 generates oxidized and cross-linked forms that are liberated from the membrane. The release of soluble Aβ presents the peptide for precipitation by the high concentrations of Zn released in the synaptic vicinity. Microglial activation by oxidized Aβ overproduces H_2O_2 and myeloperoxidase, which fosters further cross-linking of Aβ and H_2O_2 build-up outside the cortical cells. H_2O_2 enters cellular compartments and yields the hydroxyl radical through Fenton chemistry with consequent oxidation of nucleic acids, proteins, and lipids that characterize AD-affected brain tissue.

Possible mechanisms of Aβ toxicity include the formation of plasma membrane channels[251] and the generation of H_2O_2 through Cu(II) reduction by the peptide, which make cells more responsive to oxidative stress.[252] The mechanisms may be related because reactive oxygen species may cause lipid peroxidation that leads to alterations in the order and fluidity of the bilayer lipids, and may also lead to an increase of membrane permeability. The common change observed in cell membrane permeability is an increased intracellular calcium level that could occur either indirectly through Aβ modulating an existing Ca^{2+} channel or directly through cation-selective channels formed by Aβ.

The supramolecular structure of membrane-associated Aβ, either as an ion channel or as a membrane fusion promoter, is unknown, although theoretical models have been developed for the structure of ion channels formed by the membrane-bound Aβ40.[253] Atomic force microscopy, laser confocal microscopy, and fluorescent calcium imaging were used to examine in real time the acute effects of fresh and globular Aβ40, Aβ42, and Aβ(25−35) on cultured endothelial cells.[254] Aβ peptides were found to cause morphologi-

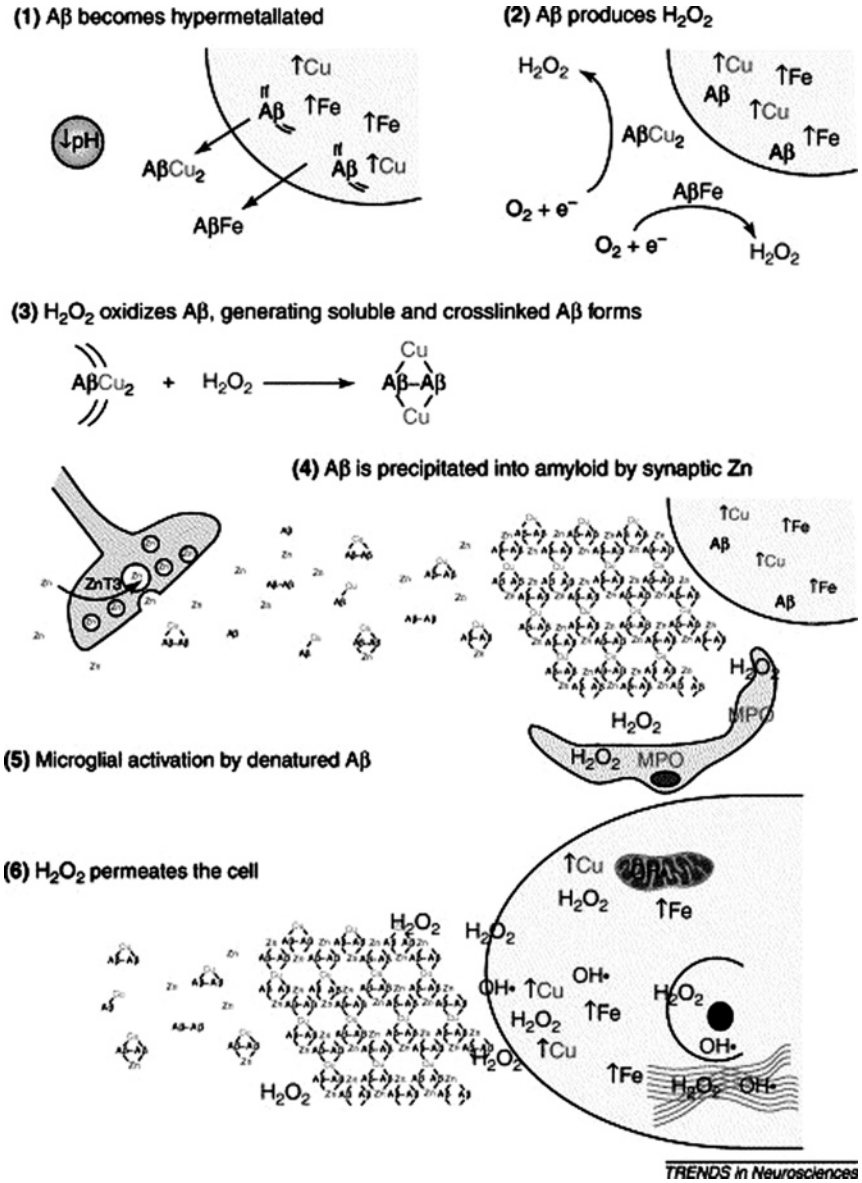

Figure 23. Model for the metallobiology of Aβ in AD. (1) Hypermetalation of Aβ. (2) Catalytic production of H_2O_2. (3) AβCu reacts with H_2O_2 to generate oxidized and cross-linked forms that are liberated from the membrane. (4) The release of soluble Aβ presents the peptide for precipitation by the high concentrations of Zn released in the synaptic vicinity. Plaques are therefore an admixture of Aβ and high concentrations of Zn, Cu, and Fe. (5) Microglial activation. (6) Production of the hydroxyl radical, and oxidation of nucleic acids, proteins, and lipids that characterize AD-affected brain tissue. Reprinted with permission from ref 218. Copyright 2003 Elsevier.

cal changes within minutes after treatment and lead to eventual cellular degeneration.

EPR was used to show that, in the presence of Cu(II) and Zn(II), Aβ42 formed allosterically ordered α-helical structures that penetrated negatively charged membranes.[217] Penetration of the bilayer was shown to be closely related to conditions favorable to oligomerization of the peptide, thus verifying that metals play an important part in the formation of amyloid plaques, the end point of oligomerization.

Direct evidence of the metal-induced amyloid formation by an Aβ fragment, which exhibits a clear-cut dependence on the amino acid sequence, has been recently reported;[255] in fact, the heptapeptide EFRHDSG, corresponding to amino acid residues 3−9 of Aβ, undergoes a conformational transition from irregular to β-sheet and is self-associated into insoluble aggregates upon Cu(II) binding. Raman spectra of the Cu(II)−Aβ(3−9) complex and aggregation assays of mutated Aβ(3−9) peptides demonstrated that a concerted Cu(II) coordination of the imidazole side chain of His6, the carboxyl groups of Glu3 and Asp7, and the amino group at the N-terminus was essential for the amyloid formation. Although Aβ(1−9) and Aβ(2−9) also contained the metal binding sites, neither of these peptides formed amyloid depositions in the presence of Cu(II).

The chemistry of the redox-active metal complexes of Aβ has been an area of intense focus in the study of AD; however, the cause/effect connection of the metallo-Aβ plaques with AD is still under debate.[256] The results obtained for the metal coordination environment of Aβ40 and Aβ42 showed that the metal binding seemed to be nonstoichiometric with approximately 3.5 metal ions per pair of aggregated peptides and a cooperative binding pattern as the amount of aggregates increases.[216,245]

Although the coagulation of the peptide plaques leaves little doubt that interaction with cytoplasmic molecules is unlikely, smaller fragments of the amyloid peptide are soluble and Aβ fibrils extend across membranes, exposing them to the cytoplasm. Moreover, the cleavage of APP by secretases

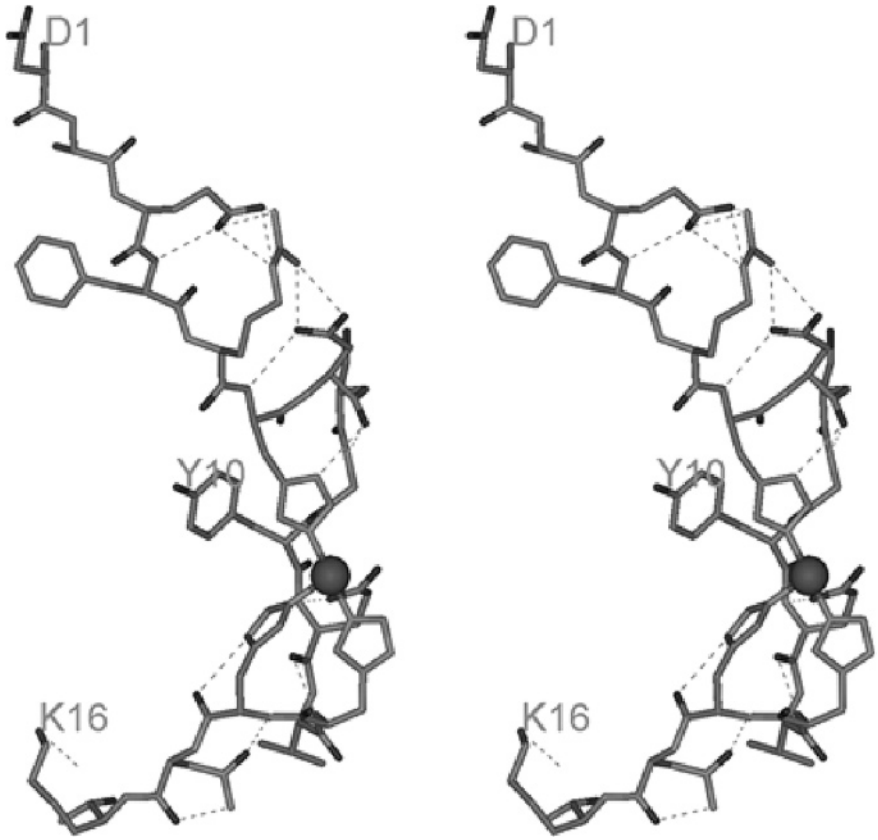

Figure 24. Proposed metal coordination and solution structure of CuAβ1−16 in a relaxed-eye stereoview based on NMR study of Co^{2+} binding and molecular mechanics calculations. According to the molecular mechanical calculations, both the two-histidine (His-13/His-14) and three-histidine binding patterns are stable, whereas NMR study suggests the latter binding pattern. The dotted lines are H-bonds, which may prevent further bending of the peptide to allow the binding of the N-terminus to the metal. Reprinted with permission from ref 258. Copyright 2005 The American Society for Biochemistry & Molecular Biology.

produces the Aβ(1−16) fragment of APP. These soluble fragments and intramembrane spanning fibrils still possess possible metal binding sites such as histidines, glutamate, aspartate, and tyrosine within the 1−20 fragment of Aβ. The redox chemistry of Aβ has been previously reported, wherein Met35 was suggested as a "built-in" reducing agent required for the redox cycling hypothesis.[257] Sufficient data are still lacking on the redox chemistry of metallo-Aβ and on the consequent oxidative stress; moreover, the discrepancies in previous studies, such as the presence or absence of free radicals and the nature of the metal−Aβ interaction, are the main shortcomings in Aβ research. Such difficulties need to be overcome since the understanding of the chemical processes associated with metallo-Aβ may provide insight into the regulatory processes that lead to AD. The oxidation chemistry of CuAβ in the presence and absence of H_2O_2 has recently been investigated,[258] showing conclusive metal-centered pre-equilibrium kinetics toward the oxidation of a simple substrate and the oxidative cleavage of double-stranded plasmid DNA. The Cu(II) complexes of the 1−16 and the 1−20 fragments of Aβ showed significant oxidative activities toward a catechol-like substrate trihydroxylbenzene and plasmid DNA cleavage. The latter reflects possible oxidative stress to biological macromolecules, yielding supporting data to the pathological role of these soluble Aβ fragments. The kinetic profiles were consistent with metal-centered redox chemistry for the action of CuAβ. A mechanism was proposed by the use of the catalytic cycle of dinuclear catechol oxidase as a working model. A tetragonally distorted octahedral metal coordination sphere with three coordinated His side chains and some specific H-bonding interactions was concluded from the electronic spectrum of CuAβ, the hyperfine-shifted ^{1}H NMR spectrum of CoAβ, and molecular mechanics calculations (Figure 24).

The single methionine located at position 35 of the Aβ plays an important role in AD-associated oxidative stress and may act as an electron donor for the reduction of Aβ-bound Cu(II) to Cu(I).[206,259,260] For many proteins, the methionine side chains are easily oxidized to the sulfoxide under physiological conditions ($Met^{red} \rightarrow Met^{ox}$) in the absence of catalytic metal ions and may function as endogenous antioxidants. Oxidized Met35 ($Met35^{ox}$) comprises 10−50% of total brain Aβ in postmortem AD plaques[261] and, thus, may be connected to AD-related oxidative stress events. Recent Raman spectroscopic analysis of AD brain tissue confirmed that the Met35 is extensively oxidized and that Zn(II) and Cu(II) are coordinated to the histidine residues, thus providing a chemical basis for the extensive oxidative damage caused by the Aβ peptide in AD.[235]

CD, thioflavin-T binding assay, atomic force microscopy, and mass spectrometry have been used to demonstrate that the Aβ40$Met35^{ox}$ and Aβ42$Met35^{ox}$ peptides undergo β-aggregation at significantly reduced rates, as compared to the Aβ peptides containing $Met35^{red}$.[262−264] Most significantly, the $Met35^{ox}$ prevented formation of the Aβ protofibril, which is believed to be a common, toxic intermediate in the amyloidosis of many proteins. Based on a working hypothesis that the inhibition might be due to the increased polarity imparted by the $Met35^{ox}$ side chain at the hydrophobic C-terminus, NMR spectroscopy was applied to obtain site-

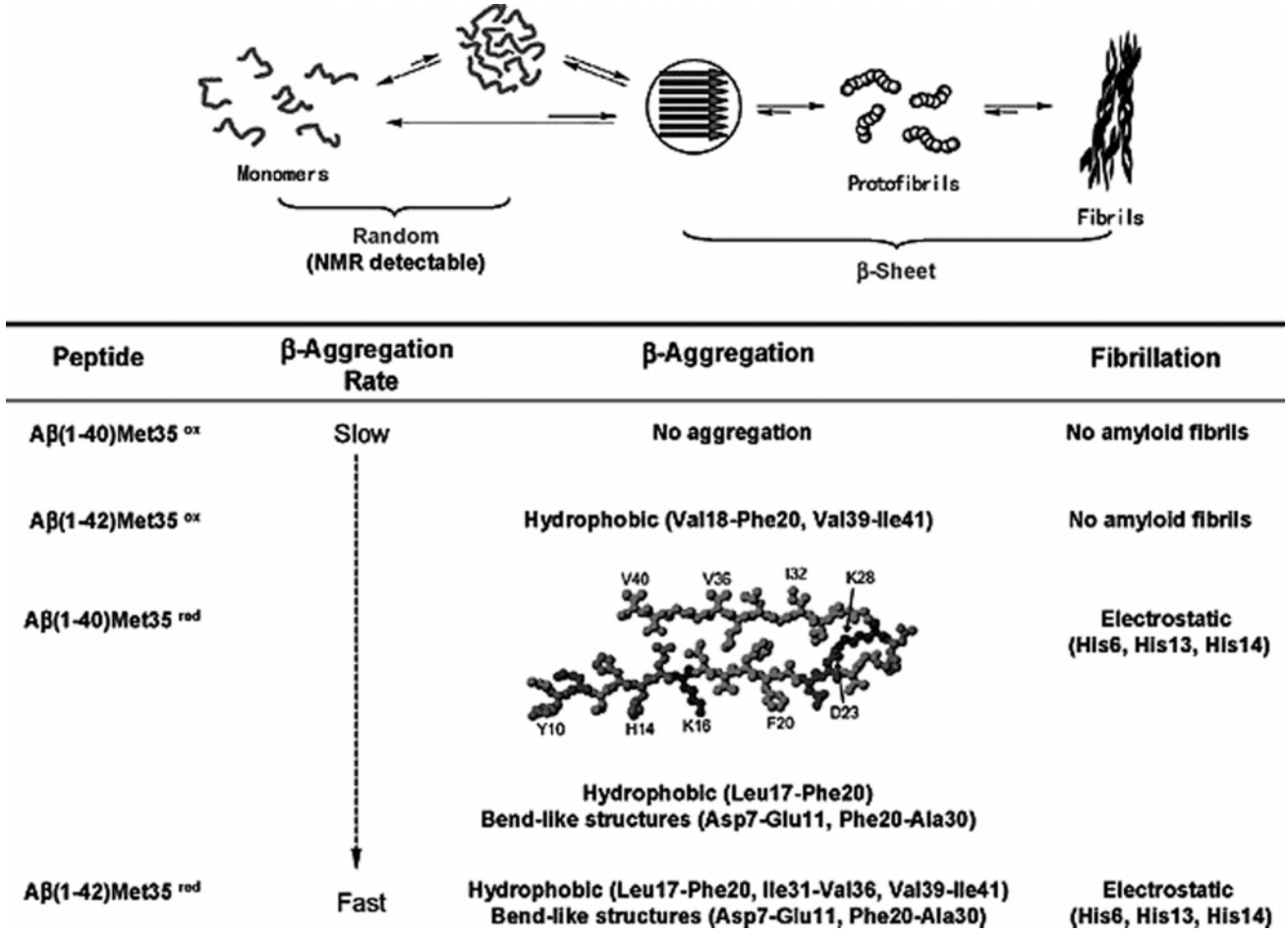

Figure 25. Schematic model showing the equilibrium among the different metal-free Aβ aggregation states, which include monomers, loosely associated disordered aggregates, soluble β-strand aggregates shown with parallel orientations, later-stage protofibrils, and end-stage fibrils. In the first step, all of the pathways involve hydrophobic association, followed by electrostatic association of the histidine side chains. Reprinted with permission from ref 265. Copyright 2004 American Chemical Society.

specific structural information.[265] A single set of conditions (aqueous solution, pH 7.2, 5 °C) was chosen for analysis of four Aβ peptides with different Met35 oxidation states (Aβ40Met35^{red}, Aβ40Met35^{ox}, Aβ42Met35^{red}, and Aβ42Met35^{ox}). The NMR data supported the absence of any well-defined secondary or tertiary structures for all four peptides. However, NOE and chemical shift data of Aβ40Met35^{red} and Aβ42Met35^{red} indicated residual β-strand structure at two hydrophobic regions (Leu17−Ala21 and Ile31−Val36) and turn- or bendlike structures at two largely hydrophilic regions (Asp7−Glu11 and Phe20−Ser26). It was therefore proposed that the Met35^{red} → Met35^{ox} conversion inhibits amyloid formation by preventing early, site-specific hydrophobic and electrostatic associations and that different association steps may be involved in amyloid formation for the Aβ40 and Aβ42 peptides (Figure 25). Solution NMR signals detect only the early stages of association, that is, monomeric peptide where the chemical shifts, NOE distances, and signal/noise ratio are influenced by the relative distribution among the various states. The table reported in Figure 25 reports on the residue-specific interactions taking place during the first step of Aβ self-assembly and second stage β-strand fibrillation, indicating that certain localized peptide regions are predisposed toward β-strand and bendlike structures. The four peptides have different β-aggregation rates and interactions, such that the oxidation state of Met-35 is demonstrated to play an influential role. The pathway of the Aβ40Met35^{red} peptide incorporates a single, central molecule taken from a larger working model of the cross-β unit that has in-register parallel β-sheets formed by residues 12−24 and 30−40 and a bend or kink for residues 25−29.

For the Met residue to serve as a source of electrons for the Cu(II)-catalyzed reduction of molecular oxygen to hydrogen peroxide, a long distance electron transfer is required from the thioether sulfur to the peptide-bound copper. The electron-transfer pathways between the Met35 sulfur atom and the cupric site in the N-terminus of Aβ congeners have been analyzed applying semiclassical models of long distance electron transfer.[266] Simulations performed for several Aβ conformers collected along the 6 ns Langevin dynamics trajectories suggested that the presence of the Phe20 residue in the peptide was required for feasibility of the electron transfer, such that the Phe20Ala mutation in Aβ could be proposed as a potential way to reduce its neurotoxicity.

The effect of mutating the methionine to valine in Aβ42 has been investigated.[267] The neurotoxic activity of AβM35V on primary mouse neuronal cortical cells was enhanced. AβM35V was binding Cu^{2+} and producing similar amounts of H_2O_2 as Aβ42 in vitro, and the neurotoxic activity was attenuated by the H_2O_2 scavenger catalase. The increased toxicity of AβM35V was associated with increased binding of this mutated peptide to cortical cells. The M35V mutation altered the interaction between Aβ and copper in a lipid environment as shown by EPR analysis, which indicated that the valine substitution made the peptide less rigid in the

bilayer region with a resulting higher affinity for the bilayer. Circular dichroism spectroscopy showed that both Aβ42 and AβM35V displayed a mixture of α-helical and β-sheet conformations.

It has been reported that, upon recruiting endogenous reductants, Aβ is able to reduce Cu(II) (and Fe(III)) with the consequent generation of H_2O_2 from O_2.[211] It has also been reported that Aβ is tyrosine cross-linked by Cu at concentrations lower than those detected in senile plaques in vivo, resulting in the generation of oligomeric Aβ species.[213] Such dityrosine modification might be significant since it is highly resistant to proteolysis and is known to play a role in increasing structural strength. It must however be remembered that many other reports have appeared where reduction to Cu(I) requires the addition of exogenous reductants[254] and that spontaneous reduction of Cu(II) is still debated.

On the basis of suggestive evidence for an oxyradical-induced cross-linking between His and Lys side chains, the Cu(II)-catalyzed oxidation of 4-alkylimidazoles was investigated in the presence of amines, as surrogates for these amino acid side chains, using ascorbic acid as a continual source of reducing equivalents.[268] A model His-Lys cross-link was isolated and structurally characterized as a 5-alkyl-5-hydroxy-4-(alkylamino)-1,5-dihydroimidazol-2-one by NMR and mass spectrometry. Evidence that the 2-imidazolone, the principal oxidation product found in the absence of amine, is an intermediate in the formation of the imidazole−amine adduct was that higher yields of the cross-link adduct were obtained starting with the 2-imidazolone.

In an attempt to elucidate the products of the metal-catalyzed oxidation of the human (H) and mouse (M) (1−10H), (1−10M), (1−16H), and (1−16M) fragments of Aβ, high-performance liquid chromatography and matrix-assisted laser desorption/ionization mass spectrometry methods and Cu(II)/H_2O_2 as a model oxidizing system were employed.[269] The oxidation targets for all peptides studied were the histidine residues coordinated to the metal ions which were converted to 2-oxo-His. Asp1 was oxidatively decarboxylated and deaminated to pyruvate. Oxidation of His residues was also ratified by analyzing the decomposition products of Aβ induced by ascorbate and/or hydrogen peroxide in the presence of Cu(II) with mass spectrometry,[270] which excluded the occurrence of Tyr modification.

Density functional theory (DFT) calculations were performed to identify molecular events underlying Aβ/Cu^{2+}-catalyzed production of H_2O_2.[271] In fact, binding of Aβ to Cu activates oxygen and, in the presence of a reducing substrate, such as ascorbic acid, catalyzes reduction of oxygen to H_2O_2 by promoting transfer of two electrons and two protons from the substrate to O_2. DFT calculations suggested that Cu(II) is reduced to Cu(I) via proton-coupled electron transfer from ascorbate to the side-chain oxygen of the tyrosinate of Tyr10, which passes the first electron to Cu(II). Next, dioxygen coordinates to Cu(I) and is reduced to superoxide. The second electron comes when Tyr10 gives up its side-chain hydroxyl hydrogen atom to superoxide via hydrogen atom transfer. Simultaneously, H_3O^+ donates its proton to superoxide via proton transfer, whereupon H_2O_2 and Tyr10 radicals form.

5. Amyotrophic Lateral Sclerosis (ALS) and Superoxide Dismutase (SOD)

Amyotrophic lateral sclerosis (ALS)[272] is a progressive neurodegenerative disease of upper and lower motor neurons affecting approximately one in 200 000 people. About 10% of ALS cases are inherited; the others are believed to be sporadic cases.[273] Of the inherited cases, about 20% are caused by mutations in the gene encoding superoxide dismutase 1 (SOD1). More than 90 different pathogenic SOD1 mutations have been described; all are dominant except for the substitution of valine for alanine at position 90, which may be recessive or dominant. The neuropathology of ALS is characterized by degeneration and loss of motor neurons and gliosis. Intracellular inclusions are found in degenerating neurons and glia.[1] Familial ALS (FALS) neuropathology is characterized by neuronal Lewy body-like inclusions (vide infra) and astrocytic inclusions composed largely of mutant SOD1 (Figure 1).

The CuZnSOD is a homodimeric enzyme (MW $\sim 2 \times$ 16 kDa) found in all eukaryotic species where it catalyzes the dismutation of the superoxide anion, according to

$$2O_2^- + 2H^+ \rightarrow H_2O_2 + O_2$$

The protein has been extensively investigated and characterized.[274,275] In the oxidized enzyme, Cu(II) is bound by four His residues and one water molecule in a distorted square-planar arrangement. One of the His ligands bridges Cu(II) to Zn(II), which is further coordinated by two His and one Asp in tetrahedral coordination.

Upon reduction, the bridging His and copper undergo a conformational rearrangement due to breakage of the His−Cu bond with the metal moving ~0.17 nm away from His N_ϵ that becomes protonated (Figure 26).[276]

CuZnSOD is located predominantly in the cytosol, nucleus, and mitochondrial intermembrane space of eukaryotic cells and in the periplasmic space of bacteria. Superoxide, as already discussed, is a potent, but chemically selective, reactive oxygen species produced in all aerobic cells. Sometimes it functions as a signaling agent, but it can also cause oxidative damage, particularly at excessive concentrations or when it reaches the wrong cellular locations. One

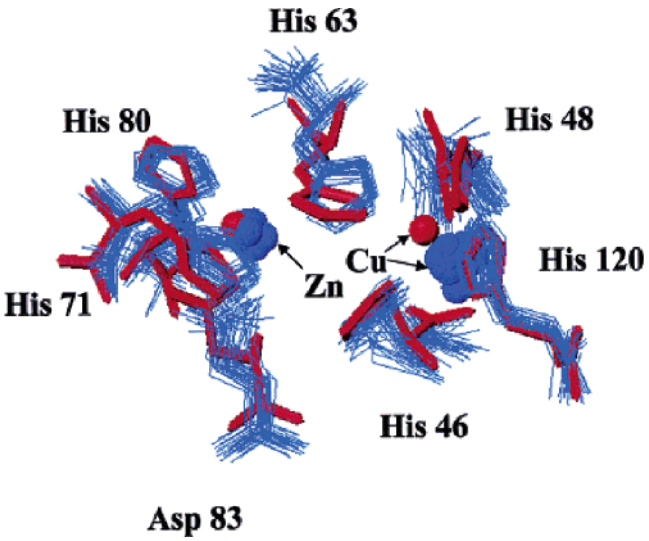

Figure 26. Active site of the family conformers of the reduced (blue) and oxidized (red) dimers of human Cu,Zn−SOD. Reprinted with permission from ref 276. Copyright 2002 Blackwell Publishing.

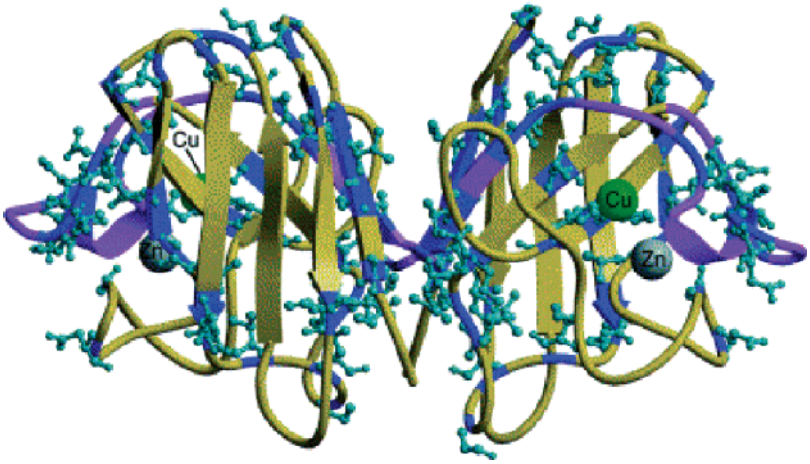

Figure 27. Sites of mutations in dimeric Cu−Zn superoxide dismutase. The side chains of mutated amino acids are shown in light blue, and the backbone as dark blue. Reprinted with permission from ref 280. Copyright 2001 Elsevier.

of the best documented examples of superoxide-mediated damage occurs when it attacks and destroys labile iron-sulfur cluster cofactors of aconitase and other similar iron-containing proteins.[277]

The work on SOD1 mutants has received a great advance in recent years, especially in the research groups of Valentine et al. at UCLA, USA, and of Bertini et al. at the University of Florence, Italy. The results obtained up to 2004 have recently been reviewed,[278] and only a few main results will be summarized herein. Over 100 distinct SOD1 mutations have been identified in FALS patients,[279] as summarized in Figure 27.[280] Most of the individual mutations are the result of substitution of one single amino acid by another; such substitutions have been identified at over one-third of the 153 amino acid residues of the wild-type CuZnSOD protein. As shown in the figure, the majority of the mutations are clustered on the top and bottom of the β barrel, in the dimer interface, or along one of the loops that forms part of the Zn binding pocket of superoxide dismutase (SOD). The only parts of the SOD molecule where mutations have not been found are in the Zn binding groups and on the residues facing out on backside of the β barrel, opposite the active site. In addition to the individual amino acid substitutions, there are also a smaller group of mutations resulting in amino acid deletions and truncations. A major part of the C-terminal region (purple in the figure) is found to be entirely deleted in a few individuals.

ALS mutant CuZnSOD proteins may be grouped into two groups:[281]

(i) A group named wild-type-like[281] in which copper and zinc levels are very similar to those found in the wild-type protein, i.e., high in zinc but with variable levels of copper.[282] The SOD activities and the spectroscopic characteristics of this class of ALS mutant CuZnSOD proteins are virtually identical to those of wild-type CuZnSOD.[282]

(ii) A second class, named "metal binding region" mutants.[281] These include mutations in the metal binding ligands themselves or in elements intimately associated with metal binding (Figure 28).[281] The side chain of Asp124 is particularly important, since it contributes to the stabilization of both the copper and zinc binding sites by simultaneously H-bonding to the nonliganding imidazole nitrogen atoms of copper ligand His46 and zinc ligand His71. These mutants are isolated from the expression systems with very low zinc but also with very low copper. This class of ALS mutant CuZnSOD proteins is very likely to exist in vivo in zinc deficient *and* copper deficient forms.

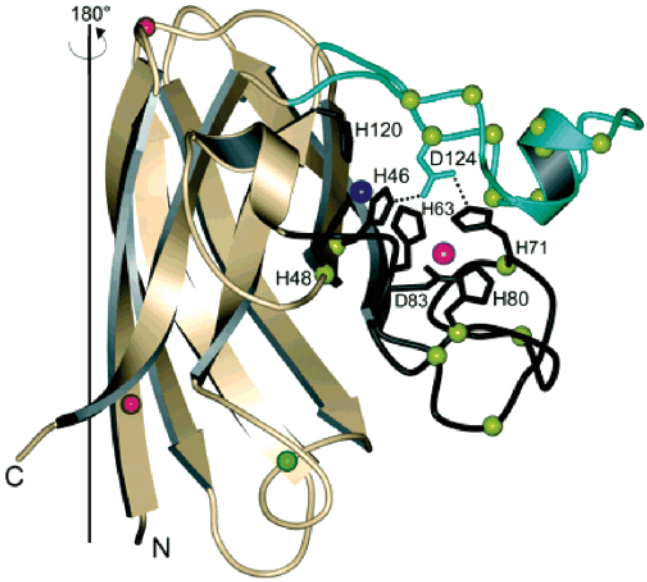

Figure 28. Structure of a monomer of the wild-type-like pathogenic SOD1 mutant G37R. The positions of the G37R and A4V mutations are indicated with red spheres. The copper and zinc ions are represented by blue and magenta spheres, respectively. The wild-type-like mutations (most of which are not shown) are found scattered throughout the β-barrel of the protein, shown in gold. The electrostatic loop is cyan, and the zinc loop and metal binding ligands are shown in black. The positions of the metal binding region mutations are represented by yellow spheres. The position of Cys-111 is represented by a green sphere. Asp-124, a residue termed the "secondary bridge", links the electrostatic and zinc loops and the copper and zinc binding sites. The second subunit of the G37R homodimer is generated by a rotation of 180° around the axis indicated. Reprinted with permission from ref 281. Copyright 2003 National Academy of Sciences. U.S.A.

Several hypotheses have been advanced that would relate SOD1 mutations with FALS:

(a) *A loss-of-function mechanism* based on impaired antioxidant functions of SOD1. Such mutations could lead to toxic accumulation of superoxide radicals, but (i) no motor neuron degeneration is seen in transgenic mice in which SOD1 expression has been eliminated and (ii) overexpression of mutant SOD1 in transgenic mice causes motor neuron disease despite elevated SOD1 activity.

(b) *A gain-of-function mechanism* based on a pro-oxidant role for mutant SOD1 contributing to motor neuron degeneration. Such a mechanism is challenged by the absence of effects on motor neuron degeneration in transgenic mice lacking the specific copper chaperone for SOD1, which deprives SOD1 of copper and eliminates enzymatic activity.[283]

(c) *An aggregation mechanism* based on the possible deleterious effects of accumulating aggregates of mutant SOD1, as supported by the observation that intracellular inclusions are found in motor neurons in murine models of mutant SOD1-mediated disease.[284] Although a variety of inclusions have been described in sporadic cases of ALS, there is poor evidence for deposition of SOD1 in these inclusions and no convincing evidence that aggregation contributes to the pathogenesis of sporadic ALS.

An aberrant redox chemistry of mutant SOD1 may arise from modification of active copper and zinc sites and yield enhanced peroxidase activity,[285] and superoxide production.[286] However, the requirement of copper ion for toxicity is not universally accepted, since ALS symptoms are observed in mice expressing the SOD1 mutant in which all of the copper ligands are mutated.[287]

The occupation of Cu and Zn binding sites not only affects the stability of SOD but it is also likely to act upon the free energy barrier to unfolding, thus affecting the so-called "kinetic stability" of SOD. As a consequence, the loss of these ions may facilitate partial or global unfolding transitions that may lead to misfolding and aggregation. As a matter of fact, the metals have been shown to contribute significantly to the kinetic stability of the protein, with apo-SOD showing acid-induced unfolding rates about 60-fold greater than those of the holoprotein.[288] However, the unfolding rates of wild-type and mutant SOD were similar to each other in both the holo and apo states, indicating that, regardless of the effect of mutation on thermodynamic stability, the kinetic barrier toward SOD unfolding is dependent on the presence of metals. In particular, the three D101N, E100K, and N139K mutants, all having normal metalation properties, were exhibiting the same thermal stability as the wild-type SOD.[289] Thus, pathogenic SOD mutations that do not significantly alter the stability of the protein may still lead to SOD aggregation by compromising its ability to bind or retain its metals and thereby decrease its kinetic stability.

As for the other hypothesis for a toxic function based on an increased propensity for cytoplasmic aggregation of mutant SOD1, ALS mutations have been considered to induce protein misfolding and/or destabilization; in fact, ALS mutations provoke a decrease of 1−6 °C in the melting temperature of SOD1,[290] while wild-type (WT) SOD1 remains active after treatment at 80 °C. While it remains unclear how SOD1 acquires zinc ions, the copper chaperone for SOD1 (CCS), as discussed in section 3.6, controls not only copper acquisition but also disulfide formation in apo-SOD1.[122] ALS mutants are more susceptible to disulfide reduction compared to the WT protein,[291] and hence, adventitious reductions may constitute an important step in the disease. It has in fact been shown that uptake of the SOD1 molecule into the intermembrane space of the mitochondria is dependent on the status of the disulfide bond.[292] The reduced form of SOD1 is imported through the mitochondrial outer membrane, but the disulfide-bonded apo-SOD1, the Zn(II)-loaded SOD1, and the holo-form or fully mature form of SOD1 are not readily transferred from the cytosol into the intermembrane space of the mitochondria. Since the effects of disulfide reduction on the SOD1 structure are so relevant to the intracellular localization and stability of the SOD1 molecule, it has been shown that, even after removal of both copper and zinc ions from the active and mature form of hSOD1, the dimeric state still persists; however, upon reduction of the disulfide bond, the protein can readily dissociate to the monomer form.[293] Zn(II) addition to the reduced apo-hSOD1 restores the dimeric state, indicating that only the most immature form of hSOD1 before any post-translational modifications favors the monomeric state.[290] Very recently, the crystal structure of the H46R mutant has disclosed a novel zinc coordination and the disruption of the Asp 124 secondary bridge between the Cu and Zn binding sites.[294] Such disruption has been suggested to account for the increased tendency to aggregate.[294]

A study on post-translational modifications influencing the stability of both wild-type and ALS-mutant SOD1 has recently been reported.[295] Consideration of the four post-translational events (Cu binding, Zn binding, disulfide formation, dimerization) preceding SOD1 activation makes it possible for the protein to adopt over 44 states. Results showed that ALS mutations have the greatest effect on the most immature form of SOD1, destabilizing the metal-free and disulfide-reduced polypeptide to the point that it is unfolded at physiological temperature. Moreover, the immature states of ALS-mutant, but not wild-type, SOD1 were readily forming oligomers at physiological concentrations. The oligomers were found to be more susceptible to mild oxidative stress, promoting incorrect disulfide cross-links between conserved cysteines and driving aggregation. It was therefore concluded that it is the earliest, disulfide-reduced polypeptides in the SOD1 assembly pathway that are most destabilized with respect to unfolding and oxidative aggregation by ALS-causing mutations.

Five FALS-related mutants (G37R, H46R, G85R, D90A, and L144F) were used to demonstrate that the unfolding rates were very similar to those of wild-type SOD in the metalated as well as in the demetalated states,[296] with demetalated SODs showing unfolding rates about 60-fold faster than the metalated proteins. As a consequence, pathogenic SOD mutations may lead to SOD aggregation by affecting its ability to bind or retain metals, and it may also be hypothesized that the loss of metals in wild-type SOD may be involved in nonfamilial forms of ALS.

The A4V mutation is responsible for a rapidly progressive disease course and is particularly prone to aggregation when expressed in *E. coli*: it remains soluble when expressed at 18 °C but aggregates in inclusion bodies when expressed at 23 °C or above.[297] Since the SOD aggregates dissolve with 4 M urea, intermolecular hydrophobic interactions are predominantly responsible for making SOD insoluble. Many of the urea-solubilized subunits were cross-linked via disulfide bridges.

The H43R and A4V mutations, when examined in the context of the C6A/C111S HSOD (HSOD-AS) parent, which retains the wild-type fold and activity, showed nearly wild-type structures; however, an overall architectural destabilization was demonstrated propagating from the point mutations and promoting the formation of fibril-like aggregates.[298] The cysteine-independent aggregation of FALS mutants was 7−80-fold enhanced compared to the case of the parent HSOD-AS, and aggregation severity could be suggested to be enhanced by the presence of free cysteine residues, which

Figure 29. Sequence alignment of human α- and *β*-synuclein (αS and *β*S). Conserved residues are written in blue. Gray boxes indicate the NAC region of α-syn.

can form disulfide bonds to covalently lock the fibrous aggregates. The fibrils were visualized for the first time by electron microscopy and atomic force microscopy and resembled those found in postmortem studies of FALS patients.

CuZnSOD mutants with modifications near the metal binding sites show altered SOD activities and spectroscopic properties. Moreover, some of them, specifically metal deficient S134N and H46R SOD1, crystallize in filament-like arrays with abnormal contacts between the individual protein dimers.[299] Concerning the hypothesis that the abnormal protein−protein contacts in the crystal structures might also be responsible for the earliest steps of the protein oligomerization in solution, NMR studies were carried out on S134N SOD that demonstrated a dramatically different behavior between the fully metalated mutant and the fully metalated wild-type SOD1, with a region of subnanosecond mobility located close to the site of the mutation.[300] In addition, concentration-dependent chemical shifts provided evidence of abnormal intermolecular contacts in solution.

6. Parkinson's Disease (PD)

Parkinson's disease (PD) is a progressive neurodegenerative disorder characterized by impaired motor function manifested by resting tremor, rigidity, bradykinesia, and postural instability. The pathophysiological features of PD include degeneration and death of dopaminergic neurons and the accumulation of intracellular inclusions designated as Lewy bodies.[301] PD is the most common neurodegenerative movement disorder. It affects more than 0.1% of the population older than 40 years of age.[302]

Lewy bodies (LBs) and dystrophic neurites (Lewy neurites) are a pathologic hallmark of PD and classically are round inclusions composed of a halo of radiating fibrils and a less defined core (Figure 1). Ultrastructurally, LBs are composed of 10−14 nm amyloid-like fibrils having α-synuclein, which can polymerize into ∼10 nm fibrils in vitro, as the primary structural component.[303]

PD has long been considered a nongenetic disorder. However, two genes have recently been discovered clearly associated with the disease: (i) α-synuclein (PARK1)[304] and (ii) parkin (PARK2),[305] and other contributing genes have been indicated. As the work on Alzheimer's disease has suggested, when multiple genes influence a single disorder, those genes may define a pathogenic biochemical pathway. It is not yet clear what this pathway might be in Parkinson's disease, but the notion that protein degradation might be the key pathogenic pathway is becoming more and more popular. Dopaminergic neurons may be more sensitive to the disease process than other neurons because they sustain more protein damage through oxidative stress induced by dopamine metabolism. However, work on the molecular basis of Parkinson's disease is currently less advanced than work on other neurodegenerative disorders; as additional genes are found, other pathogenic mechanisms may emerge.

α-Syn is a small, 14 kDa protein that has sequence homology to three other proteins termed *β*-synuclein (*β*-syn), *γ*-synuclein (*γ*-syn), and synoretin.[306] These proteins are more highly homologous within the amino-terminal half, which encompasses five to six degenerate KTKEGV repeats. Of these proteins, α-syn has the greatest sequence homology to *β*-syn (Figure 29).[307] Furthermore, the expression and intracellular localization of α- and *β*-syn are very similar. They are both predominantly expressed in neurons of the central nervous system. In contrast, *γ*-syn is predominantly expressed in neurons of the peripheral nervous system, although it is also found at low levels in the brain but diffusely distributed throughout the cytoplasm. Synoretin is similar to *γ*-syn with respect to amino acid sequence and intracellular distribution, but synoretin is mainly expressed in the retina. α-syn comprises 140 amino acids distributed in three different regions: (i) the amphipathic N-terminus (residues 1−60); (ii) the highly hydrophobic self-aggregating sequence known as NAC (non-A*β* component, residues 61−95), which is presumed to initiate fibrillation; and (iii) the acidic C-terminal region (residues 96−140).

α-Synuclein is an intrinsically unfolded or natively unfolded protein that assembles into LB-like filaments, whereas its related homologues *β*- and *γ*-synuclein do not.[308] Residues 71 to 81 of α-synuclein are essential for filament assembly. α-Synuclein appears to be associated with membrane compartments in cultured cells and brain tissue through interactions with acidic head groups of phospholipids.[309] Membrane-bound α-synuclein may play an important role in fibril formation.[310]

Studies in human postmortem material indicate that reactive oxygen species are important in the pathogenesis of sporadic PD.[311] There are also consistent findings of the impaired functioning of mitochondrial complex I (NADH CoQ10 reductase), since derangements in complex I clearly lead to aggregation and accumulation of α-synuclein,[312,313] and other forms of oxidative stress promote α-synuclein aggregation. Oxidative damage appears to play a role in the aggregation of α-synuclein in sporadic PD, as there is selective α-synuclein nitration in synuclein lesions in PD and related disorders.[314] It was therefore suggested that inhibition of complex I creates an environment of oxidative stress that ultimately leads to aggregation of α-synuclein and the subsequent death of neurons (Figure 30).[301] Dysfunction of complex I results in oxidative stress, free radical formation, and reduced ATP formation; these events lead to neuronal depolarization and contribute to excitotoxic neuronal injury

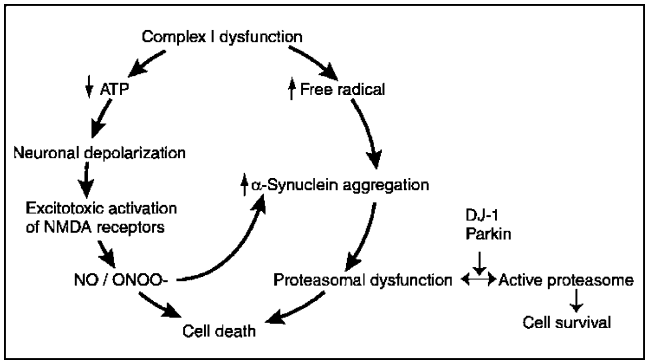

Figure 30. Complex I deficiency may be central to sporadic PD. Reprinted with permission from *Science* (http://www.aaas.org), ref 301. Copyright 2003 AAAS.

and further free radical-mediated injury involving NO and peroxynitrite and a feedforward cycle of increasing oxidative stress and injury. Complex I deficiency leads to accumulation and aggregation of α-synuclein, with dysfunction of the proteasome and consequent cell death. Familial-associated mutations in α-synuclein bypass complex I deficiency, but they promote α-synuclein accumulation and aggregation. Parkin appears to be a multipurpose neuroprotective agent that may allow the cell to more readily handle proteasomal impairment. Loss of parkin function may decrease the cells' ability to deal with proteasomal dysfunction. DJ-1 may function as a chaperone, and its absence may also decrease the cells' ability to deal with proteasomal dysfunction.[301]

The protein undergoes dramatic conformational transitions from its natively unstructured state to an α-helical conformation upon interaction with lipid membranes,[315,316] or to the characteristic crossed β-conformation in highly organized amyloid-like fibrils under conditions that trigger aggregation.[317] The kinetics of fibrillation of α-syn are consistent with a nucleation-dependent mechanism,[318] being modulated by factors and effectors of different types: low pH and high temperature,[319] organic solvents,[320] heparin,[321] polyamines,[322] and metal cations[323] all accelerate aggregation.

After having shown that α-synuclein self-oligomerizes when interacting with the peptide corresponding to Aβ_{25-35} in an orientation-specific manner,[324] the effect of various metals on such self-oligomerization was investigated and evidence was gained that (i) copper(II) is the most effective metal ion, (ii) the process depends on the acidic C-terminal region, and (iii) its underlying biochemical mechanism was distinct from that of the Aβ_{25-35}-induced oligomerization.[325] For the first time a possible link between abnormal copper homoeostasis and the onset of PD could therefore be suggested. Since oxidatively modified protein could increase its own tendency toward protein aggregation, copper-catalyzed oxidation of α-synuclein was examined in the presence of hydrogen peroxide or eosin: the protein was also self-oligomerized into an SDS-resistant ladder on the gel.[326]

Starting from the first recognition of a positive correlation between the prevalence of PD and industrialization,[327] the idea has slowly emerged that this disorder is likely to be an "environmental" disease. In fact, several studies have implicated such environmental factors as pesticides, herbicides, and heavy metals in the origin of PD.[328]

The possible involvement of heavy metals in the etiology of PD has emerged from the results of epidemiological studies. Postmortem analysis of PD brain tissues further

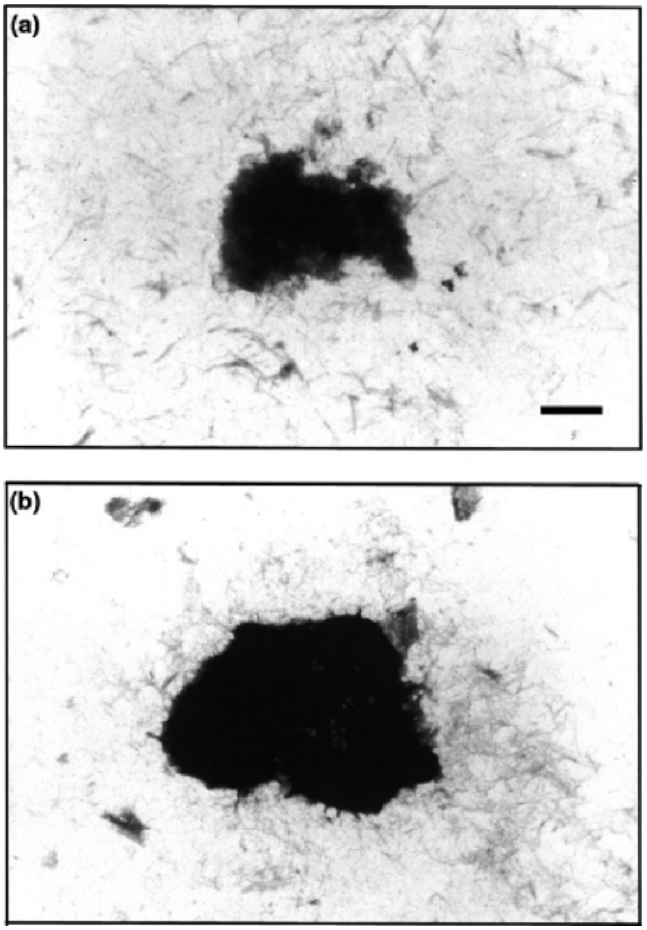

Figure 31. Copper localization to the protein aggregates of α-synuclein prepared in the absence (a) and presence (b) of phosphatidylinositol. The scale bar in part a represents 1.43 μm. Reprinted with permission from ref 332. Copyright 2003 Blackwell Publishing.

ratified a considerable increase in total iron, zinc, and aluminum content of the parkinsonian substantia nigra. A study of the effects of various metals on the kinetics of fibrillation and in inducing conformational changes of recombinant α-synuclein revealed that Al(III) and Cu(II), Fe(III), Co(III), and Mn(II) were the most effective metal ions,[329] with a strong correlation to increasing ion charge density. It was therefore suggested that the potential for ligand bridging by polyvalent metal ions is an important factor in the metal-induced conformational changes of α-synuclein.

Following the hypothesis that copper can be released from oxidatively damaged Cu,Zn−SOD, aggregation of α-synuclein was experimentally observed upon incubation with both Cu,Zn−SOD and H_2O_2.[330] Since the process was inhibited by radical scavengers, spin trapping agents, and copper chelators, the aggregation of α-synuclein was apparently mediated by the Cu,Zn−SOD/H_2O_2 system via the generation of the hydroxyl radical by the free radical-generating function of the enzyme.

Since hydrogen peroxide-mediated ceruloplasmin (CP) modification can induce the formation of free radicals and release of copper ions, the role of CP was investigated in the aggregation of α-synuclein,[331] and as in the case of Cu,-Zn−SOD, aggregation of α-synuclein was shown to possibly be mediated by the CP/H_2O_2 system via the generation of the hydroxyl radical.

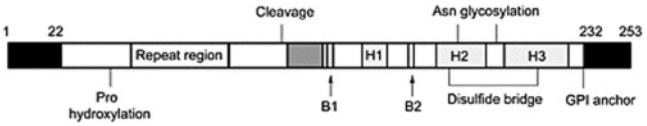

Figure 32. Schematic diagram of human PrP showing signal peptides (black), the hydrophobic region (gray), α-helical regions (denoted with H1−3), and β-strands (denoted with B1−2). Indicated are sites for glycosylation (Asn181, Asn197), hydroxylation (Pro44), and cleavage (Lys112/His113). Cysteines 179 and 214 form a disulfide bridge. Reprinted with permission from ref 342. Copyright 2003 Oxford University Press.

The coexistence of α-synuclein and lipids in Lewy bodies inspired the study of the interactions between these molecules by observing lipid-induced protein self-oligomerization in the presence of a chemical coupling reagent.[332] Self-oligomerization was induced by phosphatidic acid, phosphatidylinositol, phosphatidylserine, phosphatidylethanolamine, and even arachidonic acid but not by phosphatidylcholine. The lipid interaction site was on the N-terminal region of the protein, consistent with the structural transition to α-helices of the protein upon membrane interaction. The same lipids were also shown to enhance the self-oligomerization induced by Cu(II)/H_2O_2, and the measured fluorescence at 410−420 nm with excitation at 325 nm provided evidence of formation of a di-tyrosine cross-link. The presence of lipids was reported to enhance the affinity of Cu(II) for α-synuclein from a K_d of 44.7 μM to a K_d of 5.9 μm. Copper localization to the protein aggregates of α-synuclein was also qualitatively estimated with an electron microscope (Figure 31), which demonstrated that larger aggregates were formed with Cu(II) in the presence of phosphatidylinositol (Figure 31, panel b).

A comprehensive investigation of the effects of several metal ions on α-synuclein speciation has recently been reported.[333] Ca(II) and Co(II) were found to selectively induce rapid formation of discrete annular oligomeric species,

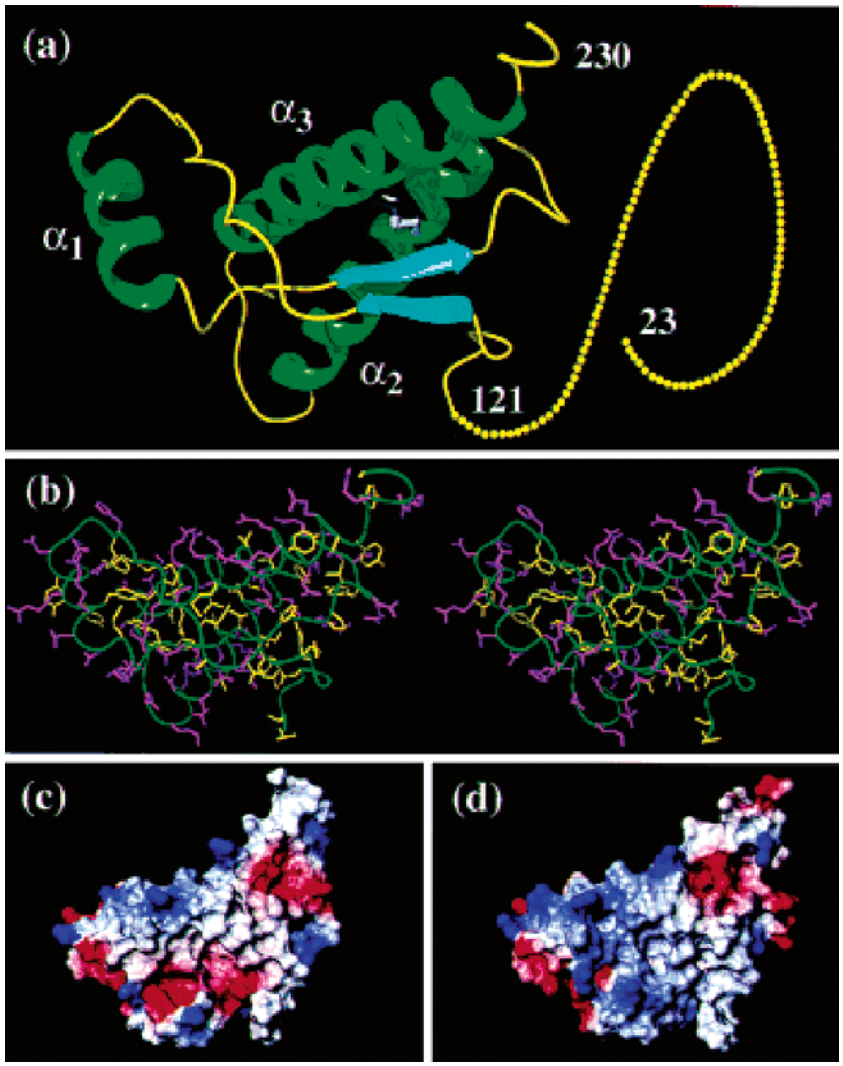

Figure 33. (a) Cartoon of the three-dimensional structure of the intact bPrP(23−230). Helices are green, β-strands are cyan, segments with nonregular secondary structure within the C-terminal domain are yellow, and the flexibly disordered "tail" of residues 23−121 is represented by 108 yellow dots, each of which represents a residue of the tail (the numeration for hPrP is used, and the insertions and deletions are placed according to the alignment in ref 23). (b) Stereoview of an all-heavy atom presentation of the globular domain in bPrP(23−230), with residues 121−230, in the same orientation as in part a. The backbone is shown as a green spline function through the Cα positions, hydrophobic side chains are yellow, and polar and charged side chains are violet. (c and d) Surface views of the globular domains of bPrP and hPrP, respectively. The orientation of the molecule is slightly changed relative to that of part a, so that residue 186 is approximately in the center. The electrostatic surface potential is indicated in red (negative charge), white (neutral), and blue (positive charge). The figures were prepared with the program MOLMOL. Reprinted with permission from ref 347 Copyright 2000 National Academy of Sciences, U.S.A.

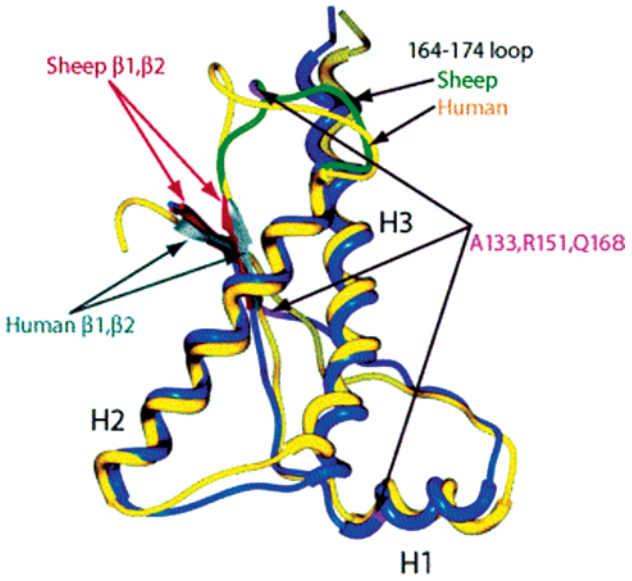

Figure 34. Comparison of the crystal structure of the globular domain of the ARQ allele of sheep PrP (blue) and the NMR structure of human PrP (yellow): least-squares superimposition of common residues, with an rmsd = 1.73 Å for 100 Cα atoms. In addition to the three helices, the intramolecular β-sheet is shown in red for sheep PrP and gray for human PrP. The loop 164−174 between β2 and H2 is shown in green for sheep PrP. The three polymorphic residues of sheep (A133, R151, Q168) are shown in magenta (Figure drawn with Spock). Reprinted with permission from ref 348. Copyright 2004 Elsevier.

and three classes of effects could be defined with different groups of metal ions: (a) Cu(II), Fe(III), and Ni(II) yielded 0.8−4 nm spherical particles, similar to the result for α-synuclein incubated without metal ions; (b) Mg(II), Cd(II), and Zn(II) gave larger, 5−8 nm spherical oligomers; and (c) Co(II) and Ca(II) gave annular oligomers, 70−90 nm in diameter with Ca(II) and 22−30 nm in diameter with Co(II).

Truncated α-synuclein (1−125), lacking the C-terminal 15 amino acids, did not form annular oligomers upon calcium addition, indicating the involvement of the calcium binding domain.

The structural characterization of Cu(II) interacting with α-syn has recently been reported.[334] Copper(II) was demonstrated to be effective in accelerating protein aggregation at physiologically relevant concentrations without altering the resultant fibrillar structures. UV−vis, CD, EPR, and NMR were used to locate the primary binding site at the N-terminus, involving His-50 as the anchoring residue and other nitrogen/oxygen donor atoms in a square-planar or distorted-tetragonal geometry. The carboxylate rich C-terminus was shown to potentially coordinate a second Cu(II) ion with a 300-fold reduced affinity.

7. Prion Diseases (PrPD)

7.1. The Prion Protein

Many lines of evidence have related certain transmissible degenerative diseases that affect humans and other mammals (bovine spongiform encephalopathy (BSE) or "mad cow disease" in cattle, scrapie in sheep, chronic wasting disease (CWD) in deer and elk, and Creutzfeldt−Jakob disease (CJD)

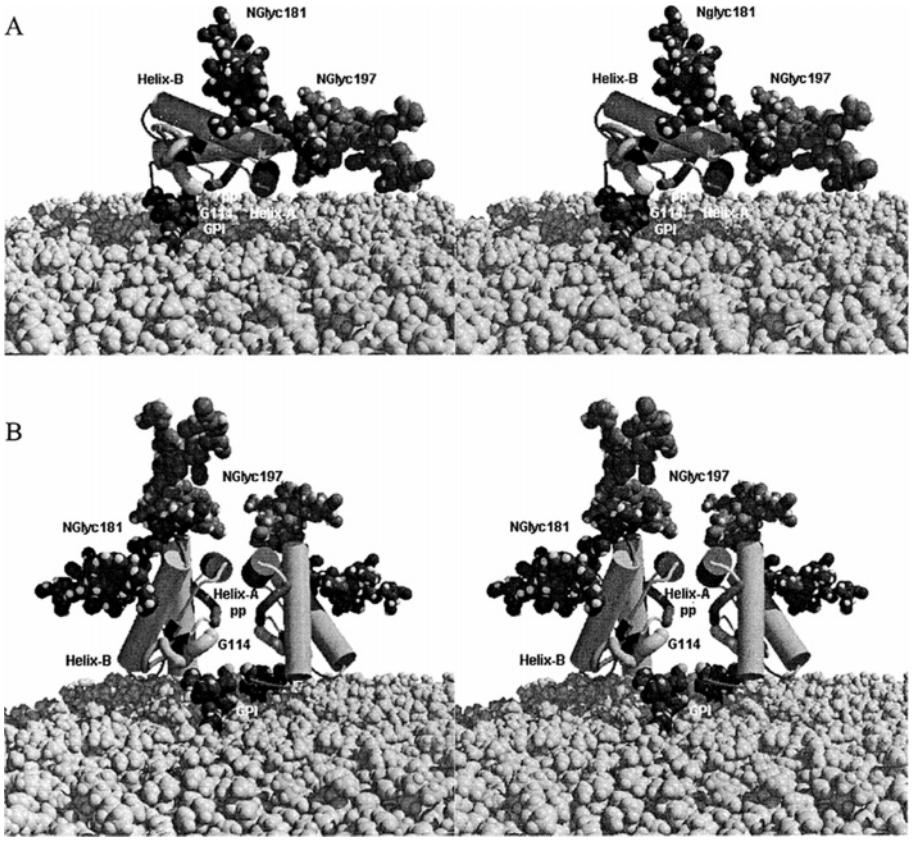

Figure 35. Stereo representation of two possible orientations of human PrP with respect to the membrane. (A) The monomeric lying-down model in which helix-A is in close contact with the polar surface of the membrane. (B) The dimeric standing model with helix-A and the C-terminal part of the PrP^{Sc}−PrP^{C} binding region, PrP(135−141), forming the interaction between the two monomers. Reprinted with permission from ref 351. Copyright 2000 Oxford University Press.

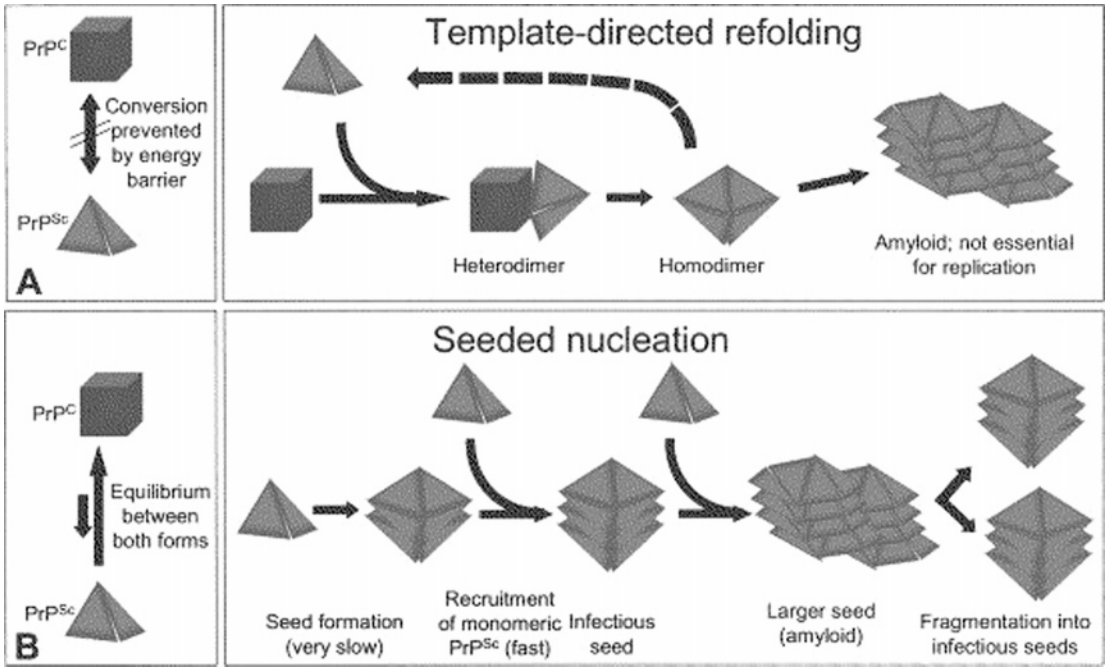

Figure 36. Models for the conformational conversion of PrP^C into PrP^{Sc}: (A) The "refolding" or template assisted model. (B) The "seeding" or nucleation−polymerization model. Reprinted with permission from ref 354. Copyright 2004 Elsevier.

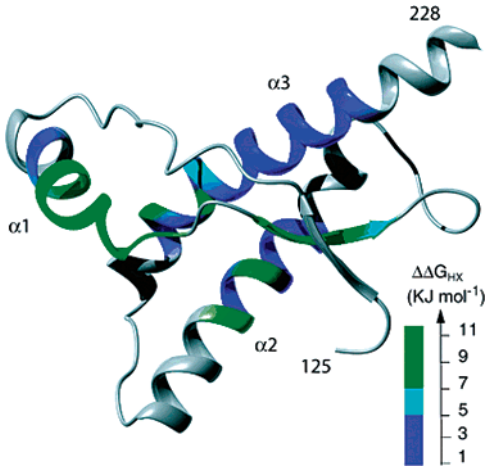

Figure 37. Difference of the free energy of exchange ($\Delta\Delta G_{HX}$) of individual backbone amide atoms between pH 7.0 and 4.5. The $\Delta\Delta G_{HX}$ values are displayed on a ribbon diagram of the 3D structure of hPrP(121−230) determined at pH 7.0. Individual amino acids are colored according to $\Delta\Delta G_{HX}$. Reprinted with permission from ref 364. Copyright 2003 The American Society for Biochemistry & Molecular Biology.

in humans) to changes in the conformation of the cellular prion protein (PrP^C). Prion diseases usually respect the species barrier,[335] but a few rare exceptions exist, as in the transmission of disease from scrapie-infected sheep to cattle, producing bovine spongiform encephalopathy (BSE) with subsequent penetration into the human population as the variant Creutzfeldt−Jakob disease (vCJD).[336]

The prion protein is a normal cellular component expressed by many cell types but found at much higher levels in neurons.[337] A glycosylphosphatidylinositol (GPI) anchor ties the protein to the outside surface of cells, and endocytosis cycles PrP^C back and forth from the endosome.[338]

PrP^c is a protease-sensitive, α-helix-containing protein, whereas its conformationally altered counterparts are partially resistant to proteinase K treatments, form aggregates or fibrils, and present a decreased content of α-helix and an increase of β-sheet structure.[339] It is not clear how conversion occurs, but PrP^c is absolutely necessary for development of prion disease, and several reports have implicated intracellular PrP^c trafficking in this process.[340]

Understanding of prion diseases has advanced over the past few years (A few years ago, it was memorably stated that "prion diseases constitute one of the best-understood groups of neurodegenerative diseases".);[341] however, despite these advances, the physiological role(s) of PrP^c is still under discussion.

PrP^c (Figure 32)[342] is encoded by *PRNP*, a small, single-copy gene on chromosome 20, which is expressed at highest levels in neurons.[343] The human PrP^c protein is synthesized as a 253 amino acid polypeptide chain from which the first 22 amino acids (signal peptide) are cleaved shortly after translation. Post-translational processing adds a C-terminal GPI anchor at residue 230, which facilitates glycolipid linkage of PrP^c to the cell membrane. Two N-linked glycosylation sites are located at residues 181 and 197. A nonapeptide followed by four identical octapeptide repeats is normally located between residues 51 and 91. A normal polymorphism (valine or methionine) resides at residue 129.

Many NMR investigations have been reported by Wüthrich et al.,[344] James et al.,[345] and Viles et al.[346] The NMR analysis of recombinant PrP^c from various species suggests that all consist of three α-helical regions (two linked by a disulfide bridge), a short antiparallel β-pleated segment, and a flexibly disordered N-terminus up to residue 120. The overall structure is that of a small globular protein (Figure 33).[347] There is a high level of structural homology between bovine and human PrP.[347]

Crystallographic studies supported this monomeric structure (Figure 34),[348] but, in the dimeric form, an unusual domain swapping of helix 3 is apparent, with creation of a novel short antiparallel β-sheet segment at the molecular interface.[349] NMR and solid-state structures refer to the non-glycosylated PrP^C despite a likely role of glycans in protecting the protein from conversion into the disease-associated form.[350] Molecular dynamics simulations shed

Figure 38. Schematic view of the structural conversion of PrP^{C} into pathogenic PrP^{Sc}. Shown are the solution structure of the carboxyl-terminal domain of PrP^{C} and a structural model of PrP^{Sc} for the corresponding amino acid sequence. Secondary structure elements are color-coded according to their occurrence in the solution structure of the cellular conformation (red = α-helix; cyan = β-sheet). Whereas helices 2 and 3 remain helical in PrP^{Sc}, helix 1, which is encircled in the structure of PrP^{C}, is incorporated into the left-handed β-helix that builds up the amino-terminal part of PrP^{Sc}. Reprinted with permission from ref 367. Copyright 2003 The American Society for Biochemistry & Molecular Biology.

light on a possible role of the two N-linked glycans and the GPI anchor.[351] It was, in fact, apparent that the glycans stabilize the structured parts of the protein, whereas the GPI anchor retains flexibility and apparently maintains the protein at 0.9−1.3 nm from the membrane surface, with little influence on its structure or orientational freedom (Figure 35).[351]

7.2. $PrP^{C} \rightarrow PrP^{Sc}$ Transition

In contrast with the detailed knowledge on PrP^{C}, little is known about PrP^{Sc} or the $PrP^{C} \rightarrow PrP^{Sc}$ transition. It is generally accepted that the formation of protease-resistant and infectious forms is driven by a template-assisted conformational change of PrP^{C}. In the case of inherited disease, abnormal forms of PrP^{C} result from mutations in the *PRNP* gene. This abnormal misfolded protein subsequently accumulates in the endoplasmic reticulum. The main drawback in prion research is the difficulty in relating in vivo and in vitro data, also exemplified by the generically defined binding partner Protein X argued from experiments on transgenic mice.[352]

A number of in vitro models have been described dealing with conversion of purified predominantly α-helical PrP into an aggregated form with high β-sheet content.[353] As anticipated, the main catalyst of the $PrP^{C} \rightarrow PrP^{Sc}$ conversion is PrP^{Sc} itself that either may act as a template for a self-perpetuating change of PrP^{C} (Figure 36A)[354] or may aggregate by a process of "nucleation" on a pre-existing seed of PrP (Figure 36B).[354] The first model postulates an interaction between exogenously introduced PrP^{Sc} and endogenous PrP^{C}, which is induced to transform itself into further PrP^{Sc}. Spontaneous conversion of PrP^{C} into PrP^{Sc} may be prevented by a high energy barrier. The second "seeding" model proposes that the two PrP isoforms are in thermodynamic equilibrium. Only when some monomeric PrP^{Sc} molecules form a highly ordered "seed" will further monomeric PrP^{Sc} be recruited and amyloid aggregates eventually form.[354]

Several lines of evidence support the view that PrP^{Sc} may exist in different interconvertible structures controlled by copper or zinc.[355−357] Based on the prion−copper connection (section 7.5), a model was suggested based on significant similarities among PrP and some transcription factors and zinc-finger proteins.[358] According to this model, copper binding could create intramolecular bridges in PrP^{C} but intermolecular bridges in PrP^{Sc}.

The pH of the environment where the conformation transition occurs is apparently very important (accumulation of even small quantities of misfolded PrP in the cytosol is strongly neurotoxic),[359] but the subcellular localization of the transition is controversial.[360] The transition is enhanced at acidic pH in vitro,[361] the free energy of unfolding of hPrP-(90−231) is lower in acid pH than in neutral pH,[362] and hPrP-(90−231) forms a folding intermediate that contains a large amount of β-sheet secondary structure in acidic guanidinium chloride, as does mouse PrP(121−231) at low pH in urea but not at neutral pH.[363] NMR structures have mainly been obtained under acidic solution conditions. The NMR structure of the globular domain of the human prion protein (hPrP) at pH 7.0 showed the same global fold, but slight, strictly localized, conformational changes were observed,[364] presumably determined by protonation of His-155 and His-187 (Figure 37). As shown in this figure, amide proton protection factors map local differences in protein stability within residues 154−157 at the C-terminal end of helix α1 and residues 161−164 of β-strand 2. These two segments appear to form a separate domain that at acidic pH has a larger tendency to unfold than the overall protein structure. It was therefore suggested that this domain, while providing a "starting point" for pH-induced unfolding, might be implicated in the endosomic PrP^{C} to PrP^{Sc} conformational transition. As a matter of fact, it was considered that the globular structured domain can be further divided into two subdomains:[365] (i) one long hairpin subdomain comprising helix 1 and the β-sheet; and (ii) one purely α-helical subdomain encompassing helices 2 and 3.

PrP^{Sc} probably incorporates the unstructured domain and the long hairpin subdomain into a left-handed β-helix while the helical subdomain is supposed to retain its structure, as suggested by electron-crystallographic data.[366] This being the case, helix 1 has to undergo a major structural rearrangement from an α-helix into a structure involving a significant amount of β-sheet (Figure 38).[367] In addition, it was noticed that helix 1 possesses several other unique features: (i) 6 of 11 residues of the helix extending from Asp-144 to Met-154 in the mean NMR structure of human prion protein are charged at neutral pH,[368] such that helix 1 was defined as "the most hydrophilic helix in all of the known protein structures";[369] (ii) very few long-range interactions occur; and (iii) a significant number of backbone hydrogen bonds are solvent-accessible.[370]

NMR and CD studies of peptides encompassing helix 1 and flanking sequences indicated intrinsic helix propensity of the helix 1 region such that the helix survives to high ionic strength, with pH variation, and in the presence of organic cosolvents.[367] These results therefore suggest that

interconversion of helix 1 represents a barrier rather than a seeding point for the $PrP^{C} \rightarrow PrP^{Sc}$ conversion.

By the same token, pH dependence was also shown to affect the structure of the octapeptide repeat region, comprising repeats of the sequence PHGGGWGQ. The structure of the octapeptide repeats at pH 6.2 revealed a new structural motif that was causing a reversible pH-dependent PrP oligomerization (Figure 39).[371] The aggregation motif is made by the segment HGGGW adopting a loop conformation and by GWGQ adopting a β-turn-like structure (Figure 40).[371] It is interesting to compare this structure with that of the HGGGW$-Cu^{2+}$complex [372] since, as it will be later discussed, the suggestion can be made of a conformational transition that may trigger PrP aggregation.

While the N-terminal region is highly conserved among mammalian species, the C-terminal part shows inter- and intraspecies variation. In sheep, animals expressing the Ala136/Arg154/Arg171 (PrP^{ARR}) variant show resistance to scrapie, whereas those with PrP^{VRQ} or PrP^{ARQ} show susceptibility.[373] Interestingly, these variants undergo different conformational changes upon interaction with copper: PrP^{VRQ} showed an increase in β-sheet content, whereas PrP^{ARR} remained structurally unchanged.[374]

7.3. Prion Synthetic Peptides

Delineation of the function of the different PrP domains has often and valuably been approached in terms of synthetic peptides.[375] In particular, the synthetic fragment PrP(106−126) has been suggested as a good model for PrP^{Sc} due to the following:[376] (i) high propensity to adopt β-sheet conformations forming amyloid fibrils in vitro; (ii) partial resistance to proteolysis; (iii) induction of apoptotic death in primary cultures of neurons; and (iv) absence of toxicity on neurons derived from mice not expressing PrP^{C}.

CD and neurotoxicity studies have shown that the peptide activity is modulated by its hydrophobic domain.[377] It was then demonstrated that the two conserved Gly-114 and Gly-119 residues, by virtue of their intrinsic flexibility, prevent the peptide from assuming a structured conformation, favoring instead aggregation in amyloid fibrils.[378] In fact, the G114A and G119A peptides assume soluble β-structured conformations. Since these mutated peptides retain neurotoxicity, it was concluded that fibrillar aggregation is not necessary for the induction of toxic effects that, on the contrary, are likely to result from the occurrence of protofibrillar intermediates.

Progress on knowledge of the structure of PrP^{Sc} or of any fibril-forming fragments of PrP was made possible by a detailed structural model for Alzheimer's disease β-amyloid fibrils proposed on the basis of solid-state NMR data[183] and of hydrogen−deuterium (H/D) exchange coupled with NMR[187] or mass spectrometry.[379] In fact, investigation of the conformational characteristics of mouse PrP106−126 with electron microscopy, CD, NMR-detected H/D exchange, and molecular dynamics simulations revealed that fibrils contain ~50% β-sheet structure and that strong amide exchange protection is limited to the central portion of the peptide spanning the palindromic sequence VAGAAAAGAV.[189] Molecular dynamics simulations indicated that the peptide assumes a stable structure in water consisting of two four-stranded parallel β-sheets that are tightly packed against each other by methyl−methyl interactions. Fibril formation involving polyalanine stacking is consistent with the experi-

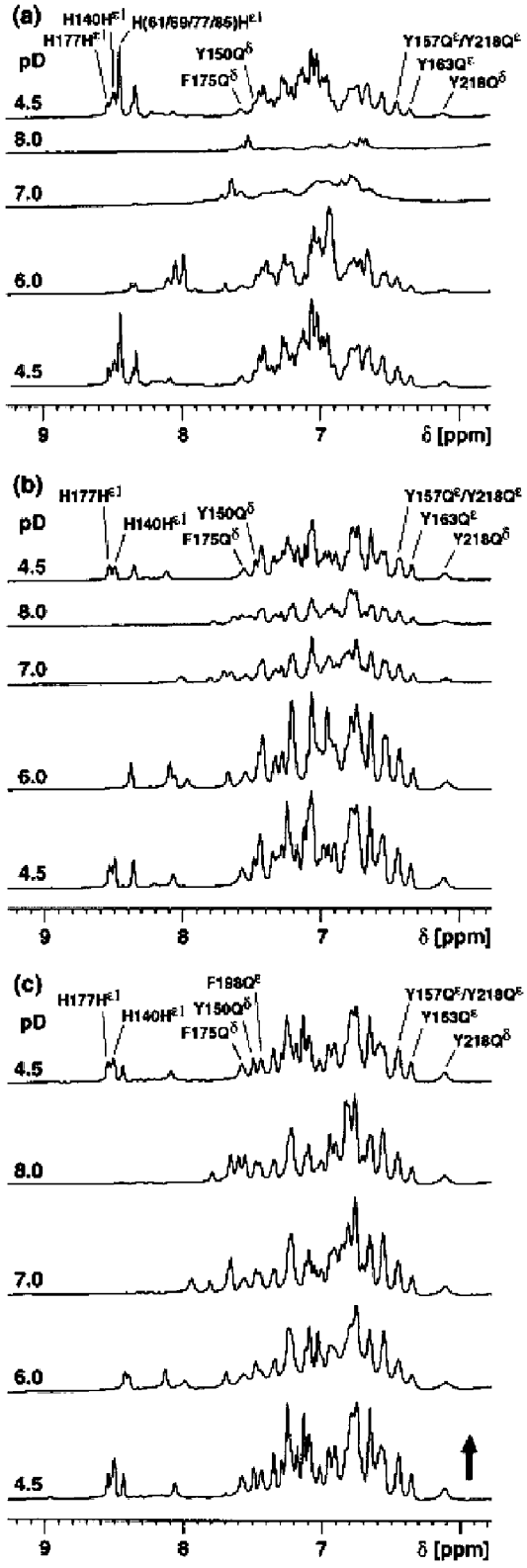

Figure 39. pD dependence of the hPrP ^{1}H NMR spectrum. Shown is the spectral region from 6 to 9 ppm in the 750 MHz ^{1}H NMR spectrum of a 0.6 mM solution of hPrP in D_2O at 20 °C. (a) hPrP(23−230). (b) hPrP(81−230). (c) hPrP(90−230). Prior to these experiments, the labile protons were exchanged with deuterons by dissolving samples in D_2O. Subsequently, the pD of the sample was increased from 4.5 to 8.0 in a stepwise fashion (see arrow bottom to top) by adding small amounts of NaOD, and finally it was decreased again to pD 4.5 by small additions of DCl (top spectrum). Assignments of selected aromatic resonances are indicated above the top spectrum in each series. Reprinted with permission from ref 371. Copyright 2003 Elsevier.

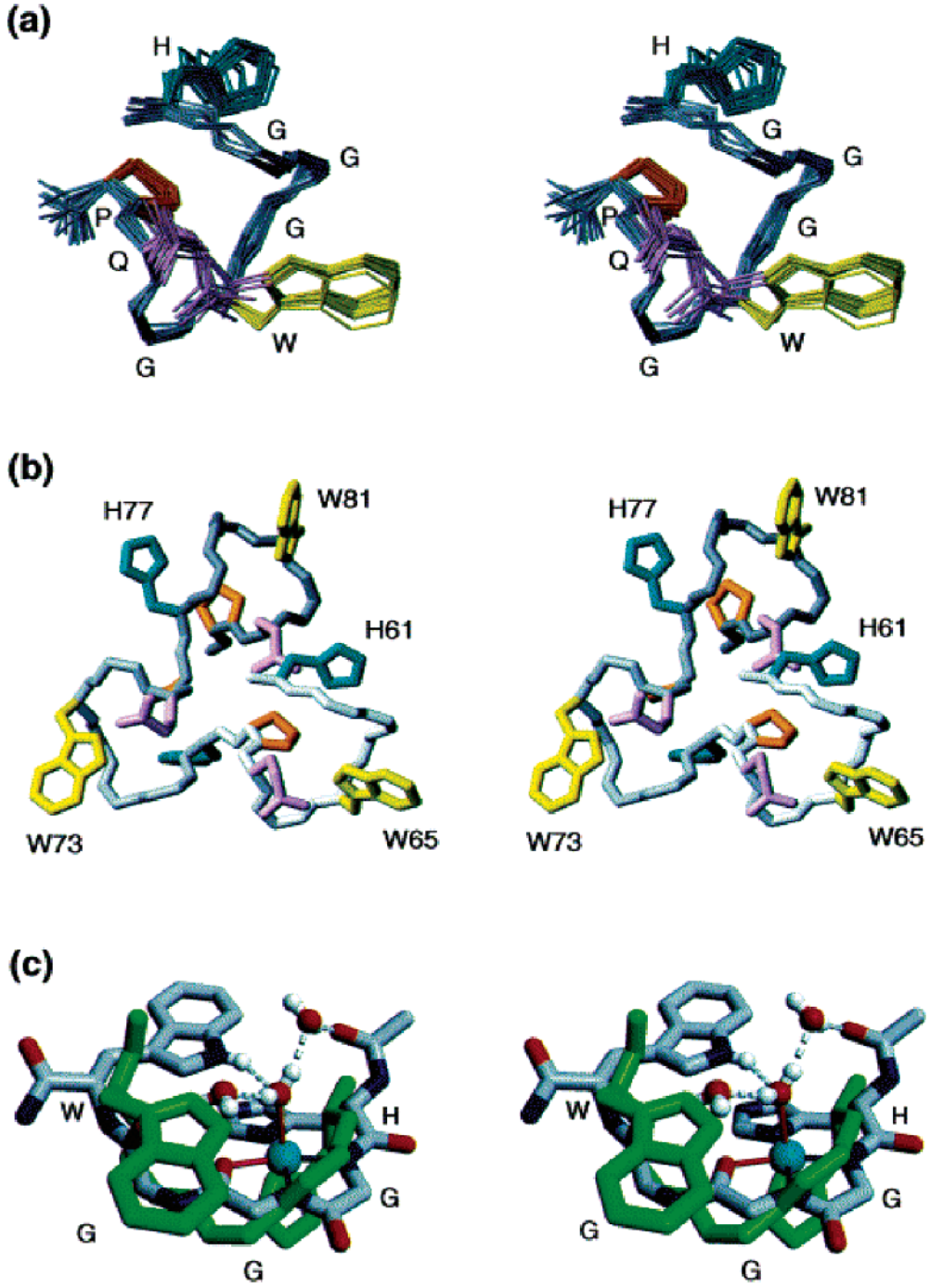

Figure 40. Stereoviews of octapeptide repeat structures. (a) All-heavy-atom representation of the 20 energy-refined DYANA conformers superimposed for best fit of the N, C· and C′ atoms of HGGGWGQP. The backbone is gray, and the side chains are shown in different colors: Trp (yellow), His (cyan), Gln (pink), and Pro (orange). (b) Representative structure of $(HGGGWGQP)_3$. The numbering corresponds to residues 61−84 in the human prion protein sequence. The same color code as in part a was used, except that the backbone atoms of the three repeats are indicated by different gray scales: light gray, residues 61−68; gray, residues 69−76; dark gray, residues 77−84. (c) Comparison of the NMR structure of unligated HGGGW and the X-ray structure of HGGGW−Cu^{2+}. The relative orientation of the two molecules resulted from a superposition for best fit of the backbone heavy atoms (RMSD 1.3 Å). The backbone and side chain heavy atoms of the NMR structure are in green. In the X-ray structure, the oxygen, nitrogen, carbon, and hydrogen atoms are displayed in red, blue, gray, and white, respectively. Hydrogen bonds between the pentapeptide and ordered water molecules are indicated as broken white lines. The position of the copper ion is indicated by a sphere in cyan. The red and blue lines indicate the coordination sites between copper and the peptide oxygen and nitrogen atoms, respectively. Reprinted with permission from ref 371. Copyright 2003 Elsevier.

mental observations. The same simulations performed on an octamer of the peptide TNVKHVAGAAAAGAVVGGLGG solvated by ∼5000 water molecules showed that two layers of parallel β-sheets (stacked in different orientations) were forming stable octameric complexes, whereas two layers of antiparallel β-sheets quickly collapsed into irregular globular structures. Two parallel β-sheets were therofere chosen for further simulation, providing the most stable complex shown in Figure 41.[189]

7.4. Prion Protein and Metal Ions

Prion infection of brain tissues has long been linked to impaired homeostasis of several metal ions, including, besides copper, also iron, manganese, and zinc. The similarity

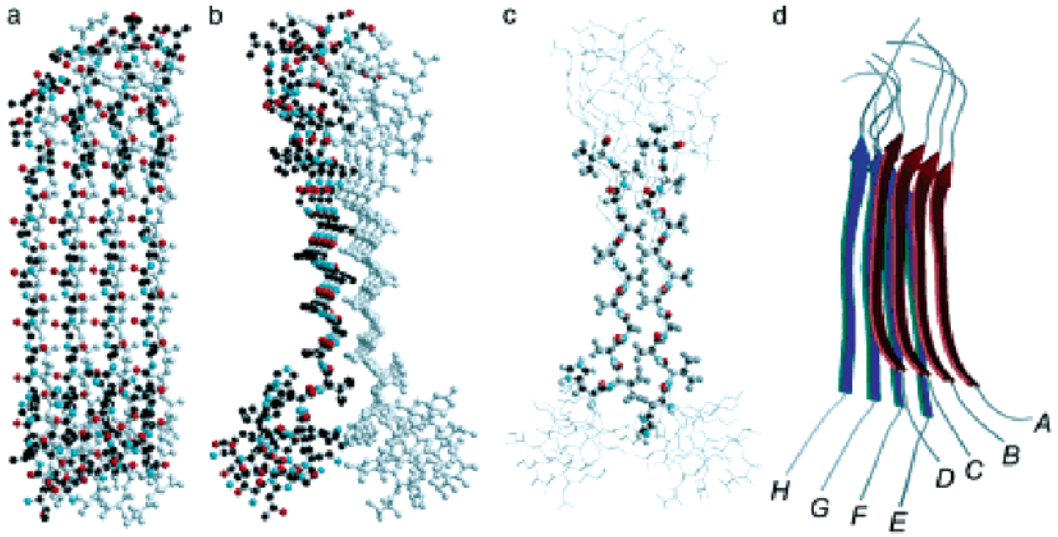

Figure 41. Representative structure of the octameric complex of PrP106−126 calculated by using MD simulations. All peptides are oriented with the N-terminus at the bottom. (a) Front view, using functional coloring for the top layer (strands A−D) and gray for the bottom layer (strands E−H). (b) Side view, using the same coloring scheme as in part a. (c) Side view, emphasizing the methyl packing interactions in the core of the complex. Residues (His-110 to Val-120) on two opposite strands (B and F) are shown as a ball-and-stick representation (including H), and other residues are shown as a wire diagram. (d) Schematic ribbon diagram of the predicted PrP106−126 fibril structure. Reprinted with permission from ref 189. Copyright 2003 National Academy of Sciences, U.S.A.

of transmissible spongiform encephalopathy (TSE) with many other neurodegenerative diseases[380] is emphasized by accumulation of PrP in cerebellar and cerebral cortices in the form of extracellular plaques.[381] Such similarity also includes various inherited human TSEs, caused by mutations of the *prnp* gene encoding PrP^C on chromosome 20.[382] All these diseases are further characterized by evident signs of oxidative damage in the affected area of the brain.[383] As a consequence, a first link with metal homeostasis is provided by the chemistry of redox-active metal ions that can produce reactive oxygen species through Fenton's reactions. As a matter of fact, PrP106−126 was observed to generate hydroxyl radicals upon preincubation with small amounts of Cu(II) followed by addition of Fe(II),[384] exactly in the same way as amyloid-β and α-synuclein do (vide supra). Moreover, when using the neurotoxic PrP121−231 fragment containing mutations (E200K, D178N, F198S) known to enhance the toxicity to cultured PrP-knockout neurones,[385] hydroxyl radicals could be generated by the addition of Fe(II).[386]

Other links with metal ions have emerged from studies showing direct interactions with PrP. In the absence of divalent cations, PrP^{Sc} molecules were >20-fold more sensitive to proteinase K digestion in low ionic strength buffers than in high ionic strength buffers. Addition of micromolar concentrations of copper restored the protease resistance of PrP^{Sc} molecules under conditions of low ionic strength. At low ionic strength, Cu(II) controls the conformation of purified truncated PrP27−30[≠] (The term PrP27−30 refers to the protease-resistant fragment of PrP^{Sc}, which has a ragged N-terminal and comprises residues 90−231.), confirming that deletion of the N-terminal octapeptide repeat region of PrP^{Sc} does not eliminate binding to copper.[387]

Disturbances in the levels of copper and manganese have been observed in prion-infected brain tissue.[388,389] A model consisting of PrP^C conversion into aggregated forms guided by changes in detergent concentration[390] was considered for investigating the effects of metal ions, and it indicated that Mn(II) more than Cu(II), Ni(II), Co(II), or Zn(II) displays a specific, strong proaggregatory effect at low milllimolar concentration that could be blocked by Cu(II) at nanomolar concentration.[391] The possible interconnection between copper and manganese was further investigated in light of the fact that loss of Cu binding occurs in prion disease,[388,389] such that substitution of Mn or other metals into the protein may occur,[356,392] and interaction with Mn causes conversion of PrP^c to PrP^{res}, as detected by in vitro studies.[393] The expected differences in the way the protein binds copper and manganese (Cu(II) is a soft metal ion with strong preference toward nitrogen donors; Mn(II) is a hard oxophilic ion) might therefore provide a relevant piece of information on the mechanism of conversion of the protein or its normal cellular activity. Near-IR spectroscopy coupled with multivariate analysis could in fact suggest that (i) PrP binds both Mn and Cu differently, (ii) PrP−Cu, and not PrP−Mn, protects the metal from the water, increasing protein stability, and (iii) PrP−Cu remains stable in solution, whereas PrP−Mn undergoes changes leading to fibril formation.[394] Substantial evidence supports the notion that, in conversion to the abnormal isoform, the Cu binding activity of PrP^c is lost,[395] and other ions, mainly Mn(II) or Mn(III), might prevent Cu from binding and affect Cu transport and resistance to oxidative stress.

7.5. The Prion–Copper Connection

A huge number of reports that have appeared so far have ratified a strong connection existing between prion biochemistry and infectivity and copper:[383,396]

(i) PrP^C binds Cu^{2+} within the octapeptide region with low micromolar affinity in a pH-dependent fashion, and more copper binding sites are located elsewhere toward the C-terminus (vide infra).[397−402]

(ii) Copper ions at concentrations ≥100 μM rapidly and reversibly stimulate clathrin-mediated endocytosis of PrP^C.[403−405]

(iii) A connection between PrP^C, copper ions, and protection of cells from oxidative stress is suggested by the SOD activity exhibited by recombinant PrP refolded in the

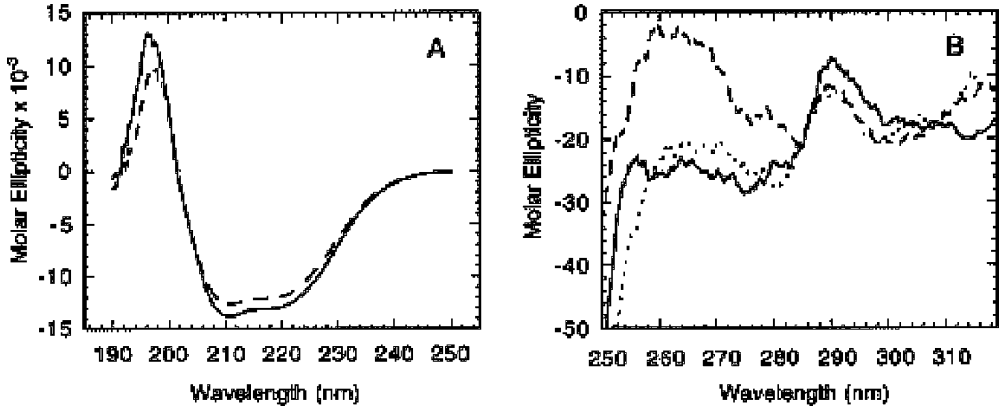

Figure 42. CD spectra of metal-free and copper-complexed SHaPrP(29−231). The near-UV CD spectra (A) indicate a mainly α-helical structure: (solid line) a metal-free preparation of SHaPrP(29−231) (4 μM) in 50 mM sodium acetate at pH 6 and (dashed line) after addition of 100 μM $CuCl_2$. The tertiary structure changes after addition of Cu^{2+}. (B): (solid line) metal-free SHaPrP(29−231) (6.7 μM) in 50 mM MES and 0.05% NaN_3 at pH 6 and (dashed line) after addition of 100 μM $CuCl_2$; (dotted line) purified PrP^C from hamster brain (2.9 μM). Reprinted with permission from ref 397. Copyright 1998 American Chemical Society.

presence of copper,[406] by the increased sensitivity to oxidative insult of neurons lacking PrP^C,[407] and by comparison of death signals in *prnp* gene deficient and wild-type mice.[408] Transition metal ions are indeed well-known catalysts of oxidative damage, and in the case of prions, induction of dimeric and truncated species has been demonstrated upon incubation with Cu(II) and dopamine.[409] It must however be mentioned that, very recently, new assays have been reported where no detectable dismutase activity was found for the recombinant prion protein.[410]

(iv) Reduced copper content and decreased SOD activity have been reported in the brains of *Prn-p*$^{0/0}$ mice,[411] a result not reproduced in other studies.[412,413]

(v) The prion protein is a target for oxidation by hydrogen peroxide which mainly directs against the His residues of the octarepeat region[414] and the two Met residues located in the PrP(106−126) region, but a significant increase in β-sheet structure occurs only in the presence of Cu(II).[415]

(vi) Cu(II) has recently been shown to inhibit the conversion of recombinant PrP(23−230) into amyloid fibrils at micromolar concentration and pH 7.2.[416] Such inhibitory activity was decreased by lowering the pH and also by using prion protein with deletion of the octarepeat region.

The role of copper in prion pathogenesis is evidently rather complex, and even the fact that the prion protein is directly involved in copper homeostasis is still a matter of debate. As an example, expression of a modified PrP molecule targeted to the secretory pathway in yeast was unable to rescue growth deficiency phenotypes of yeast strains harboring gene deletions of copper transporters, chaperones, pumps, reductases, and cuproenzymes.[417] These experiments refute the existence of a direct connection between copper utilization and PrP.

As already stated, the octapeptide repeat region selectively binds copper over other metal ions.[372,397,398,400,401,411,418−421] This region binds four Cu(II) ions likely cooperatively with identical coordination geometry,[372,399,421,422] and affinity in the range between 1 nM and 10 μM or even in the femtomolar range in one case.[399−401,423,424] A fifth Cu(II) binding site is centered at His-96 and His-111,[398,399,401,423] and coordination to a C-terminal fragment was further noticed.[425] In total, from four to approximately seven copper atoms were shown to bind purified PrP^C preparations from mouse and human brain, respectively.[388,393]

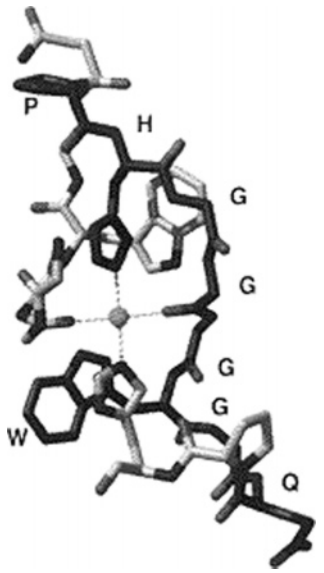

Figure 43. Possible conformation of Cu^{2+} binding to two octapeptide repeats. Copper is coordinated by two His residues and two Gly carbonyl oxygens and is bound in a square-planar geometry. Modeling was performed using the Sybyl software package (Tripos Inc.), and the structure was validated with PROCHECK. Reprinted with permission from ref 397. Copyright 1998 American Chemical Society.

CD and fluorescence spectroscopy on Syrian hamster PrP-(29−131) showed changes in the tertiary structure (from α-helical to β-sheet) induced by Cu^{2+}, which quenches the Trp fluorescence, shifts the emission spectrum to shorter wavelengths, and changes the near-UV CD spectrum (Figure 42).[397] Other ions (Ca^{2+}, Co^{2+}, Mg^{2+}, Mn^{2+}, Zn^{2+}) were not as efficient as copper. Two bound Cu(II) ions per PrP molecule were suggested, and binding was shown to strongly depend on pH (significant quench at pH ≥ 5). The possible conformation of the complex of Cu(II) with two repeats is shown in Figure 43.[397]

A series of Cu^{2+}−peptide complexes composed of 1-, 2-, and 4-octarepeats and several sub-octarepeat peptides, studied by X- and S-band EPR and CD at pH 7.45, showed two EPR active binding modes.[422] The dominant mode apparently involved coordination of three nitrogens and one oxygen, whereas two nitrogens and two oxygens were coordinated in the minor mode. Involvement of the histidine imidazole

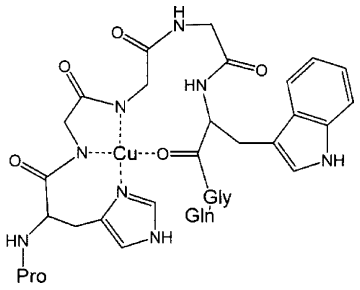

Figure 44. Proposed bond-line model of the dominant binding mode of the octarepeat segment (P**H**GGGWGQ). Reprinted with permission from ref 422. Copyright 2000 American Chemical Society.

was demonstrated by ESEEM (electron spin−echo envelope modulation). The fundamental Cu^{2+} binding unit was found to be HGGGW; a rigorous 1:1 Cu^{2+}/octarepeat binding stoichiometry was determined regardless of the number of octarepeats in a given peptide sequence. A model consistent with the data contained Cu^{2+} bound to the nitrogen of the histidine imidazole side chain, two nitrogens from sequential glycine backbone amides, and a carbonyl group from the backbone (Figure 44).[422]

The crystal structure of HGGGW in a complex with Cu^{2+} ratified previous data revealing equatorial coordination by the histidine imidazole, two deprotonated glycine amides, and a glycine carbonyl, along with an axial water bridging to the Trp indole (Figure 45).[372] The identified Gly−Cu linkage is unstable below pH ∼ 6.5 and thus suggests a pH-dependent molecular mechanism by which PrP detects Cu^{2+} in the extracellular matrix or releases PrP-bound Cu^{2+} within the endosome. An observed unusual complementary interaction between copper-structured HGGGW units suggested a mechanism for transmembrane signaling and perhaps conversion to the pathogenic form (Figure 46).[372] At extracellular pH, 7.4, each octarepeat binds a single Cu^{2+}, whereas at the endosomal pH, ∼6.0, the affinity for the metal ion is lowered by protonation of the amides competing with Cu^{2+} coordination (Figure 46a).[372] The octarepeat domain is ordered by Cu^{2+} at pH 7.4 in a way that brings the conserved Gln residues into close proximity to one another, facilitating intermolecular recognition between neighboring, membrane-bound PrP proteins. Such cross-linking may act as a molecular signal stimulating endocytosis and, when accompanied by rare events leading to partial unfolding of the globular domain, may allow for recognition between PrP-(90−120) regions, thereby facilitating formation of PrP^{Sc} (Figure 46b).[372]

Potentiometric and ^1H NMR studies on Ac-PHGGGWGQ-NH_2 interacting with Cu^{2+} ions at pH ∼ 7.4 revealed not only evidence of the binding site made of the imidazole nitrogen and the two amide nitrogens of Gly3 and Gly4, but also evidence for the folding of the peptide that brings the Trp residue into interacting distance with the metal ion, most

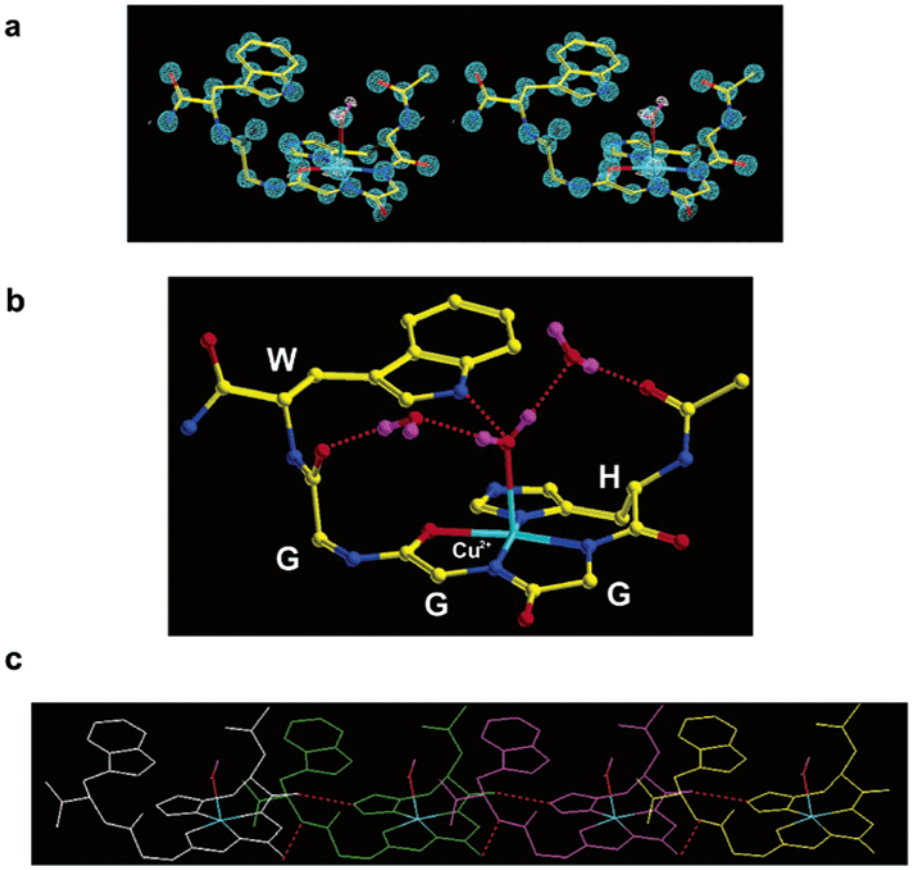

Figure 45. Crystal structure (0.7 Å resolution) of the HGGGW segment in complex with Cu^{2+}. (a) A stereo representation of the electron density is shown in blue. A difference map (white) reveals the hydrogen density for the axially bound water. (b) This molecular representation shows how copper coordination is from the histidine imidazole and deprotonated amides from the next two glycines. In addition, the NH of the indole is within hydrogen bonding distance to the oxygen of the axial water. Two additional intramolecular ordered water molecules are also shown. (c) The red dashed lines show intermolecular hydrogen bond contacts identified in the crystal. These four copies of the copper binding units suggest a possible way in which the full octarepeat domain orders. Reprinted with permission from ref 372. Copyright 2002 American Chemical Society.

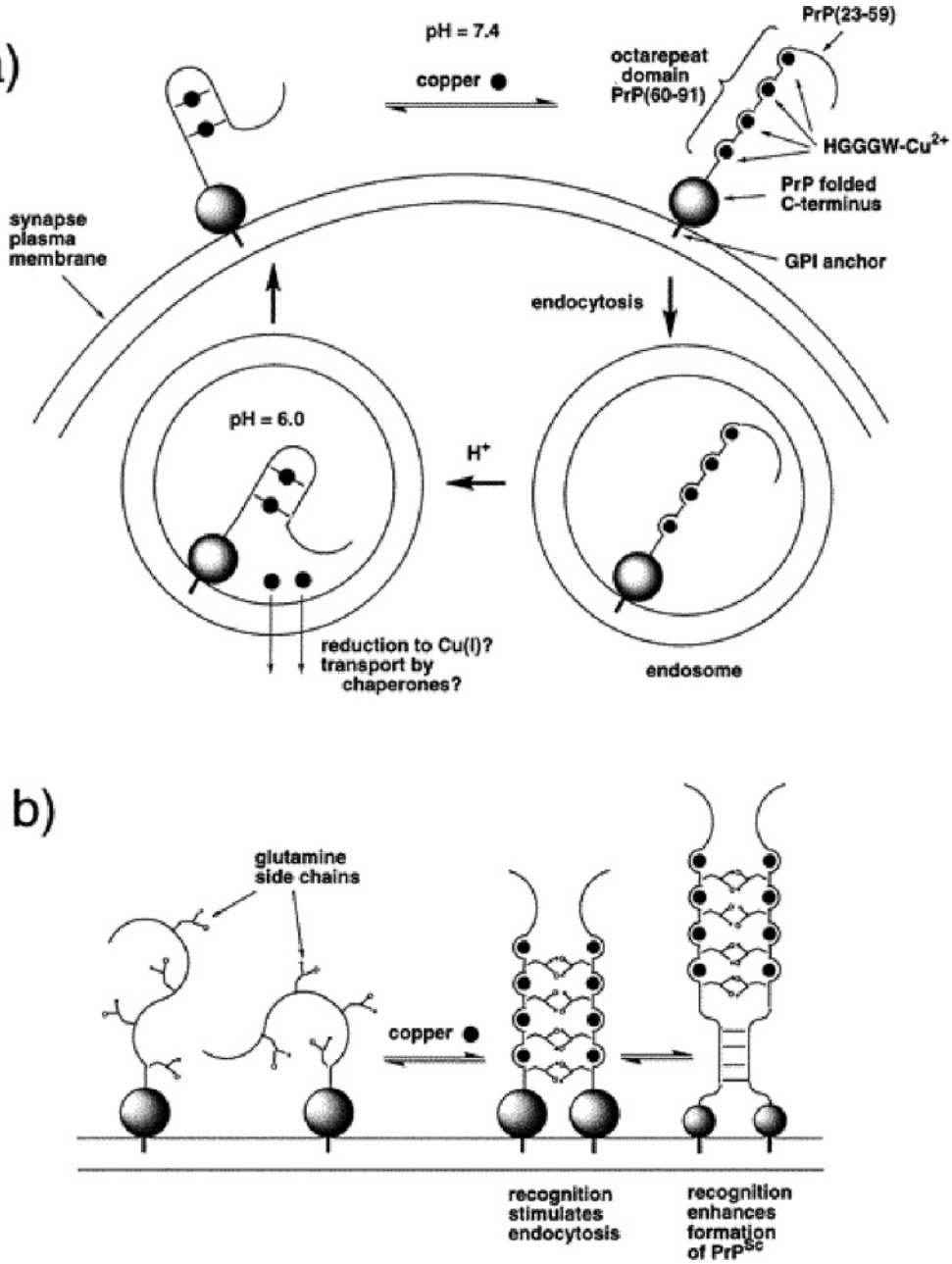

Figure 46. Working hypotheses for how the prion protein functions to transport Cu^{2+} through endocytosis and how the octarepeat domain participates in the formation of pathogenic PrP^{Sc}. Reprinted with permission from ref 372. Copyright 2002 American Chemical Society.

probably through a metal-bound water molecule (Figure 47).[50] The stability of the complex formed was similar to those of other peptides having a similar type of coordination, and the geometry around the Cu^{2+} ion was apparently slightly distorted from the tetragonal one.

EPR studies of copper interacting with full-length recombinant PrP were used to map all Cu(II) binding sites of the protein.[399] Five copper ions per protein were again determined (Figure 48), and variable pH studies demonstrated affinity for copper only above pH 6.0, as found with octarepeat peptides. Using a series of peptide constructs, along with S-band EPR and ESEEM, specific Cu^{2+} contacts in the site outside of the octarepeat domain were mapped.

CD studies on Cu^{2+} binding to various fragments of the octarepeat region of the prion protein were later reported, showing that (i) Cu^{2+} coordinates with a lower affinity for PrP than the femtomolar dissociation constant reported previously, (ii) each of the octarepeats does not form an isolated Cu^{2+} binding motif but folds up cooperatively within multiple repeats, and, (iii) in addition to the coordinating histidine side chain residues, the glycine residues and the

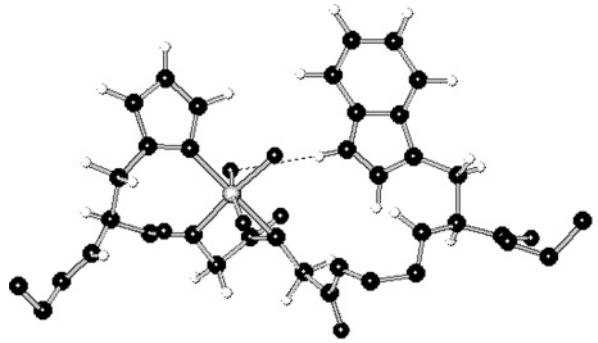

Figure 47. Molecular model of the copper(II)−PHGGGWG complex in water solution. Adapted with permission from ref 50. Copyright 2002 The Royal Society of Chemistry.

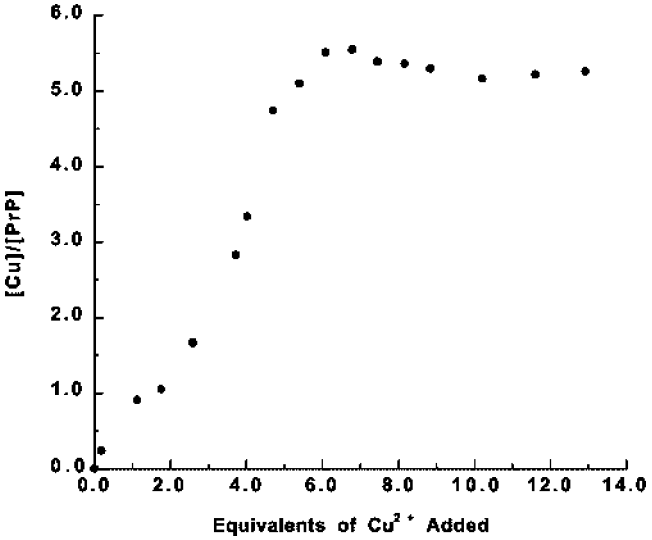

Figure 48. Integrated EPR signal intensity as a function of titrated Cu^{2+} at pH 7.4 for rSHaPrP(29−231). The protein concentration is 21 μM, and the copper ion concentration is reported in equivalents per protein. All data were collected at 85 K. Reprinted with permission from ref 399. Copyright 2003 American Chemical Society.

proline within each octarepeat are also necessary to maintain the coordination geometry.[424]

In an attempt to characterize Cu(II) binding outside the octarepeat region, a preferential binding site was located between residues 90 and 115 with a nanomolar dissociation constant.[426] Comparison of recombinant PrP with PrP(91−115) indicated that this prion fragment is a good model for Cu^{2+} binding to the full-length protein. A square-planar or square-pyramidal Cu^{2+} coordination utilizing histidine residues was demonstrated by NMR and EPR, and it was also shown that the high affinity site requires both His-96 and His-111 as Cu^{2+} ligands, rather than a complex centered on His-96, as previously suggested.[399] A loss of irregular structure on copper coordination with an increase in β-sheet conformation was shown, and the model shown in Figure 49 was provided.[426]

Following the characterization of Cu(II) binding to the octarepeat unit,[50] a similar potentiometric and spectroscopic approach was extended to prion fragments containing two and four octarepeat units.[427] Competition plots were used to compare the coordination power of the monomer, the dimer, and the tetramer, showing that (i) at pH 7.4 ~70% of the Cu(II) prefers to bind the dimer over the monomer and (ii) the tetramer is a stronger ligand than the dimer in the pH range 5.0−7.4 but not at pH ≥ 7.4. The NMR approach presented in section 2.2 allowed the structure of the Cu(II)−dimer complex (Figure 50) to be obtained, yielding evidence that the metal is bound to N_π of His-62 and N_τ of His-70.[427]

Since preferential Cu^{2+} binding to the unstructured amyloidogenic portion of PrP (residues 90−126) forms a square-planar complex,[399,426] and Ni^{2+} often replaces Cu^{2+} in square-planar diamagnetic complexes, detailed ^1H NMR and CD studies were recently reported for Ni^{2+} binding to PrP(23−231) with the octarepeat domain deleted, PrP(91−115), and PrP(90−126).[428] These data were apparently suggesting that Ni^{2+} and Cu^{2+} bind to His-96 and His-111 independently of each other in a similar coordination scheme, shown in Figure 51.

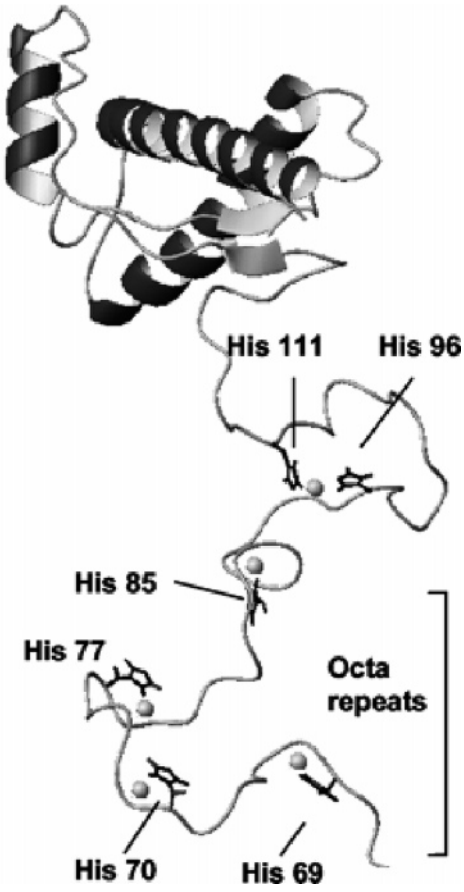

Figure 49. Model of PrP(57−231) showing binding positions of Cu^{2+} ions. The copper ligating histidine residues are highlighted, and the copper ions are shown as spheres. Distance geometry (Dyana) was used to incorporate a single copper ion at 2 Å from the N-ϵ atoms of His-96 and His-111. In addition, each HGGGW Cu^{2+} binding motif in the octarepeat region was similarly modeled using the crystal structure as a guide. Reprinted with permission from ref 426. Copyright 2004 The American Society for Biochemistry & Molecular Biology.

A different NMR approach, already discussed in section 2.2, was used for characterizing the binding properties of PrP106−126 toward Cu(II), Mn(II), and Zn(II) at pH 5.7.[41,429] ^1H and ^{13}C 1D spectra, ^1H spin−lattice relaxation rates, and $^1H-^{15}N$ and $^1H-^{13}C$ HSQC 2D spectra identified binding of Cu(II) and Mn(II) but not of Zn(II). Evaluation of the exchange rate from the metal coordination sphere allowed Cu(II)−^1H distances to be calculated and, then, restrained molecular dynamics simulations to be performed, providing a good structural model (Figure 52) with the imidazole nitrogen, the ionized amide nitrogen of His-111, and the amino-terminal group as metal ligands and the terminal carboxyl stabilizing the coordination sphere through ionic interactions. The hydrophobic C-terminal region does not affect the copper binding properties of the peptide and is left free to interact with other target molecules. As for the complex with Mn(II), qualitative information was obtained on the carbonyl oxygens of Gly-124 and Leu-125, beyond the terminal Gly-126 carboxyl, being at a close distance from the metal ion, that also interacts, most likely, through a hydrogen bond of metal-bound water, with the imidazole ring of His-111.

Very recently, a combination of X-band EPR, S-band EPR, and ESEEM allowed three distinct Cu(II) coordination modes of the octarepeat region at pH 7.4 to be identified.[430] Multiple His coordination was demonstrated at low copper stoichi-

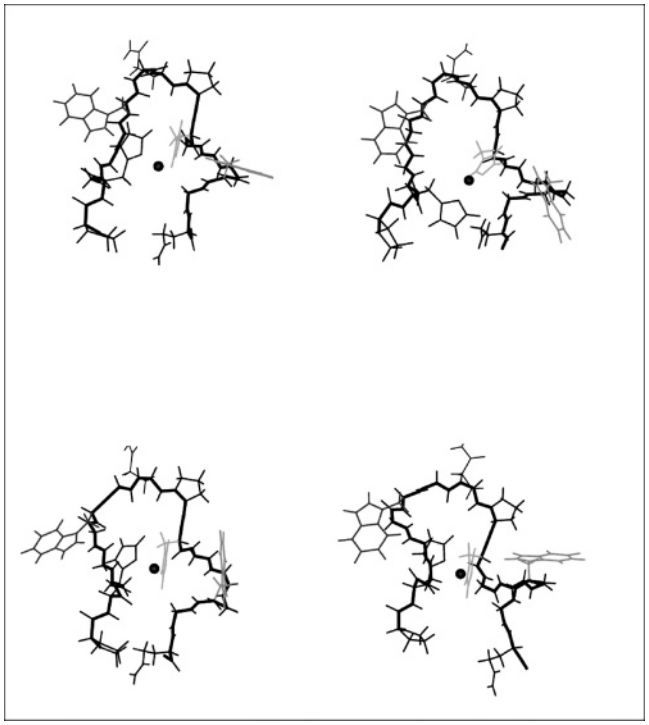

Figure 50. Structural details of the four best structures of the Cu(II)−PrP(61−76) complex. Structure calculation was performed by restrained molecular dynamics with simulated annealing in the torsional angle space. The figure was created with MOLMOL 2K.1.0. Reprinted with permission from ref 427. Copyright 2004 The Royal Society of Chemistry.

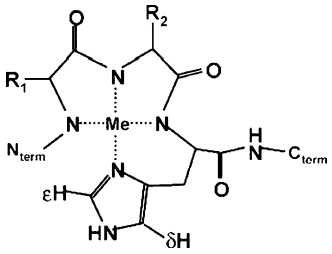

Figure 51. Schematic of the metal binding sites in PrP(91−115) and PrP(90−126). "Me" represents either a Ni^{2+} or Cu^{2+} ion. Gly-94 (R1), Thr-95 (R2), and His-96 provide ligands for one square-planar site. Met-109 (R1), Lys-110 (R2), and His-111 provide ligands for the second site. Reprinted with permission from ref 428. Copyright 2005 Elsevier.

ometry (component 3, Figure 53), whereas, at full occupancy, the octarepeat domain was (i) partially collapsing, (ii) stabilizing a specific binding mode yielding Cu−Cu dipolar interactions, and (iii) facilitating cooperative copper uptake (component 1). Detection of a third minor species (component 2) offered a view of the pathway from component 3 to component 1 at increasing Cu(II) occupancy.

The kinetic properties of Cu(II) reduction mediated by the octarepeat region have a maximal activity around pH 6.5, close to the pH in endosomes.[431] All four repeat units and, noticeably, at least one tryptophan side chain are essential for Cu(II) reduction. Evidence also was presented that supports a 1:1 Cu(II)-tetrarepeat active intermediate, where copper is coordinated by four histidine Nτ atoms (Raman spectra). Molecular mechanics calculations suggested that two tryptophan residues approach the Cu(II) site. It was therefore concluded that PrP may be active not only in capturing Cu(II) ions in the extracellular space and releasing them in the endosome but also in reducing the captured Cu(II) ions prior to their transfer to Cu(I)-specific intracellular copper-trafficking proteins.

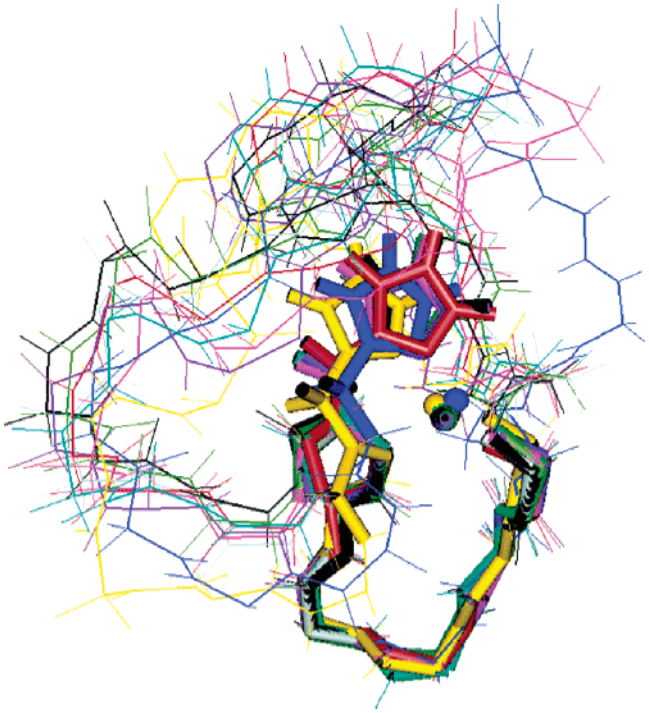

Figure 52. Superimposition of Cu(II)−PrP106−126 structures obtained from experimental data (blue); from energy minimization (yellow); and from molecular dynamics calculations (orange). All the other colored structures represent the snapshots from molecular dynamics. The figure was created with MOLMOL 2K.1.0. Reprinted with permission from ref 429. Copyright 2005 American Chemical Society.

8. Conclusions and Perspectives

This review has focused on the copper homeostasis and its eventual link with copper involvement in different neurological disorders. Copper is the redox active metal ion directly involved in reactions leading to the oxidative stress in cells and tissues. The copper homeostasis is carefully controlled by proteins including transport and storage proteins, enzymes, and chaperones. Copper plays a dual role in producing reactive oxygen species (Fenton reaction): damaging the cells and eliciting antioxidant activity (e.g. in SOD1).

Abnormal binding of metal ions to proteins or losing control over the copper homeostasis can result in serious disorders including these neurodegenerative diseases. The copper ion in SOD1 acts as the redox site, dismutating superoxide radicals O_2^- to O_2 and H_2O_2. Mutations within the SOD1 protein may result in loss of the antioxidant function of SOD or gain of a pro-oxidant function of this enzyme, leading to amyotrophic lateral sclerosis. The binding of copper ions to PrP^C may have a critical impact on metal transport, but abnormal binding of metal ions can cause conformation conversion and possibly play a role in prion disease progression. Although the exact biological implications of Cu^{2+} binding to PrP^C are not yet understood, the antioxidant properties seem to be well supported by chemical and biological data. Whether such antioxidant activity arises from sequestration of copper, SOD-type function, or more complex processes is still to be clarified. Besides creating oxidative stress, copper, together with other metal ions,

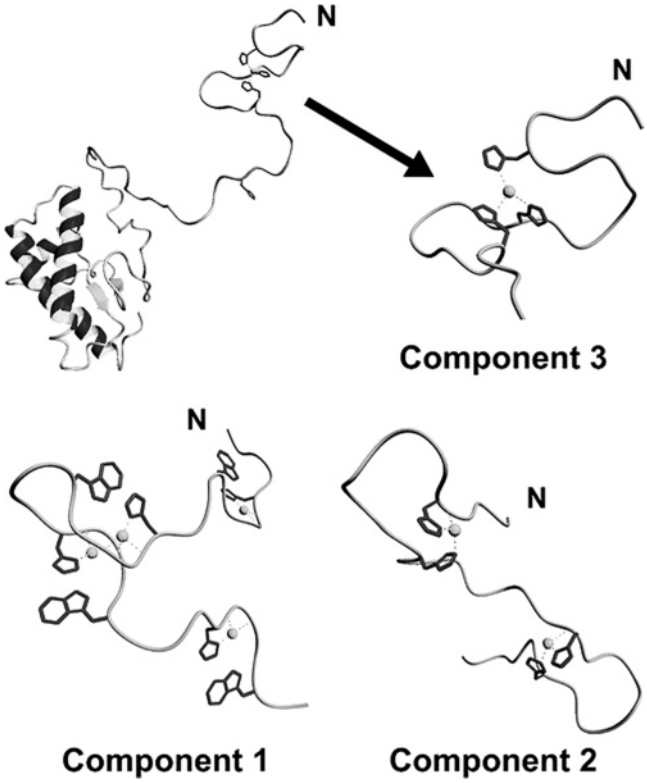

Figure 53. Models of PrP^C containing Cu^{2+} in the three coordination modes. Upper left: PrP(60−231) bound to a single Cu^{2+} with component 3 coordination. Upper right: the copper binding octarepeat domain is expanded. In this mode, an additional His imidazole may also participate in copper binding. For components 1 and 2, only the octarepeat domains are shown. Reprinted with permission from ref 430. Copyright 2005 American Chemical Society.

influences protein aggregation processes that are critical in most of the neurodegenerative diseases. Slight differences—only three amino acids are changed—between human and rat Aβ peptide sequences cause humans, but not rats, to suffer from AD. Does this variation derive from the differential interactions of metal ions with Aβ? Can we manage neurological disorders by controlling metal ion concentration, e.g. via specific chelating agents, as has been shown already in clinical trials?[432]

To answer these questions, further experimental work and collaboration among physical inorganic chemists, biochemists, neurochemists, and physicians will need to be initiated and pursued.

9. References

(1) Taylor, J. P.; Hardy, J.; Fischbeck, K. H. *Science* **2002**, *296*, 1991.
(2) Kelly J. W. *Curr. Opin. Struct. Biol.* **1998**, *8*, 101.
(3) Sigurdsson, E. M.; Wisniewski, T.; Frangione, B. *Trends Mol. Med.* **2002**, *8*, 411.
(4) Chiba, T.; Hagihara, Y.; Higurashi, T.; Hasegawa, K.; Naiki, H.; Goto, Y. *J. Biol. Chem.* **2003**, *278*, 47016.
(5) Radford, S. E.; Dobson, C. M. *Cell* **1999**, *97*, 291.
(6) Dobson, C. M. *Nature* **2003**, *426*, 884.
(7) Sitia, R.; Braakman, I. *Nature* **2003**, *426*, 891.
(8) Goldberg, A. L. *Nature* **2003**, *426*, 895.
(9) Ciechanover, A. *Cell* **1997**, *79*, 13.
(10) Uversky, V. N.; Fink, A. L. *Biochim. Biophys. Acta* **2004**, *1698*, 131.
(11) Ullrich, O.; Reinheckel, T.; Sitte, N.; Hass, R.; Grune, T.; Davies, K. J. A. *Proc. Natl. Acad. Sci., U.S.A.* **1999**, *96*, 6223.
(12) Grune, T.; Reinheckel, T.; Davies, K. J. A. *J. Biol. Chem.* **1996**, *271*, 15504.
(13) Shringarpure, R.; Grune, T.; Mehlhase, J.; Davies, K. J. A. *J. Biol. Chem.* **2003**, *278*, 311.
(14) Selkoe, D. J. *Nature* **2003**, *426*, 900.
(15) Dobson, C. M. *Science* **2004**, *304*, 1259.
(16) Bucciantini, M.; Giannoni, E.; Chiti, F.; Baroni, F.; Formigli, L.; Zurdo, J.; Taddei, N.; Ramponi, G.; Dobson, C. M.; Stefani, M. *Nature* **2002**, *416*, 507 and references therein.
(17) Sunde, M.; Blake, C. *Adv. Protein Chem.* **1997**, *50*, 123.
(18) Dumoulin, M.; Dobson, C. M. *Biochimie* **2004**, *86*, 589.
(19) Kayed, R.; Bernhagen, J.; Greenfield, N.; Sweimeh, K.; Brunner, H. Voelter, W.; Kapurniotu, A. *J. Mol. Biol.* **1999**, *287*, 781.
(20) Harper, J. D.; Lansbury, P. T., Jr. *Annu. Rev. Biochem.* **1997**, *66*, 385.
(21) Nelson, R.; Sawaya, M. R.; Balbirnie, M.; Madsen, A. O.; Riekel, C.; Grothe, R.; Eisenberg, D. *Nature* **2005**, 435, 773.
(22) Perry, G.; Sayre, L. M.; Atwood, C. S.; Castellani, R. J.; Cash, A. D.; Rottkamp, C. A.; Smith, M. A. *CNS Drugs* **2002**, *16*, 339.
(23) Reiter, R. J. *FASEB J.* **1995**, *9*, 526.
(24) Halliwell, B.; Gutteridge, J. M. C. *Methods Enzymol.* **1990**, *186*, 1.
(25) Barnham, K. J.; Masters, C. L.; Bush, A. I. *Nat. Rev. Drug Discovery* **2004**, *3*, 205 and references therein.
(26) Cui, K.; Luo, X.; Xu, K.; Ven Murthy, M. R. *Prog. Neuropsychopharmacol. Biol. Psychiatry* **2004**, *28*, 771 and references therein.
(27) Burdette, S. C.; Lippard, S. J. *Proc. Natl. Acad. Sci., U.S.A.* **2003**, *100*, 3605.
(28) Brown, D. R.; Kozlowski, H. *Dalton Trans.* **2004**, 1907.
(29) Lovell, M. A.; Robertson, J. D.; Teesdale, W. J.; Campbell, J. L.; Markesbery, W. R. *J. Neurol. Sci.* **1998**, *158*, 47.
(30) Bush, A. I. *Curr. Opin. Chem. Biol.* **2000**, *4*, 184.
(31) Tiffany-Castiglioni, E.; Qian, Y. *Neurotoxicology* **2001**, *22*, 577.
(32) Sigel, H.; Martin, R. B. *Chem. Rev.* **1982**, *82*, 385.
(33) Bal, W.; Kozlowski, H.; Kupryszewski, G.; Mackiewicz, Z.; Pettit, L.; Robbins, R. *J. Inorg. Biochem.* **1993**, *52*, 79.
(34) Formicka-Kozlowska, G.; Pettit, L. D.; Steel, I.; Livera, C. E.; Kupryszewski, G.; Rolka, K. *J. Inorg. Biochem.* **1985**, *24*, 299.
(35) Kozlowski, H. *Proceedings of the 9th Conference on Coordinaton Chemistry*, Smolenice, Bratislava, 1983; p 201.
(36) Tumer, Z.; Horn, N.; Tonnesen, T.; Christodoulou, J.; Clarke, J. T.; Sarkar, B. *Nat. Genet.* **1996**, *12*, 11.
(37) Sjoberg, S. *Pure Appl. Chem.* **1997**, *69*, 1549.
(38) Daniele, P.; Zerbinati, O.; Zelano, V.; Ostacoli, G. *J. Chem. Soc., Dalton Trans.* **1991**, 2711.
(39) Hay, R.; Hassan, M.; You-Quan, C. *J. Inorg. Biochem.* **1993**, *52*, 17.
(40) Gaggelli, E.; D'Amelio, N.; Valensin, D.; Valensin, G. *Magn. Reson. Chem.* **2003**, *41*, 877.
(41) Belosi, B.; Gaggelli, E.; Guerrini, R.; Kozlowski, H.; Łuczkowski, M.; Mancini, F. M.; Remelli, M.; Valensin, D.; Valensin, G. *ChemBioChem* **2004**, *5*, 349.
(42) Lehnert, N.; George, S. D.; Solomon, E. I. *Curr. Opin. Chem. Biol.* **2001**, *5*, 176.
(43) Szilagyi, R. K.; Solomon, E. I. *Curr. Opin. Chem. Biol.* **2002**, *6*, 250.
(44) Andersson, K. K.; Schmidt, P. P.; Katterle, B.; Strand, K. R.; Palmer, A. E.; Lee, S. K.; Solomon, E. I.; Graslund, A.; Barra, A. L. *J. Biol. Inorg. Chem.* **2003**, *8*, 235.
(45) Solomon, E. I.; Szilagyi, R. K.; DeBeer George, S.; Basumallick, L. *Chem. Rev.* **2004**, *104*, 419.
(46) Mirica, L. M.; Ottenwaelder, X.; Stack, T. D. *Chem. Rev.* **2004**, *104*, 1013.
(47) Bertini, I.; Luchinat, C. *Coord. Chem. Rev.* **1996**, *150*, 1.
(48) Conato, C.; Kamysz, W.; Kozlowski, H.; Luczkowski, M.; Mackiewicz, Z.; Mlynarz, P.; Remelli, M.; Valensin, D.; Valensin, G. *J. Chem. Soc., Dalton Trans.* **2002**, 3939.
(49) Remelli, M.; Luczkowski, M.; Bonna, A. M.; Mackiewicz, Z.; Conato, C.; Kozlowski, H. *New J. Chem.* **2003**, *27*, 245.
(50) Luczkowski, M.; Kozlowski, H.; Stawikowski, M.; Rolka, K.; Gaggelli, E.; Valensin, D.; Valensin, G. *J. Chem. Soc., Dalton Trans.* **2002**, 2269.
(51) Kozlowski, H.; Bal, W.; Dyba, M.; Kowalik-Jankowska, T. *Coord. Chem. Rev.* **1999**, *184*, 319.
(52) Valensin, D.; Mancini, F. M.; Luczkowski, M.; Janicka, A.; Wis'niewska, K.; Gaggelli, E.; Valensin, G.; Lankiewicz, L.; Kozlowski, H. *J. Chem. Soc., Dalton Trans.* **2004**, 16.
(53) Gaggelli, E.; Kozlowski, H.; Valensin, D.; Valensin G. *Mol. Biosyst.* **2005**, *1*, 79.
(54) Solomon, I. *Phys. Rev.* **1955**, *99*, 559.
(55) Hall, L. D.; Hill, H. D. W. *J. Am. Chem. Soc.* **1976**, *98*, 1269.
(56) Freeman, R-; Hill, H. D. W.; Hall, L. D.; Tomlinson, B. L. *J. Chem. Phys.* **1974**, *61*, 4466.
(57) Peters, T. jr. *Biochim. Biophys. Acta* **1960**, *39*, 546.
(58) Peters, T., Jr.; Blumenstock, F. A. *J. Biol. Chem.* **1967**, *242*, 1574.
(59) Laussac, J.-P.; Sarkar, B. *Biochemistry* **1984**, *23*, 2832.
(60) Harford, C.; Sarkar, B. *Acc. Chem. Res.* **1997**, *30*, 123.

(61) Kimoto, E.; Tanaka, H.; Gyotoku, J.; Morishige, F.; Pauling, L. *Cancer Res.* **1983**, *43*, 824.
(62) Machczynski, M. C.; Gray, H. B.; Richards, J. H. *J. Inorg. Biochem.* **2002**, *82*, 375.
(63) Feiters, M. C. *Met. Ions Biol. Syst.* **2001**, *38*, 461.
(64) Banci, L.; Pieratelli, R.; Vila, A. J. *Adv. Protein Chem.* **2002**, *60*, 347.
(65) Reeds, D. C. *Annu. Rev. Biochem.* **2002**, *71*, 221.
(66) Szilagyi, R. K.; Solomon, E. I. *Curr. Opin. Chem. Biol.* **2002**, *6*, 250.
(67) Solomon, E. I.; Szilagyi, R. K.; DeBeer George, S.; Basumallick, L. *Chem. Rev.* **2004**, *104*, 419.
(68) Koch, K. A.; Pena, M. M.; Thiele, D. J. *Chem. Biol.* **1997**, *4*, 549.
(69) McGuirl, M. A.; Dooley, D. M. *Curr. Opin. Chem. Biol.* **1999**, *3*, 138.
(70) Solomon, E. D.; Baldwin, M. J.; Lowery, M. D. *Chem. Rev.* **1992**, *92*, 521.
(71) Malmstrom, B. G.; Leckner, J. *Curr. Opin. Chem. Biol.* **1998**, *2*, 286.
(72) Bertini, I.; Sigel, A.; Sigel, H. *Handbook of Metalloproteins*; Marcel Dekker Inc.: New York, 2001.
(73) *Handbook of Metalloproteins*; Messerschmidt, A., Huber, R., Poulos, T., Wieghardt, K., Eds.; John Wiley & Sons, Ltd: New York, 2001; Vol. 2.
(74) Rae, T. D.; Schmidt, P. J.; Pufahl, R. A.; Culotta, V. C.; O'Halloran, T. V. *Science* **1999**, *284*, 805.
(75) Lippard, S. J. *Science* **1999**, *284*, 748.
(76) Linder, M. C. *Biochemistry of Copper*; Plenum Press: New York, 1991.
(77) *Dietary Reference Intakes for Vitamin A, Vitamin K, Arsenic, Boron, Chromium, Copper, Iodine, Iron, Manganese, Molybdenum, Nickel, Silicon, Vanadium and Zinc*; National Academy Press: Washington, DC, 2001; Chapter 7.
(78) Mercer, J. F. B.; Llanos, R. M. *J. Nutr.* **2003**, *133*, 1481S.
(79) Zhou, B.; Gitschier, J. *Proc. Natl. Acad. Sci., U.S.A.* **1997**, *94*, 7481.
(80) Lee, J.; Prohaska, J. R.; Dagenais, S. L.; Glover, T. W.; Thiele, D. J. *Gene* **2000**, *254*, 87.
(81) Amaravadi, R.; Glerum, D. M.; Tzagollof, A. *Hum. Genet.* **1997**, *99*, 329.
(82) Culotta, V. C.; Klomp, L. W. J.; Strain, J.; Casareno, R. L. B.; Krems, B.; Gitlin, J. D. *J. Biol. Chem.* **1997**, *272*, 23469.
(83) Klomp, L. W. J.; Lin, S.-J.; Yuan, D. S.; Klausner, R. D.; Culotta, V. C.; Gitlin, J. D. *J. Biol. Chem.* **1997**, *272*, 9221.
(84) Shim, H.; Harris, Z. L. *J. Nutr.* **2003**, *133*, 1527S.
(85) Eisses, J. F.; Kaplan, J. H. *J. Biol. Chem.* **2002**, *277*, 29162.
(86) Guo, Y.; Smith, K.; Lee, J.; Thiele, D. J.; Petris, M. J. *J. Biol. Chem.* **2004**, *279*, 17428.
(87) Klomp, A. E. M.; Tops, B. B. J.; Van Den Berg, I. E. T.; Berger, R.; Klomp, L. W. J. *Biochem. J.* **2002**, *364*, 497.
(88) Petris, M. J.; Smith, K.; Lee, J.; Thiele, D. J. *J. Biol. Chem.* **2003**, *278*, 9639.
(89) Eisses, J. F.; Chi, Y.; Kaplan, J. H. *J. Biol. Chem.* **2005**, *280*, 9635.
(90) Barnes, N.; Tsivkovskii, R.; Tsivkovskaia, N.; Lutsenko, S. *J. Biol. Chem.* **2005**, *280*, 9640.
(91) Banci, L.; Bertini, I.; Del Conte, R.; D'Onofrio, M.; Rosato, A. *Biochemistry* **2004**, *43*, 3396.
(92) DeSilva, T. M.; Veglia, G.; Opella, S. J. *Proteins* **2005**, *61*, 1038.
(93) Banci, L.; Bertini, I.; Cantini, F.; Migliardi, M.; Rosato, A.; Wang, S. *J. Mol. Biol.* **2005**, *352*, 409.
(94) Hamer, D. H. *Annu. Rev. Biochem.* **1986**, *55*, 913.
(95) Cobbett, C.; Goldsbrough, P. *Annu. Rev. Plant Biol.* **2002**, *53*, 159.
(96) Vasak, M.; Hasler. D. W. *Curr. Opin. Chem. Biol.* **2000**, *4*, 177.
(97) Zhou, J. M.; Goldsbrough. P. B. *Plant Cell* **1994**, *6*, 875.
(98) Murphy, A.; Zhou, J. M.; Goldsbrough, P. B.; Taiz. L. *Plant Physiol.* **1997**, *113*, 1293.
(99) Riek, R.; Prêcheur, B.; Wang, Y,; MacKay, E. A.; Wider, G.; Güntert, P.; Liu, A.; Kägi, J. H. R.; Wüthrich, K. *J. Mol. Biol.* **1999**, *291*, 417.
(100) Peterson, C. W.; Narula, S. S.; Armitage, I. M. *FEBS Lett.* **1996**, *379*, 85.
(101) Bertini, I.; Klein, T.; Gaohua, L.; Luchinat, C.; Weser, U. *Eur. J. Biochem.* **2000**, *267*, 1008.
(102) Calderone, V.; Dolderer, B.; Hartmann, H. J.; Echner, H.; Luchinat, C.; Del Bianco, C.; Mangani, S.; Weser, U. *Proc. Natl. Acad. Sci., U.S.A.* **2005**, *102*, 51.
(103) Lin, S. J.; Culotta, V. C. *Proc. Natl. Acad. Sci., U.S.A.* **1995**, *92*, 3784.
(104) Pufahl, R. A.; Singer, C. P.; Peariso, K. L.; Lin, S. J.; Schmidt, P. J.; Fahrni, C. J.; Culotta, V. C.; Penner-Hahn, J. E.; O'Halloran, T. V. *Science* **1997**, *278*, 853.
(105) Lockhart, P. J.; Mercer, J. F. *Biochim. Biophys. Acta* **2000**, *1490*, 11.
(106) Nishihara, E.; Furuyama, T.; Yamashita, S.; Mori, N. *Neuroreport* **1998**, *9*, 3259.
(107) Himelblau, E.; Mira, H.; Lin, S. J.; Culotta, V. C.; Penarrubia, L.; Amasino, R. M. *Plant Physiol.* **1998**, *117*, 1227.
(108) Wakabayashi, T.; Nakamura, N.; Sambongi, Y.; Wada, Y.; Oka, T.; Futai, M. *FEBS Lett.* **1998**, *440*, 141.
(109) Huffman, D. L.; O'Halloran, T. V. *J. Biol. Chem.* **2000**, *275*, 18611.
(110) Lin, S. J.; Pufahl, R. A.; Dancis, A.; O'Halloran, T. V.; Culotta, V. C. *J. Biol. Chem.* **1997**, *272*, 9215.
(111) Klomp, L. W.; Lin, S. J.; Yuan, D. S.; Klausner, R. D.; Culotta, V. C.; Gitlin, J. D. *J. Biol. Chem.* **1997**, *272*, 9221.
(112) Rosenzweig, A. C.; Huffman, D. L.; Hou, M. Y.; Wernimont, A, K.; Pufahl, R. A.; O'Halloran, T. V. *Structure* **1999**, *7*, 605.
(113) Arnesano, F.; Banci, L.; Bertini, I.; Ciofi-Baffoni, S.; Molteni, E.; Huffman, D. L.; O'Halloran, T. V. *Genome Res.* **2002**, *12*, 255.
(114) Hung, I. H.; Casareno, R. L. B.; Labesse, G.; Mathews, F. S.; Gitlin, J. D. *J. Biol. Chem.* **1998**, *273*, 1749.
(115) Wernimont, A. K.; Huffman, D. L.; Lamb, A. L.; O'Halloran, T. V.; Rosenzweig, A. C. *Nat. Struct. Biol.* **2000**, *7*, 766.
(116) Tanchou, V.; Gas, F.; Urvoas, A.; Cougouluègne, F.; Ruat, S.; Averseng, O.; Quéméneur, E. *Biochem. Biophys. Res. Commun.* **2004**, *325*, 388.
(117) Anastassopoulou, I.; Banci, L.; Bertini, I.; Cantini, F.; Katsari, E.; Rosato A. *Biochemistry* **2004**, *43*, 13046.
(118) Casareno, R. L.; Waggoner, D.; Gitlin, J. D. *J. Biol. Chem.* **1998**, *273*, 23625.
(119) Lamb, A. L.; Wernimont, A. K.; Pufahl, R. A.; Culotta, V. C.; O'Halloran, T. V.; Rosenzweig, A. C. *Nat. Struct. Biol.* **1999**, *6*, 724.
(120) Falconi, M.; Iovino, M.; Desideri, A. *Structure* **1999**, *7*, 903.
(121) Lamb, A. L.; Wernimont, A. K.; Pufahl, R. A.; O'Halloran, T. V.; Rosenzweig, A. C. *Biochemistry* **2000**, *39*, 1589.
(122) Lamb, A. L.; Torres, A. S.; O'Halloran, T. V.; Rosenzweig, A. C. *Biochemistry* **2000**, *39*, 14720.
(123) Rae, T. D.; Torres, A. S.; Pufahl, R. A.; O'Halloran, T. V. *J. Biol. Chem.* **2001**, *276*, 5166.
(124) Furukawa, Y.; Torres, A. S.; O'Halloran, T. V. *EMBO J.* **2004**, *23*, 2872.
(125) Brown, N. M.; Torres, A. S.; Doan, P. E.; O'Halloran, T. V. *Proc. Natl. Acad. Sci., U.S.A.* **2004**, *101*, 5518.
(126) Glerum, D. M.; Shtanko, A.; Tzagoloff, A. *J. Biol. Chem.* **1996**, *271*, 14504.
(127) Carr, H. S.; Winge, D. R. *Acc. Chem. Res.* **2003**, *36*, 309.
(128) Heaton, D. N.; George, G. N.; Garrison, G.; Winge, D. R. *Biochemistry* **2001**, *40*, 743.
(129) Abajian, C.; Yatsunyk, L. A.; Ramirez, B. E.; Rosenzweig, A. C. *J. Biol. Chem.* **2004**, *279*, 53584.
(130) Arnesano, F.; Balatri, E.; Banci, L.; Bertini, I.; Winge, D. R. *Structure* **2005**, *13*, 713.
(131) Williams, J. C.; Sue, C.; Banting, G. S.; Yang, H.; Glerum, D. M.; Hendrickson, W. A.; Schon, E. A. *J. Biol. Chem.* **2005**, *280*, 15202.
(132) Banci, L.; Bertini, I.; Cantini, F.; Ciofi-Baffoni, S.; Gonnelli, L.; Mangani, S. *J. Biol. Chem.* **2004**, *279*, 34833.
(133) Carr, H. S.; George, G. N.; Winge, D. R. *J. Biol. Chem.* **2002**, *277*, 31237.
(134) Horng, Y. C.; Cobine, P. A.; Maxfield, A. B.; Carr, H. S.; Winge, D. R. *J. Biol. Chem.* **2004**, *279*, 35334.
(135) Fillit, H. M.; O'Connell, A. W.; Brown, W. M.; Altstiel, L. D.; Anand, R.; Collins, K.; Ferris, S. H.; Khachaturian, Z. S.; Kinoshita, J.; Van Eldik, L.; Dewey, C. F. *Alzheimer Dis. Assoc. Disord.* **2002**, *16*, S1.
(136) Alzheimer, A. *Allg. Z. Psychiatr. Ihre Grenzgeb.* **1907**, *64*, 146.
(137) Leslie, R. A. *Trends Neurosi.* **2002**, *25*, 232.
(138) Torreilles, F.; Touchan, J. *Prog. Neurobiol.* **2002**, *66*, 191.
(139) Hardy, J.; Selkoe, D. J. *Science* **2002**, *297*, 353.
(140) De Ferrari, G. V.; Inestrosa, N. C *Brain Res. Rev.* **2000**, *33*, 1.
(141) Goate, A.; Chartier-Harlin, M. C.; Mullan, M.; Brown, J.; Crawford, F.; Fidani, L.; Giuffra, L.; Haynes, A.; Irving, N.; James, L.; Mant, R.; Newton, P.; Rooke, K.; Roques, P.; Talbot, C.; Pericak-Vance, M.; Roses, A.; Williamson, R.; Rossor, M.; Owen, M.; Hardy, J. *Nature* **1991**, *349*, 704.
(142) Sherrington, R.; Rogaev, E. I.; Liang, Y.; Rogaeva, E. A.; Levesque, G.; Ikeda, M.; Chi, H.; Lin, C.; Li, G.; Holman, K.; Tsuda, T.; Mar, L.; Foncin, J.-F.; Bruni, A. C.; Montesi, M. P.; Sorbi, S.; Rainero, I.; Pinessi, L.; Nee, L.; Chumakov, I.; Pollen, D.; Brookes, A.; Sanseau, P.; Polinsky, R. J.; Wasco, W.; Da Silva H. A. R.; Haines, J. L.; Pericak-Vance, A.; Tanzi, R. E.; Roses, A. D.; Fraser, P. E.; Rommens, J. M.; StGeorge-Hyslop, P. H. *Nature* **1995**, *375*, 754.
(143) Levy-Lahad, E.; Wasco, W.; Poorkaj, P.; Romano, D. M.; Oshima, J.; Pettingell, W. H.; Yu, C. E.; Jondro, P. D.; Schmidt, S. D.; Wang, K.; Crowley, A. C.; Fu, Y. H.; Guenette, S. Y.; Galas, D.; Nemens, E.; Wijsman E. M.; Bird, T. D.; Schellenberg, C. D.; Tanzi, R. E. *Science* **1995**, *269*, 973.
(144) Selkoe, D. J. *Science* **2002**, *298*, 789.

(145) Selkoe, D. J. *Ann. Intern. Med.* **2004**, *140*, 627.
(146) Braak, E.; Braak, H. *Acta Neuropathol.* **1997**, *93*, 323.
(147) Hoshi, M.; Sato, M.; Matsumoto, S.; Noguchi, A.; Yasutake, K.; Yoshida, N.; Sato, K. *Proc. Natl. Acad. Sci., U.S.A.* **2003**, *100*, 6370.
(148) Giacobini, E. *Jpn. J. Pharmacol.* **1997**, *74*, 225.
(149) Alvarez, A.; Opazo, C.; Alarcón, R.; Garrido, J.; Inestrosa, N. C. *J. Mol. Biol.* **1997**, *272*, 348.
(150) Inestrosa, N. C.; Alvarez, A.; Pérez, C. A.; Moreno, R, D,; Vicente, M.; Linker, C.; Casanueva, O. I.; Soto, C.; Garrido, J. *Neuron* **1996**, *16*, 881.
(151) Reyes, A. E.; Perez, D.; Alvarez, A.; Garrido, J.; Gentry, M. K.; Doctor, B. P.; Inestrosa, N. C. *Biochem. Biophys. Res. Commun.* **1997**, *232*, 652.
(152) Wang, H. Y.; Lee, D. H. S.; D'Andrea, M. R.; Peterson, P. A.; Shank, R. P.; Reitz, A. B. *J. Biol. Chem.* **2000**, *275*, 5626.
(153) Wang, H. Y.; Lee, D. H. S.; Davis, C. B.; Shank, R. P. *J. Neurochem.* **2000**, *75*, 1155.
(154) Espinoza-Fonseca, L. M. *Biochem. Biophys. Res. Commun.* **2004**, *320*, 587.
(155) Kang, J.; Lemaire, H. G.; Unterbeck, A.; Salbaum, J. M.; Masters, C. L.; Grzeschik, K. H.; Multhaup, G.; Beyreuther, K.; Müller-Hill, B. *Nature* **1987**, *325*, 733.
(156) Tanzi, R. E.; Gusella, J. F.; Watkins, P. C.; Bruns, G. A. P.; St. George-Hyslop, P. H.; VanKeuren, M. L.; Patterson, D.; Pagan, S.; Kurnit, D. M.; Neve, R. L. *Science* **1987**, *235*, 880.
(157) Checler, F.; Vincent, B. *Trends Neurosci.* **2002**, *25*, 616.
(158) Turner, P. R.; O'Connor, K.; Tate, W. P.; Abraham, W. C. *Prog. Neurobiol.* **2003**, *70*, 1.
(159) Selkoe, D. J. *Physiol. Rev.* **2001**, *81*, 741.
(160) Okamoto, T.; Takeda, S.; Murayama, Y.; Ogata, E.; Nishimoto, I. *J. Biol. Chem.* **1995**, *270*, 4205.
(161) Sabo, S. L.; Ikin, A. F.; Buxbaum, J. D.; Greengard, P. *J. Cell Biol.* **2001**, *153*, 1403.
(162) White, A. R.; Reyes, R.; Mercer, J. F.; Camakaris, J.; Zheng, H.; Bush, A. I.; Multhaup, G.; Beyreuther, K.; Masters, C. L.; Cappai, R. *Brain Res.* **1999**, *842*, 439.
(163) Maynard, C. J.; Cappai, R.; Volitakis, I.; Cherny, R, A.; White, A. R.; Beyreuther, K.; Masters, C. L.; Bush, A. I.; Li, Q. X. *J. Biol. Chem.* **2002**, *277*, 44670.
(164) Multhaup, G.; Schlicksupp, A.; Hesse, L.; Beher, D.; Ruppert, T.; Masters, C. L.; Beyreuther, K. *Science* **1996**, *271*, 1406.
(165) Ruiz, F. H.; Gonzalez, M.; Bodini, M.; Opazo, C.; Inestrosa, N. C. *J. Neurochem.* **1999**, *73*, 1288.
(166) Ruiz, F. H.; Silva, E.; Inestrosa, N. C. *Biochem. Biophys. Res. Commun.* **2000**, *269*, 491.
(167) Hardy, J. *Neurobiol. Aging* **2002**, *23*, 1073.
(168) Tsubuki, S.; Takaki, Y.; Saido, T. C. *Lancet* **2003**, *361*, 1957.
(169) Wilquet, V.; De Strooper, B. *Curr. Opin. Neurobiol.* **2004**, *14*, 582.
(170) De Strooper, B.; Saftig, P.; Craessaerts, K.; Vanderstichele, H.; Guhde, G.; Annaert, W.; Von Figura, K.; Van Leuven, F. *Nature* **1998**, *391*, 387.
(171) Lambert, M. P.; Barlow, A. K.; Chromy, B. A.; Edwards, C.; Freed, R.; Liosatos, M.; Morgan, T. E.; Rozovsky, I.; Trommer, B.; Viola, K. L.; Wals, P.; Zhang, C.; Finch, C. E.; Krafft, G. A.; Klein, W. L. *Proc. Natl. Acad. Sci., U.S.A.* **1998**, *95*, 6448.
(172) Hartley, D. M.; Walsh, D. M.; Ye, C. P.; Diehl, T.; Vasquez, S.; Vassilev, P. M.; Teplow, D. B.; Selkoe, D. J. *J. Neurosci.* **1999**, *19*, 8876.
(173) LeVine, H. 3rd. *Arch. Biochem. Biophys.* **2002**, *404*, 106 and references therein.
(174) Kayed, R.; Head, E,; Thompson, J. L.; McIntire, T. M.; Milton, S. C.; Cotman, C. W.; Glabe, C. G. *Science* **2003**, *300*, 486.
(175) Suzuki, N.; Cheung, T. T.; Cai, X. D.; Odaka, A.; Otvos, L.; Eckman, C.; Golde, T. E.; Younkin, S. G. *Science* **1994**, *264*, 1336.
(176) Scheuner, D.; Eckman, C.; Jensen, M.; Song, X.; Citron, M.; Suzuki, N.; Bird, T. D.; Hardy, J.; Hutton, M.; Kukull, W.; Larson, E.; Levy-Lahad, E.; Viitanen, M.; Peskind, E.; Poorkaj, P.; Schellenberg, G.; Tanzi, R.; Wasco, W.; Lannfelt, L.; Selkoe, D.; Younkin, S. *Nat. Med.* **1996**, *2*, 864.
(177) Weggen, S.; Eriksen, J. L.; Das, P.; Sagi, S. A.; Wang, R.; Pietrzik, C. U.; Findlay, K. A.; Smith, T. E.; Murphy, M. P.; Bulter, T.; Kang, D. E.; Marquez-Sterling, N.; Golde, T, E.; Koo, E. H. *Nature* **2001**, *414*, 212.
(178) Selkoe, D. J. *Nature* **1999**, *399*, A23.
(179) Jarrett, J. T.; Berger, E. P.; Lansbury, P. T., Jr. *Biochemistry* **1993**, *32*, 4693.
(180) Bitan, G.; Kirkitadze, M. D.; Lomakin, A.; Vollers, S. S.; Benedek, G. B.; Teplow, D. B. *Proc. Natl. Acad. Sci.* **2003**, *100*, 330.
(181) Zhang, S.; Iwata, K.; Lachenmann, M. J.: Peng, J. W.; Li, S.; Stimson, E. R.; Lu, Y.-A.; Felix, A. M.; Maggio, J. E.; Lee, J. P. *J. Struct. Biol.* **2000**, *130*, 130.
(182) Riek, R.; Gunthert, P.; Dobeli, H.; Wipf, B.; Wuthrich, K. *Eur. J. Biochem.* **2001**, *268*, 5930.
(183) Shao, H.; Jao, S.; Ma, K.; Zagorski, M. G. *J. Mol. Biol.* **1999**, *285*, 755 and references therein.
(184) Petkova, A. T.; Ishii, Y.; Balbach, J. J.; Antzutkin, O. N.; Leapman, R. D.; Delaglio, F.; Tycko, R. *Proc. Natl. Acad. Sci., U.S.A.* **2002**, *99*, 16742.
(185) Narayanan, S.; Reif, B. *Biochemistry* **2005**, *44*, 1444.
(186) Englander, S. W.; Sosnick, T. R.; Englander, J. J.; Mayne, L. *Curr. Opin. Struct. Biol.* **1996**, *6*, 18.
(187) Hoshino, M.; Katou, H.; Hagihara, Y.; Hasegawa, K.; Naiki, H.; Goto, Y. *Nat. Struct. Biol.* **2002**, *9*, 332.
(188) Ippel, J. H.; Olofsson, A.; Schleucher, J.; Lundgren, E.; Wijmenga, S. S. *Proc. Natl. Acad. Sci., U.S.A.* **2002**, *99*, 8648.
(189) Kuwata, K.; Matumoto, T.; Cheng, H.; Nagayama, K.; James T. L.; Roder, H. *Proc. Natl. Acad. Sci., U.S.A.* **2003**, *100*, 14790.
(190) Olofsson, A.; Ippel, J. H.; Wijmenga, S. S.; Lundgren, E.; Ohman, A. *J. Biol. Chem.* **2004**, *279*, 5699.
(191) Whittemore, N. A.; Mishra, R.; Kheterpal, I.; Williams, A. D.; Wetzel, R.; Serpersu, E. H. *Biochemistry* **2005**, *44*, 4434.
(192) Bernstein, S. L.; Wyttenbach, T.; Baumketner, A.; Shea, J.-E.; Bitan, G.; Teplow, D. B.; Bowers, M. T. *J. Am. Chem. Soc.* **2005**, *127*, 2075.
(193) Bitan, G.; Vollers, S. S.; Teplow, D. B. *J. Biol. Chem.* **2003**, *278*, 34882.
(194) Tarus, B.; Straub, J. E.; Thirumalai, D. *J. Mol. Biol.* **2005**, *345*, 1141.
(195) Smith, M. A.; Perry, G.; Richey, P. L.; Sayre, L. M.; Anderson, V. E.; Beal, M. F.; Kowall, N. *Nature* **1996**, *382*, 120.
(196) Sayre, L. M.; Perry, G.; Harris, P. L.; Liu, Y.; Schubert, K. A.; Smith, M. A. *J. Neurochem.* **2000**, *74*, 270.
(197) Castellani, R. J.; Honda, K.; Zhu, X.; Cash, A. D.; Nunomura, A.; Perry, G.; Smith, M. A. *Ageing Res. Rev.* **2004**, *3*, 319.
(198) Varadarajan, S.; Yatin, S.; Aksenova, M.; Butterfield D. A. *J. Struct. Biol.* **2000**, *130*, 184.
(199) Butterfield, D. A:; Boyd-Kimball, D.; Castegna, A. *J. Neurochem.* **2003**, *86*, 1313.
(200) Atwood, C. S.; Huang, X.; Moir, R. D.; Tanzi, R. E.; Bush, A. I. In *Metal Ions in Biological Systems*; Sigel, A., Sigel, S., Eds.; Marcel Dekker: New York, Basel, Hong Kong, 1999; Vol. 36, pp 309−364.
(201) Gabuzda, D.; Busciglio, J.; Chen, L. B.; Matsudaira, P.; Yankner, B. A. *J. Biol. Chem.* **1994**, *269*, 13623.
(202) Misonou, H.; Morishima-Kawashima, M.; Ihara, Y. *Biochemistry* **2000**, *39*, 6951.
(203) Cuajungco, M. P.; Goldstein, L. E.; Nunomura, A.; Smith, M. A.; Lim, J. T.; Atwood, C. S.; Huang, X.; Farrag, Y. W.; Perry, G.; Bush, A. I. *J. Biol. Chem.* **2000**, *275*, 19439.
(204) Atwood, C. S.; Moir, R. D.; Huang, X.; Scarpa, R. C.; Bacarra, N. M.; Romano, D. M.; Hartshorn, M. A. Tanzi, R. E.; Bush, A. I. *J. Biol. Chem.* **1998**, *273*, 12817.
(205) Hesse, L.; Beher, D.; Masters, C. L.; Multhaup, G. *FEBS Lett.* **1994**, *349*, 109.
(206) Huang, X.; Cuajungco, M. P.; Atwood, C. S.; Hartshorn, M. A.; Tyndall, J. D.; Hanson, G. R.; Stokes, K. C.; Leopold, M.; Multhaup, G.; Goldstein, L. E.; Scarpa, R. C.; Saunders: A. J.; Lim, J.; Moir, R. D.; Glabe, C.; Bowden, E. F.; Masters, C. L.; Fairlie, D. P.; Tanzi, R. E.; Bush, A. I. *J. Biol. Chem.* **1999**, *274*, 37111.
(207) Cherny, R. A.; Legg, J. T.; McLean, C. A.; Fairlie, D. P.; Huang, X.; Atwood, C. S.; Beyreuther, K.; Tanzi, R. E.; Masters, C. L.; Bush, A. I. *J. Biol. Chem.* **1999**, *274*, 23223.
(208) Opazo, C.; Barria, M. I.; Ruiz, F. H.; Inestrosa, N. C. *BioMetals* **2003**, *16*, 91.
(209) Atwood, C. S.; Scarpa, R. C.; Huang, X.; Moir, R. D.; Jones, W. D.; Fairlie, D. P.; Tanzi, R. E.; Bush, A. I. *J. Neurochem.* **2000**, *75*, 1219.
(210) Bush, A. I.; Pettingell, W. H.; Multhaup, G.; Paradis, M.; Vonsattel, J. P.; Gusella, J. F.; Beyreuther, K.; Masters, C. L.; Tanzi, R. E. *Science* **1994**, *265*, 1464.
(211) Opazo, C.; Huang, X.; Cherny, R. A.; Moir, R. D.; Roher, A. E.; White, A. R.; Cappai, R.; Masters, C. L.; Tanzi, R. E.; Inestrosa, N. C.; Bush, A. I. *J. Biol. Chem.* **2002**, *277*, 40302.
(212) Cherny, R. A.; Atwood, C. S.; Xilinas, M. E.; Gray, D, N,; Jones, W. D.; McLean, C. A.; Barnham, K. J.; Volitakis, I.; Fraser, F. W.; Kim, Y.; Huang, X.; Goldstein, L. E.; Moir, R. D.; Lim, J. T.; Beyreuther, K.; Zheng, H.; Tanzi, R. E.; Masters, C. L.; Bush, A. I. *Neuron* **2001**, *30*, 665.
(213) Atwood, C. S.; Perry, G.; Zeng, H.; Kato, Y.; Jones, W. D.; Ling, K. Q.; Huang, X.; Moir, R. D.; Wang, D.; Sayre, L. M.; Smith, M. A.; Chen, S. G.; Bush, A. I. *Biochemistry* **2004**, *43*, 560.
(214) Perry, G.; Taddeo, M. A.; Petersen, R. B.; Castellani, R. J.; Harris, P. L.; Siedlak, S. L.; Cash, A. D.; Liu, Q.; Nunomura, A.; Atwood, C. S.; Smith, M. A. *BioMetals* **2003**, *16*, 77.
(215) Sparks, D. L.; Schreurs, B. G. *Proc. Natl. Acad. Sci., U.S.A.* **2003**, *100*, 11065.

(216) Curtain, C. C.; Ali, F.; Volitakis, I.; Cherny, R. A.; Norton, R. S.; Beyreuther, K.; Barrow, C. J.; Masters, C. L.; Bush, A. I.; Barnham, K. J. *J. Biol. Chem.* **2001**, *276*, 20466 and references therein.
(217) Curtain, C. C.; Ali, F. E.; Smith, D. G.; Bush, A. I.; Masters, C. L.; Barnham, K. J. *J. Biol. Chem.* **2003**, *278*, 2977.
(218) Bush, A. I. *Trends Neurosci.* **2003**, *26*, 207.
(219) Cerpa, W. F.; Barría, M. I.; Chacón, M. A.; Suazo, M.; González, M.; Opazo, C.; Bush, A. I.; Inestrosa, N. C. *FASEB J.* **2004**, *18*, 1701.
(220) Rossjohn, J.; Cappai, R.; Feil, S. C.; Henry, A.; McKinstry, W. J.; Galatis, D.; Hesse, L.; Multhaup, G.; Beyreuther, K.; Masters, C. L.; Parker, M. W. *Nat. Struct. Biol.* **1999**, *6*, 327.
(221) Barnham, K. J.; McKinstry, W. J.; Multhaup, G.; Galatis, D.; Morton, C. J.; Curtain, C. C.; Williamson, N. A.; White, A. R.; Hinds, M. G.; Norton, R. S.; Beyreuther, K.; Masters, C. L.; Parker, M. W.; Cappai, R. *J. Biol. Chem.* **2003**, *278*, 17401.
(222) White, A. R.; Multhaup, G.; Maher, F.; Bellingham, S.; Camakaris, J.; Zheng, H.; Bush, A. I.; Beyreuther, K.; Masters, C. L.; Cappai, R. *J. Neurosci.* **1999**, *19*, 9170.
(223) White, A. R.; Multhaup, G.; Galatis, D.; McKinstry, W. J.; Parker, M. W.; Pipkorn, R.; Beyreuther, K.; Masters, C. L.; Cappai, R. *J. Neurosci.* **2002**, *22*, 365.
(224) Multhaup, G.; Ruppert, T.; Schlicksupp, A.; Hesse, L.; Eckhard, E.; Pipkorn, R.; Masters, C. L.; Beyreuther, K. *Biochemistry* **1998**, *37*, 7224.
(225) Borchardt, T.; Camakaris, J.; Cappai, R.; Masters, C. L.; Beyreuther, K.; Multhaup, G. *Biochem. J.* **1999**, *344*, 461.
(226) Adman, E. T. In *Advances in Protein Chemistry*; Anfinsen, C. B., Edsall, J. T., Richards, F. M., Eisenberg, D. S., Eds.; Academic Press Inc.: San Diego, CA, 1991; Vol. 42, pp 145−197.
(227) Prigge, S. T.; Kolhekar, A. S.; Eipper, B. A.; Mains, R. E.; Amzel, L. M. *Science* **1997**, *278*, 1300.
(228) Hart, P. J.; Nersissian, A. M.; Herrmann, R. G.; Nalbandyan, R. M.; Valentine, J. S.; Eisenberg, D. *Protein Sci.* **1996**, *5*, 2175.
(229) Poulos, T. L. *Nat. Struct. Biol.* **1999**, *6*, 709.
(230) Scheuermann, S.; Hambsch, B.; Hesse, L.; Stumm, J.; Schmidt, C.; Beher, D.; Bayer, T. A.; Beyreuther, K.; Multhaup, G. *J. Biol. Chem.* **2001**, *276*, 33923.
(231) White, A. R.; Multhaup, G.; Galatis, D.; McKinstry, W. J.; Parker, M. W.; Pipkorn, R.; Beyreuther, K.; Masters C. L.; Cappai, R. *J. Neurosci.* **2002**, 22, 365.
(232) Merz, P. A.; Wisniewski, H. M.; Somerville, R. A.; Bobin, S. A.; Masters, C. L.; Iqbal, K. *Acta Neuropathol.* **1983**, *60*, 113.
(233) Kirschner DA, Abraham C, Selkoe DJ. *Proc. Natl. Acad. Sci., U.S.A.* **1986**, *83*, 503−507.
(234) Lansbury, P. T., Jr. Costa, P. R.; Griffiths, J. M.; Simon, E. J.; Auger, M.; Halverson, K. J.; Kocisko, D. A.; Hendsch, Z. S.; Ashburn, T. T.; Spencer, R. G. *Nat. Struct. Biol*. **1995** *2*, 990.
(235) Dong, J.; Atwood, C. S.; Anderson, V. E.; Siedlak, S. L.; Smith, M. A.; Perry, G.; Carey, P. R. *Biochemistry* **2003**, *42*, 2768.
(236) Sieber, V.; Jurnak, F.; Moe, G. R. *Proteins* **1995**, *23*, 32.
(237) Beauchemin, D.; Kisilevsky, R. *Anal. Chem.* **1998**, *70*, 1026.
(238) Morgan, D. M.; Dong, J.; Jacob, J.; Lu, K.; Apkarian, R. P.; Thiyagarajan, P.; Lynn, D. G. *J. Am. Chem. Soc*. **2002**, *124*, 12544.
(239) Huang, X.; Atwood, C. S.; Hartshorn, M. A.; Multhaup, G.; Goldstein, L. E.; Scarpa, R. C.; Cuajungco, M. P.; Gray, D. N.; Lim, J.; Moir, R. D.; Tanzi, R. E.; Bush, A. I. *Biochemistry* **1999**, *38*, 7609.
(240) Yoshiike, Y.; Tanemura, K.; Murayama, O.; Akagi, T.; Murayama, M.; Sato, S.; Sun, X.; Tanaka, N.; Takashima, A. *J. Biol. Chem.* **2001**, *276*, 32293.
(241) Kowalik-Jankowska, T.; Ruta-Dolejsz, M.; Wisniewska, K.; Ł ankiewicz. L. *J. Inorg. Biochem.* **2001**, *86*, 535.
(242) Kowalik-Jankowska, T.; Ruta-Dolejsz, M.; Wisniewska, K.; Ł ankiewicz, L.; Koz×b8owski. H. *J. Chem. Soc., Dalton Trans.* **2000**, 4511.
(243) Karr, J. W.; Kaupp, L. J.; Szalai, V. A. *J. Am. Chem. Soc*. **2004**, *126*, 13534.
(244) Syme, C. D.; Nadal, R. C.; Rigby, S. E. J.; Viles, J. H. *J. Biol. Chem.* **2004**, *279*, 18169.
(245) Miura, T.; Suzuki, K.; Kohata, N.; Takeuchi, H. *Biochemistry* **2000**, *39*, 7024.
(246) Huang, X.; Atwood, C. S.; Moir, R. D.; Hartshorn, M. A.; Vonsattel, J. P.; Tanzi, R. E.; Bush, A. I. *J. Biol. Chem*. **1997**, *272*, 26464.
(247) Morgan, D. M.; Dong, J.; Jacob, J.; Lu, K.; Apkarian, R. P.; Thiyagarajan, P.; Lynn, D. G. *J. Am. Chem. Soc*. **2002**, *124*, 12644.
(248) Liu, T.; Howlett, G.; Barrow, C. J. *Biochemistry* **1999**, *38*, 9373.
(249) Rottkamp, C, A.; Raina, A. K.; Zhu, X.; Gaier, E.; Bush, A. I.; Atwood, C. S.; Chevion, M.; Perry, G.; Smith, M. A. *Free Radical Biol. Med.* **2001**, *30*, 447.
(250) Nunomura, A.; Perry, G.; Aliev, G.; Hirai, K.; Takeda, A.; Balraj, E. K.; Jones, P. K.; Ghanbari, H.; Wataya, T.; Shimohama, S.; Chiba, S.; Atwood, C. S.; Petersen, R. B.; Smith, M. A. *J. Neuropathol. Exp. Neurol*. **2001**, *60*, 759.
(251) Schendel, S. L.; Xie, Z.; Montal, M. O.; Matsuyama, S.; Montal, M.; Reed, J. C. *Proc. Natl. Acad. Sci., U.S.A.* **1997**, *94*, 5113.
(252) Antonsson, B.; Conti, F.; Ciavatta, A.; Montessuit, S.; Lewis, S.; Martinou, I.; Bernasconi, L.; Bernard, A.; Mermod, J. J.; Mazzei, G.; Maundrell, K.; Gambale, F.; Sadoul, R.; Martinou, J. C. *Science* **1997**, *277*, 370.
(253) Durell, S. R.; Guy, H. R.; Arispe, N.; Rojas, E.; Pollard, H. B. *Biophys. J.* **1994**, *67*, 2137.
(254) Lin, H.; Bhatia, R.; Lal, R. *FASEB J.* **2001**, *15*, 2433.
(255) Miura, T.; Mitani, S.; Takanashi, C.; Mochizuki, N. *J. Inorg. Biochem.* **2004**, *98*, 10.
(256) Kontush, A.; Berndt, C.; Weber, W.; Akopian, V.; Arlt, S.; Schippling, S.; Beisiegel, U. *Free Radical Biol. Med*. **2001**, *30*, 119.
(257) Schõneich, C.; Pogocki, D.; Hug, G. L.; Bobrowski, K. *J. Am. Chem. Soc*. **2003**, *125*, 13700.
(258) Da Silva, G. F. Z.; Tay, W. M.; Ming, L.-J. *J. Biol. Chem.* **2005**, *280*, 16601.
(259) Varadarajan, S.; Kanski, J.; Aksenova, M.; Lauderback, C.; Butterfield, D. A. *J. Am. Chem. Soc.* **2001**, *123*, 5625.
(260) Schoneich, C. *Arch. Biochem. Biophys.* **2002**, *397*, 370.
(261) Kuo, Y. M.; Kokjohn, T. A.; Beach, T. G.; Sue, L. I.; Brune, D.; Lopez, J. C.; Kalback, W. M.; Abramowski, D.; Sturchler-Pierrat, C.; Staufenbiel, M.; Roher, A. E. *J. Biol. Chem.* **2001**, *276*, 12991.
(262) Watson, A. A.; Fairlie, D. P.; Craik, D. J. *Biochemistry* **1998**, *37*, 12700.
(263) Palmblad, M.; Westlind-Danielsson, A.; Bergquist, J. *J. Biol. Chem.* **2002**, *277*, 19506.
(264) Hou, L.; Kang, I.; Marchant, R. E.; Zagorski, M. G. *J. Biol. Chem.* **2002**, *277*, 40173.
(265) Hou, L.; Shao, H.; Zhang, Y.; Li, H.; Menon, N. K.; Neuhaus, E. B.; Brewer, J. M.; Byeon, I. L.; Ray, D. G.; Vitek, M. P.; Iwashita, T.; Makula, R. A.; Przybyla, A. B.; Zagorski, M. G. *J. Am. Chem. Soc.* **2004**, *126*, 1992.
(266) Pogocki, D. *Chem. Res. Toxicol.* **2004**, *17*, 325.
(267) Ciccotosto, G. D.; Tew, D.; Curtain, C. C.; Smith, D.; Carrington, D.; Masters, C. L.; Bush, A. I.; Cherny, R. A.; Cappai, R.; Barnham, K. J. *J. Biol. Chem.* **2004**, *279*, 42528.
(268) Liu, Y.; Sun, G.; David, A.; Sayre, L. M. *Chem. Res. Toxicol*. **2004**, *17*, 110.
(269) Kowalik-Jankowska, T.; Ruta, M.; Wiœniewska, K.; Łankiewicz, L.; Dyba, M. *J. Inorg. Biochem.* **2004**, *98*, 940.
(270) Lim, J.; Vachet, R. W. *Anal. Chem.* **2003**, *75*, 1163.
(271) Barnham, K. J.; Haeffner, F.; Ciccotosto, G. D.; Curtain, C. C.; Tew, D.; Mavros, C.; Beyreuther, K.; Carrington, D.; Masters, C. L.; Cherny, R. A.; Cappai, R.; Bush, A. I. *FASEB J.* **2004**, *18*, 1427.
(272) Charcot, J. M.; Joffory, A. *Arch. Physiol. Neurol. Pathol.* **1869**, *2*, 744.
(273) Cole, N.; Siddique, T. *Semin. Neurol.* **1999**, *19*, 407.
(274) Shipp, E. L.; Cantini, F.; Bestini, I.; Valentine, J. S.; Banci, L. *Biochemistry* **2003**, *42*, 1890.
(275) Potter, S. Z.; Valentine, J. S. *J. Biol. Inorg. Chem.* **2003**, *8*, 373.
(276) Banci, L.; Bertini, I.; Cramaro, F.; Del Conte, R.; Viezzoli, M. S. *Eur. J. Biochem.* **2002**, *269*, 1905.
(277) Valentine, J. S.; Wertz, D. L.; Lyons, T. J.; Liou, L. L.; Goto, J. J.; Gralla, E. B. *Curr. Opin. Chem. Biol.* **1998**, *2*, 253.
(278) Valentine, J. S.; Doucette, P. A.; Potter, S. Z. *Annu. Rev. Biochem.* **2005**, *74*, 563.
(279) Guegan, C.; Przedborski, S. *J. Clin. Invest.* **2003**, *111*, 153.
(280) Beckman, J. S.; Estévez, A. G.; Crow, J. P.; Barbeito, L. *Trends Neurosci.* **2001**, *24*, S15.
(281) Valentine, J. S.; Hart, P. J. *Proc. Natl. Acad. Sci., U.S.A.* **2003**, *100*, 3617.
(282) Hayward, L. J.; Rodriguez, J. A.; Kim, J. W.; Tiwari, A.; Goto, J. J.; Cabelli, D. E.; Valentine, J. S.; Brown, R. H., Jr. *J. Biol. Chem.* **2002**, *277*, 15923.
(283) Subramaniam, J. R.; Lyons, W. E.; Liu, J.; Bartnikas, T. B.; Rothstein. J.; Price, D. L.; Cleveland, D. W.; Gitlin, J. D.; Wong. P. C. *Nat. Neurosci.* **2002**, *5*, 301.
(284) Cleveland, D. W.; Liu, J. *Nat. Med.* **2000**, *6*, 1320.
(285) Wiedau-Pazos, M.; Goto, J. J.; Rabizadeh, S.; Gralla, E. B.; Roe, J. A.; Lee, M. K.; Valentine, J. S.; Bredesen, D. E. *Science* **1996**, *271*, 515.
(286) Estevez, A. G.; Crow, J. P.; Sampson, J. B.; Reiter, C.; Zhuang, Y. X.; Richardson, G. J.; Tarpey, M. M.; Barbeito, L.; Beckman, J. S. *Science* **1999**, *286*, 2498.
(287) Wang, J.; Slunt, H.; Gonzales, V.; Fromholt, D.; Coonfield, M.; Copeland, N. G.; Jenkins, N. A.; Borchelt, D. R. *Hum. Mol. Genet.* **2003**, *12*, 2753.
(288) Lynch, S. M.; Boswell, S. A.; Colon, W. *Biochemistry* **2004**, *43*, 16525.

(289) Rodriguez, J. A.; Shaw, B. F.; Durazo, A.; Sohn, S. H.; Doucette, P. A.; Nersissian, A. M.; Faull, K. F.; Eggers, D. K.; Tiwari, A.; Hayward, L. J.; Valentine, J. S. *Proc. Natl. Acad. Sci., U.S.A.* **2005**, *102*, 10516.
(290) Rodriguez, J. A.; Valentine, J. S.; Eggers, D. K.; Roe, J. A.; Tiwari, A.; Brown, R. H.; Hayward, L. J. *J. Biol. Chem*. **2002**, *277*, 15932.
(291) Tiwari, A.; Hayward, L. J. *J. Biol. Chem.* **2003**, *278*, 5984.
(292) Field, L. S.; Furukawa, Y.; O'Halloran, T. V.; Culotta, V. C. *J. Biol. Chem.* **2003**, *278*, 28052.
(293) Arnesano, F.; Banci, L.; Bertini, I.; Martinelli, M.; Furukawa, Y.; O'Halloran T. V. *J. Biol. Chem.* **2004**, *279*, 47998.
(294) Antonyuk, S.; Stine Elam, J.; Hough, M. A.; Strange, R. W.; Doucette. P. A.; Rodriguez, J. A.; Hayward, L. J.; Valentine, J. S.; Hart, P. J.; Hasnain, S. S. *Protein Sci.* **2005**, *14*, 1201.
(295) Furukawa, Y.; O'Halloran, T. V. *J. Biol. Chem.* **2005**, *280*, 17266.
(296) Lynch, S. M.; Boswell, S. A.; Colon, W. *Biochemistry* **2004**, *43*, 16525.
(297) Leinweber, B.; Barofsky, E.; Barofsky, D. F.; Ermilov, V.; Nylin, K.; Beckman, J. S. *Free Radical Biol. Med.* **2004**, *36*, 911.
(298) DiDonato, N.; Craig, L.; Huff, M. E.; Thayer, M. M.; Cardoso, R. M. F.; Kassmann, C. J.; Lo, T. P.; Bruns, C. K.; Powers, E. T.; Kelly, J. W.; Getzoff, E. D.; Tainer, J. A. *J. Mol. Biol.* **2003**, *332*, 601.
(299) Elam, J. S.; Taylor, A. B.; Strange, R.; Antonyuk, S.; Doucette, P. A.; Rodriguez, J. A.; Hasnain, S. S.; Hayward, L. J.; Valentine, J. S.; Yeates, T. O.; and Hart, P. J. *Nature Struct. Biol.* **2003**, *10*, 461.
(300) Banci, L.; Bertini, I.; D'Amelio, N.; Gaggelli, E.; Libralesso, E.; Matecko, I.; Turano, P.; Valentine, J. S. *J. Biol. Chem*. **2005**, *280*, 35815.
(301) Dawson, T. M.; Dawson, V. L. *Science* **2003**, *302*, 819.
(302) Siderowf, A.; Stern, M. *Ann. Intern. Med.* **2003**, *138*, 651.
(303) Goedert, M. *Nat. Rev. Neurosci.* **2001**, *2*, 492.
(304) Polymeropoulos, M. H.; Lavedan, C.; Leroy, E.; Ide, S. E.; Dehejia, A.; Dutra, A.; Pike, B.; Root, H.; Rubenstein, J.; Boyer, R.; Stenroos, E. S.; Chandrasekharappa, S.; Athanassiadou, A.; Papapetropoulos, T.; Johnson, W. G.; Lazzarini, A. M.; Duvoisin, R. C.; Di Iorio, G.; Golbe, L. I.; Nussbaum, R. L. *Science* **1997**, *276*, 2045.
(305) Kitada, T.; Asakawa, S.; Hattori, N.; Matsumine, H.; Yamamura, Y.; Minoshima, S.; Yokochi, M.; Mizuno, Y.; Shimizu, N. *Nature* **1998**, *392*, 605.
(306) Clayton, D. F.; George, J. M. *Trends Neurosci.* **1998**, *21*, 249.
(307) Giasson, B. I.; Murray, I. V. J.; Trojanowski, J. Q.; Lee, V. M.-Y. *J. Biol. Chem.* **2001**, *276*, 2380.
(308) George, J. M. *Genome Biol.* **2002**, *3*, REVIEWS3002.
(309) Perrin, R. J.; Woods, W. S.; Clayton, D. F.; George, J. M. *J. Biol. Chem.* **2001**, *276*, 41958.
(310) Sharon, R.; Bar-Joseph, I.; Frosch, M. P.; Walsh, D. M.; Hamilton, J. A.; Selkoe, D. J. *Neuron* **2003**, *37*, 583.
(311) Zhang, Y.; Dawson, V. L.; Dawson, T. M. *Neurobiol. Dis.* **2000**, *7*, 240.
(312) Manning-Bog, A. B.; McCormack, A. L.; Li, J.; Uversky, V. N.; Fink, A. L.; Di Monte, D. A. *J. Biol. Chem.* **2002**, *277*, 1641.
(313) Betarbet, R.; Sherer, T. B.; MacKenzie, G.; Garcia-Osuna, M.; Panov, A. V.; Greenamyre, J. T. *Nat. Neurosi.* **2000**, *3*, 1301.
(314) Giasson, B. I.; Duda, J. E.; Murray, I. V.; Chen, Q.; Souza, J. M.; Hurtig, H. I.; Ischiropoulos, H.; Trojanowski, J. Q.; Lee, V. M. *Science* **2000**, *290*, 985.
(315) Chandra, S.; Chen, X.; Rizo, J.; Jahn, R.; Sudhof, T. C. *J. Biol. Chem.* **2003**, *278*, 15313.
(316) Jao, C. C.; Der-Sarkissian, A.; Chen, J.; Langen, R. *Proc. Natl. Acad. Sci., U.S.A.* **2004**, *101*, 8331.
(317) Der-Sarkissian, A.; Jao, C. C.; Chen, J.; Langen, R. *J. Biol. Chem.* **2003**, *278*, 37530.
(318) Fernandez, C. O.; Hoyer, W.; Zweckstetter, M.; Jares-Erijman, E. A.; Subramaniam, V.; Griesinger, C.; Jovin, T. M. *EMBO J.* **2004**, *23*, 2039.
(319) Bernstein, S. L.; Liu, D.; Wyttenbach, T.; Bowers, M. T.; Lee, J. C.; Gray, H. B.; Winkler, J. R. *J. Am. Soc. Mass Spectrom.* **2004**, *15*, 1435 and references therein.
(320) Munishkina, L. A.; Phelan, C.; Uversky, V. N.; Fink, A. L. *Biochemistry* **2003**, *42*, 2720.
(321) Cohlberg, J. A.; Li, J.; Uversky, V. N.; Fink, A. L. *Biochemistry* **2002**, *41*, 1502.
(322) Antony, T.; Hoyer, W.; Cherny, D.; Heim, G.; Jovin, T. M.; Subramaniam, V. *J. Biol. Chem.* **2003**, *278*, 3235.
(323) Yamin, G.: Glaser, C. B.; Uversky, V. N.; Fink, A. L. *J. Biol. Chem.* **2003**, *278*, 27630.
(324) Paik, S. R.; Lee, J.-H.; Kim, D.-H.; Chang C.-S.; Kim, Y.-S. *FEBS Lett.* **1998**, *421*, 73.
(325) Paik, S. R.; Shin, H.-J.; Lee, J.-H-; Chang, C.-S.; Kim, J. *Biochem. J.* **1999**, *340*, 821.
(326) Kim, Y. S.; Lee, D.; Lee, E. K.; Sung, J. Y.; Chung, K. C.; Kim, J.; Paik, S. R. *Brain Res.* **2001**, *908*, 93.
(327) Tanner, C. M. *Trends Neurosci.* **1989**, *12*, 49.
(328) Altschuler, E. *Med. Hypotheses* **1999**, *53*, 22.
(329) Uversky, V. N.; Li, J.; Fink, A. L. *J. Biol. Chem.* **2001**, *276*, 44284.
(330) Kim, K. S.; Choi, S. Y.; Kwon, H. Y.; Won, M. H.; Kang, T.-C.; Kang, J. H. *Free Radical Biol. Med.* **2002**, *32*, 544.
(331) Kim, K. S.; Choi, S. Y.; Kwon, H. Y.; Won, M. H.; Kang, T.-C,; Kang, J. H. *Biochimie* **2002**, *84*, 625.
(332) Lee, E. N.; Lee, S. Y.; Lee, D.; Kim, J.; Paik, S. R. *J. Neurochem.* **2003**, *84*, 1128.
(333) Lowe, R.; Pountney, D. L.; Jensen, P. H.; Gai, W. P.; Voelcker, N. H. *Protein Sci.* **2004**, *13*, 3245.
(334) Rasia, R. M.; Bertoncini, C. W.; Marsh, D.; Hoyer, W.; Cherny, D.; Zweckstetter, M.; Griesinger, C.; Jovin, T. M.; Fernandez, C. O. *Proc. Natl. Acad. Sci., U.S.A.* **2005**, *102*, 4294.
(335) Prusiner, S. B. *Science* **1997**, *278*, 245.
(336) Scott, M. R.; Will, R.; Ironside, J.; Nguyen, H. O.; Tremblay, P.; DeArmond, S. J.; Prusiner, S. B. *Proc. Natl. Acad. Sci., U.S.A.* **1999**, *96*, 15137.
(337) Kretzschmar, H. A.; Prusiner, S. B.; Stowring, L. E.; DeArmond, S. J. *Am. J. Pathol.* **1986**, *122*, 1.
(338) Caughey, B.; Chesebro, B. *Trends Cell Biol.* **1997**, *7*, 56.
(339) Prusiner S. B. *Proc. Natl Acad. Sci., U.S.A.* **1998**, *95*, 13363.
(340) Borchelt, D. R.; Taraboulos, A.; Prusiner S. B. *J. Biol. Chem.* **1992**, *267*, 16188.
(341) DeArmond, S. J.; Prusiner, S. B. *Am. J. Pathol.* **1995**, *146*, 785.
(342) van Rheede, T.; Smolenaars, M. M.; Madsen, O.; de Jong, W. W. *Mol. Biol. Evol.* **2003**, *20*, 111.
(343) Oesch, B.; Westaway, D.; Wälchli, M.; McKinley, M. P.; Kent, S. B. H.; Aebersold, R.; Barry, R. A.; Tempst, P.; Teplow, D. B.; Hood, L. E.; Prusiner, S. B.; Weissmann, C. *Cell* **1985**, *40*, 735.
(344) Calzolai, L.; Lysek, D. A.; Perez, D. R.; Guntert, P.; Wuthrich, K. *Proc. Natl. Acad. Sci., U.S.A.* **2005**, *102*, 651 and references therein.
(345) Kuwata, K.; Kamatari, Y. O.; Akasaka, K.; James, T. L. *Biochemistry* **2004**, *43*, 4439 and references therein.
(346) Viles, J. H.; Donne, D.; Kroon, G.; Prusiner, S. B.; Cohen, F. E.; Dyson, H. J.; Wright, P. E. *Biochemistry* **2001**, *40*, 2743.
(347) Lopez Garcia, F.; Zahn, R.; Riek, R.; Wuthrich, K. *Proc. Natl. Acad. Sci., U.S.A.* **2000**, *97*, 8334.
(348) Haire, L. F.; Whyte, S. M.; Vasisht, N.; Gill, A. C.; Verma, C.; Dodson, E. J.; Dodson, G. G.; Bayley, P. M. *J. Mol. Biol*. **2004**, *336*, 1175.
(349) Knaus, K. J.; Morillas, M.; Swietnicki, W.; Malone, M.; Surewicz, W. K.; Yee, V. C. *Nat. Struct. Biol.* **2001**, *8*, 770.
(350) Varki, A. *Glycobiology* **1993**, *3*, 97.
(351) Zuegg, J.; Gready, J. E. *Glycobiology* **2000**, *10*, 959.
(352) Kaneko, K.; Zulianello, L.; Scott, M.; Cooper, C. M.; Wallace, A. C.; James, T. L.; Cohen, F. E.; Prusiner, S. B. *Proc. Natl. Acad. Sci., U.S.A.* **1997**, *94*, 10069 and references therein.
(353) Baskakov, I. V.; Legname, G.; Baldwin, M. A.; Prusiner, S. B.; Cohen, F. E. *J. Biol. Chem.* **2002**, *277*, 21140 and references therein.
(354) Aguzzi, A.; Polymenidou, M. *Cell* **2004**, *116*, 313.
(355) McKenzie, D.; Bartz, J.; Mirwald, J.; Olander, D.; Marsh, R.; Aiken, J. *J. Biol. Chem.* **1998**, *273*, 25545.
(356) Wadsworth, J. D.; Hill, A. F.; Joiner, S.; Jackson, G. S.; Clarke, A. R.; Collinge, J. *Nat. Cell Biol.* **1999**, *1*, 55.
(357) Sigurdsson, E. M.; Brown, D. R.; Alim, M. A.; Scholtzova, H.; Carp, R.; Meeker, H. C.; Prelli, F.; Frangione, B.; Wisniewski, T. *J. Biol. Chem.* **2003**, *278*, 46199.
(358) Biro, J. C. *Appl. Bioinf.* **2003**, *2*, S25.
(359) Ma, J.; Wollmann, R.; Lindquist, S. *Science* **2002**, *298*, 1781.
(360) Horwich, A. L.; Weissman, J. S. *Cell* **1997**, *89*, 499.
(361) Zou, W. Q.; Cashman, N. R. *J. Biol. Chem.* **2002**, *277*, 43942.
(362) Swietnicki, W.; Petersen, R.; Gambetti, P.; Surewicz, W. K. *J. Biol. Chem.* **1997**, *272*, 27517.
(363) Hornemann, S.; Glockshuber, R. *Proc. Natl. Acad. Sci., U.S.A.* **1998**, *95*, 6010.
(364) Calzolai, L.; Zahn, R. *J. Biol. Chem.* **2003**, *278*, 35592.
(365) Jamin, N.; Coic, Y. M.; Landon, C.; Ovtracht, L.; Baleux, F.; Neumann, J. M.; Sanson, A. *FEBS Lett.* **2002**, *529*, 256.
(366) Wille, H.; Michelitsch, M. D.; Guenebaut, V.; Supattapone, S.; Serban, A.; Cohen, F. E.; Agard, D. A.; Prusiner, S. B. *Proc. Natl. Acad. Sci., U.S.A.* **2002**, *99*, 3563.
(367) Ziegler, J.; Sticht, H.; Marx, U. C.; Müller, W.; Rösch, P.; Schwarzinger, S. *J. Biol. Chem.* **2003**, *278*, 50175.
(368) Zahn, R.; Liu, A.; Luhrs, T.; Riek, R.; von Schroetter, C.; Lopez Garcia, F.; Billeter, M.; Calzolai, L.; Wider, G.; Wüthrich, K. *Proc. Natl. Acad. Sci., U.S.A.* **2000**, *97*, 145.
(369) Morrissey, M. P.; Shakhnovich, E. I. *Proc. Natl. Acad. Sci., U.S.A.* **1999**, *96*, 11293.
(370) Fernandez, A. *Eur. J. Biochem*. **2002**, *269*, 4165.
(371) Zahn, R. *J. Mol. Biol.* **2003**, *334*, 477.
(372) Burns, C. S.; Aronoff-Spencer, E.; Dunham, C. M.; Lario, P.; Avdievich, N. I.; Antholine, W. E.; Olmstead, M. M.; Vrielink, A.;

Gerfen, G. J.; Peisach, J.; Scott, W. G.; Millhauser, G. L. *Biochemistry* **2002**, *41*, 3991.
(373) Goldmann, W.; Hunter, N.; Smith, G.; Foster, J.; Hope, J. *J. Gen. Virol.* **1994**, *75*, 989.
(374) Wong, E.; Thackray, A. M.; Bujdoso, R. *Biochem. J.* **2004**, *380*, 273.
(375) Tagliavini, F.; Forloni, G.; D'Ursi, P.; Bugiani, O.; Salmona, M. *Adv. Protein Chem.* **2001**, *57*, 171.
(376) Tagliavini, F.; Lievens, P. M.; Tranchant, C.; Warter, J. M.; Mohr, M.; Giaccone, G.; Perini, F.; Rossi, G.; Salmona, M.; Piccardo, P.; Ghetti, B.; Beavis, R. C.; Bugiani, O.; Frangine, B.; Prelli, F. *J. Biol. Chem.* **200**1, *276*, 6009 and references therein.
(377) Jobling, M. F.; Stewart, L. R.; White, A. R.; McLean, C.; Friedhuber, A.; Maher, F.; Beyreuther, K.; Masters, C. L.; Barrow, C. J.; Collins, S. J.; Cappai, R. *J. Neurochem.* **1999**, *73*, 1557.
(378) Florio, T.; Paludi, D.; Villa, V.; Rossi Principe, D.; Corsaro, A.; Millo, E.; Damonte, G.; D'Arrigo, C.; Russo, C.; Schettini, G.; Aceto, A. *J. Neurochem.* **2003**, *85*, 62.
(379) Kheterpal, I.; Zhou, S.; Cook, K. D.; Wetzel, R. *Proc. Natl. Acad. Sci., U.S.A.* **2000**, *97*, 13597.
(380) Soto, C. *Nat. Rev. Neurosci.* **2003**, *4*, 49.
(381) McKinley, M. P.; Meyer, R. K.; Kenaga, L.; Rahbar, F.; Cotter, R.; Serban, A.; Prusiner, S. B. *J. Virol.* **1991**, *65*, 1340.
(382) Brown, D. R. *Mol. Neurobiol.* **2002**, *25*, 287.
(383) Lehmann, S. *Curr. Opin. Chem. Biol.* **2002**, *6*, 187.
(384) Turnbull, S.; Tabner, B. J.; Brown, D. R.; Allsop, D. *Neurosci. Lett.* **2003**, *336*, 159.
(385) Daniels, M.; Cereghetti, G. M.; Brown, D. R. *Eur. J. Biochem.* **2001**, *268*, 6155.
(386) Turnbull, S.; Tabner, B. J.; Brown, D. R.; Allsop, D. *Biochemistry* **2003**, *42*, 7675.
(387) Nishina, K.; Jenks, S.; Supattapone, S. *J. Biol. Chem.* **2007**, *279*, 40788.
(388) Wong, B. S.; Chen, S. G.; Colucci, M.; Xie, Z.; Pan, T.; Liu, T.; Li, R.; Gambetti, P.; Sy, M. S.; Brown, D. R. *J. Neurochem.* **2001**, *78*, 1400.
(389) Thackray, A. M.; Knight, R.; Haswell, S, J,; Bujdoso, R.; Brown, D. R. *Biochem. J.* **2002**, *362*, 253.
(390) Post, K.; Pitschke, M.; Schafer, O.; Wille, H.; Appel, T. R.; Kirsch, D.; Mehlhorn, I.; Serban, H.; Prusiner, S. B.; Riesner, D. *Biol. Chem.* **1998**, *379*, 1307.
(391) Giese, A.; Levin, J.; Bertsch, U.; Kretzschmar, H. *Biochem. Biophys. Res. Commun.* **2004**, *320*, 1240.
(392) Brown, D. R.; Hafiz, F.; Glasssmith, L. L.; Wong, B. S.; Jones, I. M.; Clive, C.; Haswell, S, J. *EMBO J.* **2000**, *19*, 1180.
(393) Brown, D. R.; Clive, C.; Haswell, S. J. *J. Neurochem.* **2001**, *76*, 69.
(394) Tsenkova, R. N.; Iordanova, I. K.; Toyoda, K.; Brown, D. R. *Biochem. Biophys. Res. Commun.* **2004**, *325*, 1005.
(395) Brown, D. R. *Biochem. Soc. Symp.* **2004**, 193.
(396) Brown, L. R.; Harris, D. A. In *Handbook of Copper Pharmacology and Toxicology*; Massaro, E. J., Ed.; Humana Press: Totowa, NJ, 2002; pp 103−113.
(397) Stöckel, J.; Safar, J.; Wallace, A. C.; Cohen, F. E.; Prusiner, S. B. *Biochemistry* **1998**, *37*, 7185.
(398) Hasnain, S. S.; Murphy, L. M.; Strange, R. W.; Grossmann, J. G.; Clarke, A. R.; Jackson, G. S.; Collinge, J. *J. Mol. Biol.* **2001**, *311*, 467.
(399) Burns, C. S.; Aronoff-Spencer, E.; Legname, G.; Prusiner, S. B.; Antholine, W. E.; Gerfen, G. J.; Peisach, J.; Millhauser, G. L. *Biochemistry* **2003**, *42*, 6794.
(400) Whittal, R. M.; Ball, H. L.; Cohen, F. E.; Burlingame, A. L.; Prusiner, S. B.; Baldwin, M. A. *Protein Sci.* **2000**, *9*, 332.
(401) Jackson, G. S.; Murray, I.; Hosszu, L. L.; Gibbs, N.; Waltho, J. P.; Clarke, A. R.; Collinge, J. *Proc. Natl. Acad. Sci., U.S.A.* **2001**, *98*, 8531.
(402) Qin, K.; Yang, Y.; Mastrangelo, P.; Westaway, D. *J. Biol. Chem.* **2002**, *277*, 1981.
(403) Pauly, P. C.; Harris, D. A. *J. Biol. Chem.* **1998**, *273*, 33107.
(404) Sumudhu, W.; Perera, S.; Hooper, N. M. *Curr. Biol.* **2001**, *11*, 519.
(405) Brown, L. R.; Harris, D. A. *J. Neurochem.* **2003**, *87*, 353.
(406) Brown, D. R.; Wong, B.-S.; Hafiz, F.; Clive, C.; Haswell, S. J.; Jones, I. M. *Biochem. J.* **1999**, *344*, 1.
(407) Brown, D. R.; Nicholas, R. S.; Canevari, L. *J. Neurosci. Res.* **2002**, *67*, 211.
(408) Nishimura, T.; Sakudo, A.; Nakamura, I.; Lee, D.; Taniuchi, Y.; Saeki, K.; Matsumoto, Y.; Ogawa, M.; Sakaguchi, S.; Itohara, S.; Onodera, T. *Biochem. Biophys. Res. Commun.* **2004**, *323*, 218.
(409) Shiraishi, N.; Inai, Y.; Bi, W.; Nishikimi, M. *Biochem. J.* **2005**, *387*, 247.
(410) Jones, S.; Batchelor, M.; Bhelt, D.; Clarke, A. R.; Collinge, J.; Jackson, G. S. *Biochem. J.* **2005**, *392*, 309.
(411) Brown, D. R.; Qin, K.; Herms, J. W.; Madlung, A.; Manson, J.; Strome, R.; Fraser, P. E.; Kruck, T.; von Bohlen, A.; Schulz-Schaeffer, W.; Giese, A.; Westaway, D.; Kretzschmar, H. A. *Nature* **1997**, *390*, 684.
(412) Waggoner, D. J.; Drisaldi, B.; Bartnikas, T. B.; Casareno, R. L. B.; Prohaska, J. R.; Gitlin, J. D.; Harris, D. A. *J. Biol. Chem.* **2000**, 275, 7455.
(413) Hutter, G.; Heppner, F. L.; Aguzzi, A. *Biol. Chem.* **2003**, *384*, 1279.
(414) J. R.; Groth, D.; Legname, G.; Stadtman, E. R.; Prusiner, S. B.; Levine, R. L. *Proc. Natl. Acad. Sci., U.S.A.* **2001**, *98*, 7170.
(415) Requena, J. R.; Dimitrova, M. N.; Legname, G.; Teijeira, S.; Prusiner, S. B.; Levine, R. L. *Arch. Biochem. Biophys.* **2004**, *432*, 188.
(416) Bocharova, O. V.; Breydo, L.; Salnikov, V. V.; Baskakov, I. V. *Biochemistry* **2005**, *44*, 6776.
(417) Li, A.; Dong, J.; Harris, D. A. *J. Biol. Chem.* **2004**, *279*, 29469.
(418) Hornshaw, M. P.; McDermott, J. R.; Candy, J. M. *Biochem. Biophys. Res. Commun.* **1995**, *207*, 621.
(419) Hornshaw, M. P.; McDermott, J. R.; Candy, J. M.; Lakey, J. H. *Biochem. Biophys. Res. Commun.* **1995**, *214*, 993.
(420) Miura, T.; Hori-i, A.; Mototani, H.; Takeuchi, H. *Biochemistry* **1999**, *38*, 11560.
(421) Viles, J. H.; Cohen, F. E.; Prusiner, S. B.; Goodin, D. B.; Wright, P. E.; Dyson, H. J. *Proc. Natl. Acad. Sci., U.S.A.* **1999**, *96*, 2042.
(422) Aronoff-Spencer, E.; Burns, C. S.; Avdievich, N. I.; Gerfen, G. J.; Peisach, J.; Antholine, W. E.; Ball, H. L.; Cohen, F. E.; Prusiner, S. B.; Millhauser, G. L. *Biochemistry* **2000**, *39*, 13760.
(423) Kramer, M. L.; Kratzin, H. D.; Schmidt, B.; Romer, A.; Windl, O.; Liemann, S.; Hornemann, S.; Kretzschmar, H. *J. Biol. Chem.* **2001**, *276*, 16711.
(424) Garnett, A. P.; Viles, J. H. *J. Biol. Chem.* **2003**, *278*, 6795.
(425) Brown, D. R.; Guantieri, V.; Grasso, G.; Impellizzeri, G.; Pappalardo, G.; Rizzarelli, E. *J. Inorg. Biochem.* **2004**, *98*, 133.
(426) Jones, C. E.; Abdelraheim, S. R.; Brown, D. R.; Viles, J. H. *J. Biol. Chem.* **2004**, *279*, 32018.
(427) Valensin, D.; Luczkowski, M.; Mancini, F. M.; Legowska, A.; Gaggelli, E.; Valensin, G.; Rolka, K.; Kozlowski, H. *Dalton Trans.* **2004**, 1284.
(428) Jones, C. E.; Klewpatinond, M.; Abdelraheim, S. R.; Brown, D. R.; Viles, J. H. *J. Mol. Biol.* **2005**, *346*, 1393.
(429) Gaggelli, E.; Bernardi, F.; Molteni, E.; Pogni, R.; Valensin, D.; Valensin, G.; Remelli, M.; Luczkowski, M.; Kozlowski, H. *J. Am. Chem. Soc.* **2005**, *127*, 996.
(430) Chattopadhyay, M.; Walter, E. D.; Newell, D. J.;, Jackson, P. J.; Aronoff-Spencer, E.; Peisach, J.; Gerfen, G. J.; Bennett, B.; Antholine, W. E.; Millhauser, G. L. *J. Am. Chem. Soc.* **2005**, *127*, 12647.
(431) Miura, T.; Sasaki, S.; Toyama, A.; Takeuchi, H. *Biochemistry* **2005**, *44*, 8712.
(432) Ritchie, C. W.; Bush, A. I.; Masters, C. L. *Exp. Opin. Invest. Drugs* **2004**, *13*, 1585.
(433) Kowalik-Jankowska, T.; Ruta, M.; Wiœniewska, M.; Łankiewicz, L. *J. Inorg. Biochem.* **2003**, *95*, 270.
(434) Karr, J. W.; Akintoye, H.; Kaupp, L. J.; Szalai V. A. *Biochemistry* **2005**, *44*, 5478.
(435) Garzon-Rodriguez, W.; Yatsimirsky, A. K.; Glabe, C. G. *Bioorg. Med. Chem. Lett.* **1999**, *9*, 2243.

CR040410W